






Statens vegvesen

Ferry free E39 -Fjord crossings Bjørnafjorden

304624

Rev.	Publish date	Description	Made by	Checked by	Project appro.	Client appro.
0	15.08.19	Issued for use	JOM/KNHBE/JOH	GUNHEN	KH	
Client		 <b>Statens vegvesen</b>				
Contractor		Contract no.:				
 		18/91094				

Tillatt for offentliggjøring.  
Batymetridata er nedskalert til  
50x50 m oppløsning.

Document name:

K12 - Marine geotechnical design

Document no.:

SBJ-33-C5-OON-22-RE-022

Rev.:

0

Pages:

90



# CONCEPT DEVELOPMENT FLOATING BRIDGE E39 BJØRNAFJORDEN

## K12 – MARINE GEOTECHNICAL DESIGN

Norconsult 

 DR. TECHN.  
OLAV OLSEN

 Prodtex  
Næringsmiddel / Saltvann / Trækløst

 IFE  
Pure Logic  
— The essence of production connectivity

HEYERDAHL ARKITEKTER AS

 H&BB

 MIKO  
MARINE AS

 BUKSÉR OG  
BERGING

 FORCE  
TECHNOLOGY

 SWERIM

# REPORT

**Project name:**

CONCEPT DEVELOPMENT FLOATING BRIDGE E39  
BJØRNAFJORDEN

**Document name:**

K12 – MARINE GEOTECHNICAL DESIGN

**Project number:**

5187772/12777

**Document number:**

SBJ-33-C5-OON-22-RE-022

**Date:**

15.08.2019

**Revision:**

0

**Number of pages:**

90

**Prepared by:**

Johannes Mydland, Knut-Helge Bergset, Jon Hermstad

**Controlled by:**

Gunhild Hennum

**Approved by:**

Kolbjørn Høyland

## Summary

This report describes the geotechnical design for the recommended bridge concept K12. The K12 concept is an end-anchored floating bridge with mooring system for increased robustness and redundancy. There is a pylon support at Svarvhelleholmen in south, and a filling at Gullholmane in the north. Mooring pontoons are at two locations, with 4 anchors in each direction, which gives 16 anchor locations in total.

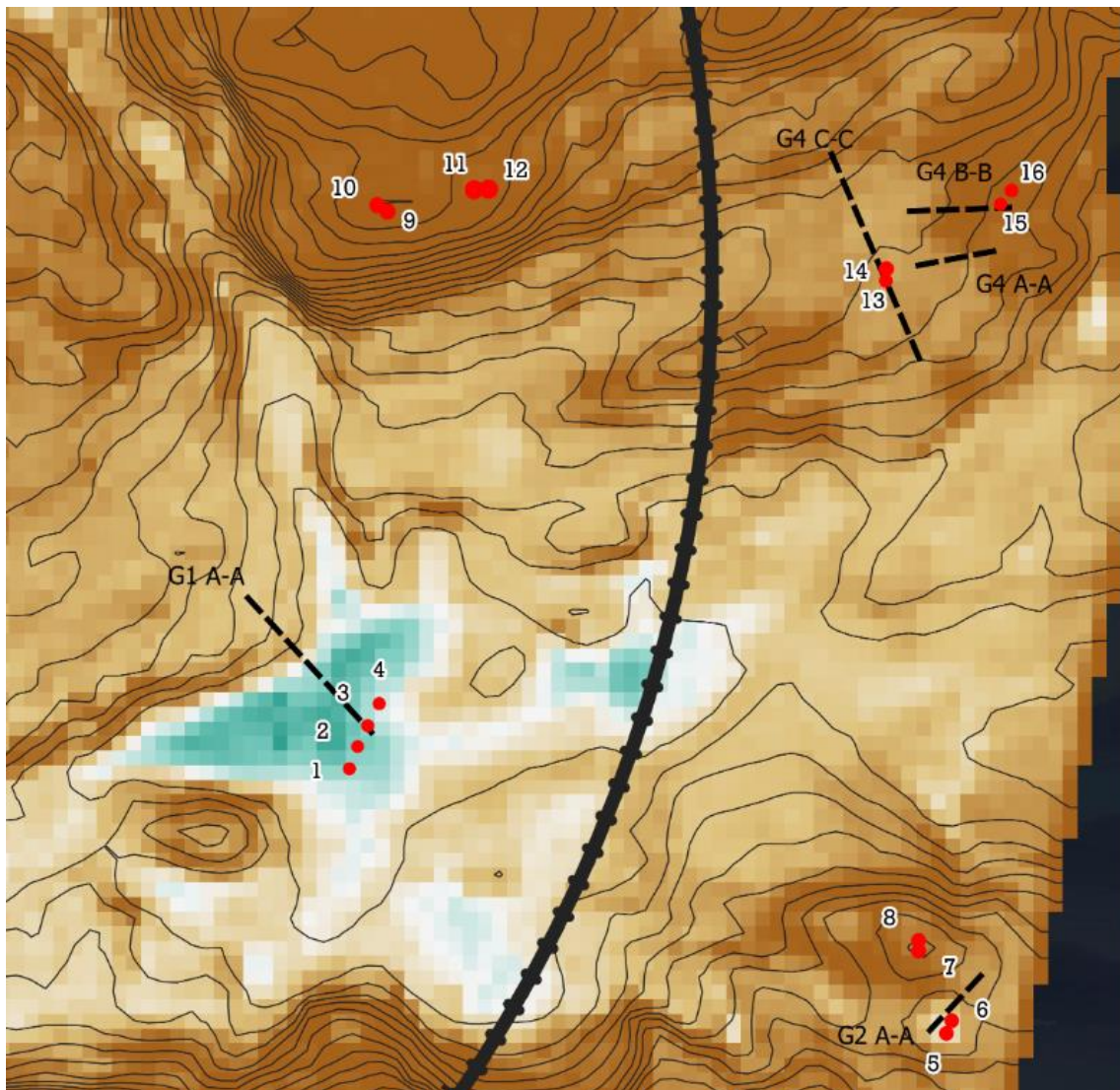
The bathymetry of Bjørnafjorden is characterized by steep slopes in the south and a hilly seabed in the north, with ridges and valleys. The mid part basin is covered by slightly over-consolidated soft clay down to more 50 meters depth. The sediment thickness is varying from 0 to about 80 m. The hilly and steep areas are partly covered by soil, with bedrock outcrops. So far the soil investigations indicate soft soil of the same character in those areas as in the basin. The fjord is characterized by many old landslides, which can clearly be seen on the maps from subsea surveys.

Existing slopes have generally low safety against failure related to earthquake, and there is a challenge to find anchor locations suitable for the bridge, and at the same time robust with respect to geotechnical stability.

Introductorily, an overall screening was performed to find possible areas for anchor locations, with respect to load transfer, static and dynamic stability, and exposure for runout debris. Locations permitting either gravity anchors or suction anchors were aimed at. In cooperation with the mooring discipline the limiting geometric conditions are set to:

- Maximum mooring line length 2000 m
- Inclination max. 45 °

After more detailed analysis, as a result of an iterative process, the anchor positions suggested for K12 are:



The anchors are divided into 4 groups:

Group 1: anchor 1- 4

Group 2: anchor 5 – 8

Group 3: anchor 9 – 12

Group 4: anchor 13 – 16

Control of static slope stability show that the safety factor for failure slopes that reach the anchors are within the requirement of 1.4. Safety factors for failure surfaces that do not reach the anchors but may affect the anchors due to run-out, are however low for some of the anchors. These are: Anchor 1- 4, 5, 6, 13 and 14, where the safety factors are varying between 1.1 and 1.3. Pseudo static calculations show far too low safety factors, and therefore dynamic analysis are performed. These analyses show permanent shear strain of maximum 10 % for certain slopes. The requirement is 3 % and thus neither acceptable. Therefore run-out consequences have also been evaluated. Note that the profiles with high permanent dynamic shear strain corresponds very well with the profiles giving low safety factors.

Run-out evaluations are performed with emphasize on the anchors with low safety factors and high shear strains. Anchor group 1 is exposed for landslide debris from several directions. For anchor group 2 the two suction anchors 5 and 6 have limited risk to be affected by landslide and the consequences are considered to be small since the potential debris volume is lower compared to group 1, and anchors 7 and 8 is safely located with respect to landslide. Anchors 9–12 are not exposed for landslides, and the same goes for anchors 15 and 1. In anchor group 4, anchor 13 and 14 may be influenced by landslide and/or retro-progressive landslide from different directions. The risk is limited and sensitive to soil conditions and depth to bedrock.

The overall philosophy is that the anchor exposed for landslide, should be suction anchors. The sediment thickness makes it possible to lengthen the skirts, to increase the holding capacity and robustness against landslide. For Anchor 1–6, 13 and 14 the required skirt depth is calculated, assuming remoulded soil in the upper 3 m. This is to include the effect of a landslide with 3 m ploughing depth. Thereby the anchors have sufficient holding capacity in case the peak design load occur after a post-landslide situation. In practice, the suction anchors will have spare capacity prior to landslide. Additional load from debris flow is not taken into account and assumed to be less than the peak mooring load when accounting for the loss of two lines.

The bridge is designed to lose two random anchors, with the bridge and mooring system still intact. The design anchor loads are consequently calculated in the ULS-condition with two random anchors out of operation.

Design resulting anchor load for a gravity anchor is in the order of 5000 MN and for a suction anchor 6300 kN. The design of gravity anchors was carried out before to the mooring analysis was complete, thus the design load used in calculation is set to 6000 MN.

Suction anchors are suggested for anchor number 1 – 6, 13 and 14:

Geometry: diameter 9 m and skirt length 10 m and 12.5 m. The stability calculations show that the safety factors are minimum 1.55, within good margins to the required 1,2.

Gravity anchors are suggested for anchor number 7 – 12, 15 and 15:

Geometry: B x L = 15 x 15 m and H = 5.3 m, where 0.3 m is skirts.

Design horizontal capacity in ULS is 6.76 MN, while the horizontal design load is 4.6 MN.

The bridge is not sensitive for deformation caused by consolidation and creep of the suction anchors, as relative deformations between anchors and bridge have minimal effect on the stiffness of the mooring system. Additionally, the mooring lines may be tightened up if required.

For the filling at Gulholmane, a solution with seabed dredging of soft soils prior to fill construction is recommended. This alternative will also eliminate the risk of significant long-term settlement damage to the road. Depending on results from supplementary soil investigations, a solution without or with partly exchange of existing soil may be possible

# Table of Content

<b>1</b>	<b>INTRODUCTION .....</b>	<b>9</b>
1.1	Current report .....	9
1.2	Project context .....	9
1.3	Project team .....	10
1.4	Project scope .....	11
<b>2</b>	<b>BRIDGE CONCEPT DESCRIPTION .....</b>	<b>12</b>
<b>3</b>	<b>RULES AND REGULATIONS .....</b>	<b>15</b>
3.1	Abbreviations and definitions .....	15
3.2	Design basis documents .....	15
3.3	Rules and regulations .....	15
3.4	Project category .....	16
3.5	Summary of design requirements .....	17
<b>4</b>	<b>DESIGN PREMISES .....</b>	<b>18</b>
4.1	Bathymetry and isopach .....	18
4.2	Coordinate system .....	21
4.3	Soil conditions .....	21
4.4	Softwares .....	23
4.5	Seismic loads .....	24
<b>5</b>	<b>GEOHAZARD AND SLOPE STABILITY .....</b>	<b>25</b>
5.1	Overall screening .....	25
5.2	Static global slope stability .....	32
5.3	Seismic slope stability .....	41
5.4	Run-Out evaluations .....	47
5.5	Recommended anchor locations .....	53
5.6	Risk assessment for anchor groups .....	56
<b>6</b>	<b>ANCHOR DESIGN .....</b>	<b>60</b>
6.1	Anchor types considered .....	60
6.2	Anchor loads .....	60
6.3	Anchor deformations .....	62
6.4	Gravity anchor calculations .....	64
6.5	Suction anchor calculation .....	67
<b>7</b>	<b>LANDFALL GULHOLMANE .....</b>	<b>79</b>

7.1	Soil conditions.....	79
7.2	Possible solutions for the rock fill construction.....	82
7.3	Recommendation.....	83
<b>8</b>	<b>RECOMMENDED PRIORITIES FOR FUTURE STUDIES .....</b>	<b>84</b>
<b>9</b>	<b>ADDITIONAL SOIL INVESTIGATIONS .....</b>	<b>85</b>
9.1	General .....	85
9.2	Anchor group 1 .....	85
9.3	Anchor group 2 .....	86
9.4	Anchor group 3 .....	87
9.5	Anchor group 4 .....	88
9.6	Gullholmane.....	89
<b>10</b>	<b>REFERENCES .....</b>	<b>90</b>
<b>Appendix A</b>	<b>Design brief</b>	
<b>Appendix B</b>	<b>Seismic evaluation</b>	
<b>Appendix C</b>	<b>Static slope stability</b>	
<b>Appendix D</b>	<b>Pseudo Static slope stability</b>	
<b>Appendix E</b>	<b>Plaxis – Slope calculations</b>	
<b>Appendix F</b>	<b>Plaxis – Suction anchor, failure modes</b>	
<b>Appendix G</b>	<b>Map of anchor groups</b>	



# 1 INTRODUCTION

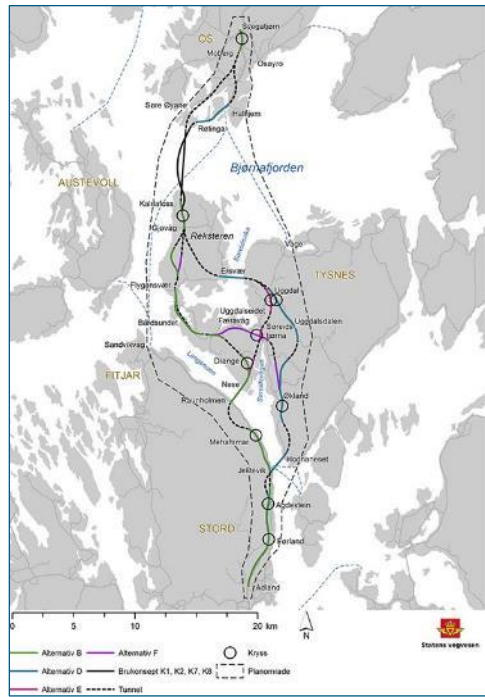
## 1.1 Current report

This report describes the marine geotechnical design for the recommended bridge concept K12.

## 1.2 Project context

Statens vegvesen (SVV) has been commissioned by the Norwegian Ministry of Transport and Communications to develop plans for a ferry free coastal highway E39 between Kristiansand and Trondheim. The 1100 km long coastal corridor comprise today 8 ferry connections, most of them wide and deep fjord crossings that will require massive investments and longer spanning structures than previously installed in Norway. Based on the choice of concept evaluation (KVU) E39 Akسدal Bergen, the Ministry of Transport and Communications has decided that E39 shall cross Bjørnafjorden between Reksteren and Os.

SVV is finalizing the work on a governmental regional plan with consequence assessment for E39 Stord-Os. This plan recommends a route from Stord to Os, including crossing solution for Bjørnafjorden, and shall be approved by the ministry of Local Government and Modernisation. In this fifth phase of the concept development, only floating bridge alternatives remain under consideration.



### 1.3 Project team

Norconsult AS and Dr.techn.Olav Olsen AS have a joint work collaboration for execution of this project. Norconsult is the largest multidiscipline consultant in Norway and is a leading player within engineering for transportation and communication. Dr.techn.Olav Olsen is an independent structural engineering and marine technology consultant firm, who has a specialty in design of large floating structures. The team has been strengthened with selected subcontractors who are all highly qualified within their respective areas of expertise:

- Prodtex AS is a consultancy company specializing in the development of modern production and design processes. Prodtex sits on a highly qualified staff who have experience from design and operation of automated factories, where robots are used to handle materials and to carry out welding processes.
- Pure Logic AS is a consultancy firm specializing in cost- and uncertainty analyses for prediction of design effects to optimize large-scale constructs, ensuring optimal feedback for a multidisciplinary project team.
- Institute for Energy Technology (IFE) is an independent nonprofit foundation with 600 employees dedicated to research on energy technologies. IFE has been working on high-performance computing software based on the Finite-Element-Method for the industry, wind, wind loads and aero-elasticity for more than 40 years.
- Buksér og Berging AS (BB) provides turn-key solutions, quality vessels and maritime personnel for the marine operations market. BB is currently operating 30 vessels for harbour assistance, project work and offshore support from headquarter at Lysaker, Norway.
- Miko Marine AS is a Norwegian registered company, established in 1996. The company specializes in products and services for oil pollution prevention and in-water repair of ship and floating rigs, and is further offering marine operation services for transport, handling and installation of heavy construction elements in the marine environment.
- Heyerdahl Arkitekter AS has in the last 20 years been providing architect services to major national infrastructural projects, both for roads and rails. The company shares has been sold to Norconsult, and the companies will be merged by 2020.
- Haug og Blom-Bakke AS is a structural engineering consultancy firm, who has extensive experience in bridge design.
- FORCE Technology AS is engineering company supplying assistance within many fields, and has in this project phase provided services within corrosion protection by use of coating technology and inspection/maintenance/monitoring.
- Swerim is a newly founded Metals and Mining research institute. It originates from Swerea-KIMAB and Swerea-MEFOS and the metals research institute IM founded in 1921. Core competences are within Manufacturing of and with metals, including application technologies for infrastructure, vehicles / transport, and the manufacturing industry.

In order to strengthen our expertise further on risk and uncertainties management in execution of large construction projects Kåre Dybwad has been seconded to the team as a consultant.

## 1.4 Project scope

The objective of the previous project phase was to develop 4 nominated floating bridge concepts, document all 4 concepts sufficiently for ranking, and recommend the best suited alternative. The characteristics of the 4 concepts are as follows:

- K11: End-anchored floating bridge. In previous phase named K7.
- K12: End-anchored floating bridge with mooring system for increase robustness and redundancy.
- K13: Straight side-anchored bridge with expansion joint. In previous phase named K8.
- K14: Side-anchored bridge without expansion joint.

The concept K12 was selected as the best suited alternative. We refer to Concept Selection and Risk Management report, ref. [1].

In order to ensure a safe and robust foundation design, we have performed evaluations with respect to anchor location, anchor design and capacity.

Key tasks are:

- Study of reports with analysis and evaluations performed in earlier phases of the project, used for screening of possible anchor locations and anchor types
- Static slope stability analysis
- Dynamic slope stability analysis for seismic condition
- Watershed and Run-out evaluations
- Risk assessment for anchor cluster
- Global sizing for anchor design
- Control of anchor holding capacity
- Calculation of anchor deformations due to consolidation settlements and creep
- Evaluations and description of solution for rock-fill at Landfall Gullholmane

## 2 BRIDGE CONCEPT DESCRIPTION

The alternative K12 is a curved bridge with two anchor clusters at approximately 1/3 and 2/3 of the arc length. The bridge is firmly anchored at both ends, and part of the bridge in the south is cable-stayed allowing for ship traffic to pass. The curvature of the bridge provides stability and better performance with respect to external load compared to a straight bridge. The addition of the two anchor clusters ensures two holding points which is beneficial by reducing the effective span length, increasing the life expectancy with respect to fatigue and in general making the bridge overall more robust against possible unforeseen accidents. A summary of key figures is given in Table 2-1.

A general overview is shown below.

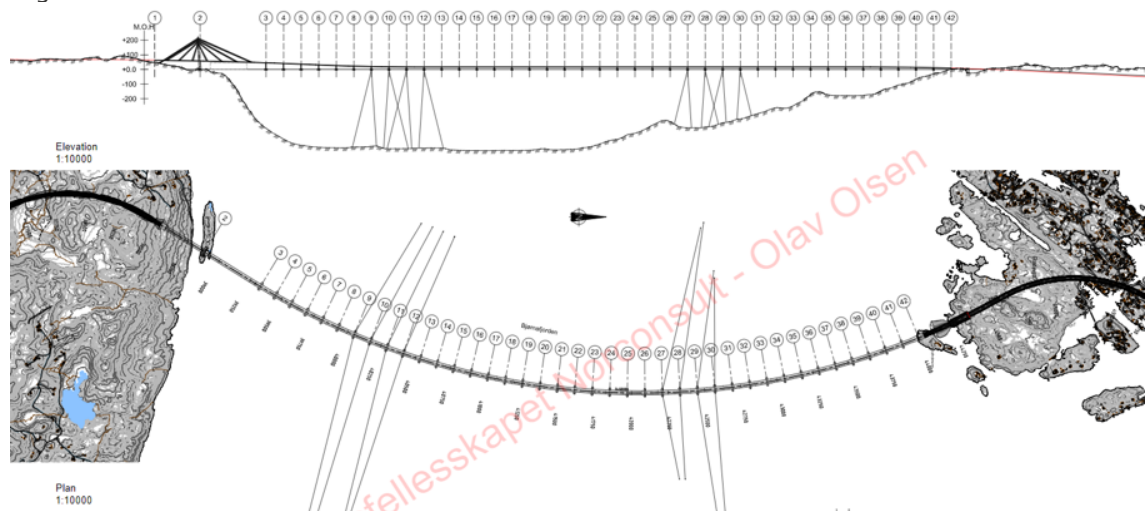


> Figure 2-1 General elevation and plan view

> Table 2-1: Key conceptual figures.

Geometry - arch	R = 5 000 m
Length	5 440 m
Cable stayed bridge main span – pylon to first pontoon	710 m
No of pontoons	39
Pontoon spacing	120 m
No of expansion joints	0
No of bearings	0
No of mooring groups	2
Mooring position Approx.	0,33L 0,67L
Horizontal mooring stiffness – anchor group	800 kN/m
First 5 horizontal eigenperiods	61, 51, 33, 21, 16 s

The mooring lines are connected to four pontoons in each anchor cluster, thereby reducing the risk of line loss due to ship impact. Another benefit is that the load is distributed across the bridge length and thus reducing high local stress concentrations in the bridge girder. Layout of the mooring configuration is shown in Figure 2-2.

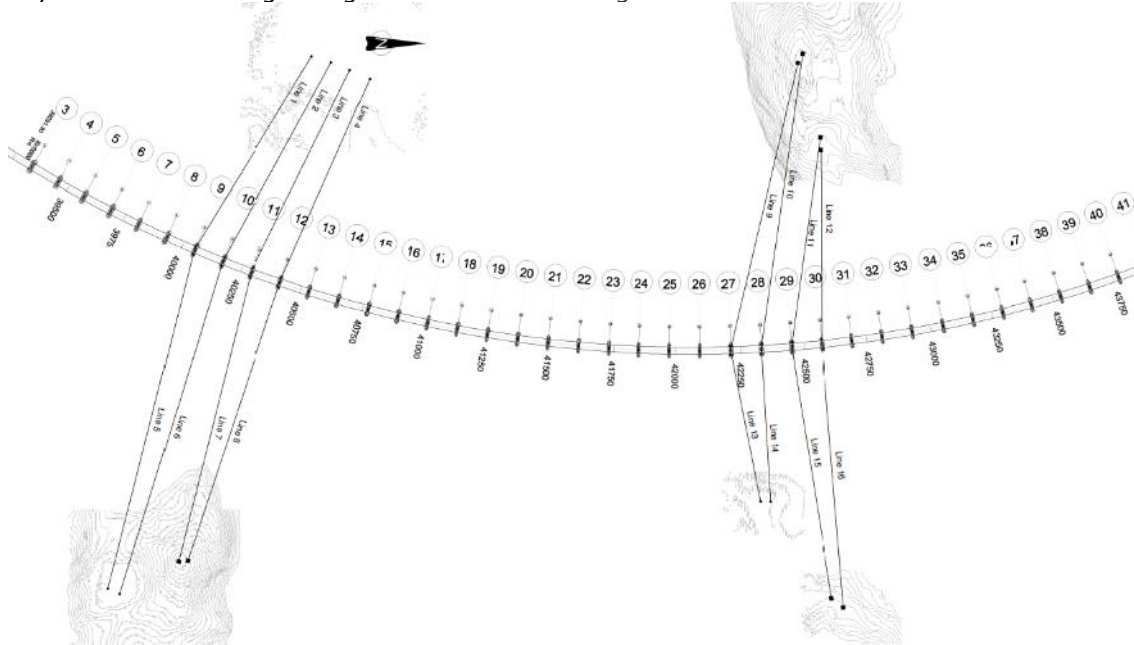


> Figure 2-2 Mooring plan view.

The southernmost anchor group is located at the deepest part of the Bjørnafjorden, while the anchors in the north is located at a higher elevation. One should however note that due to uneven ground surface and large distances between the anchors, there is a considerable difference in elevation between the anchors in east and west.

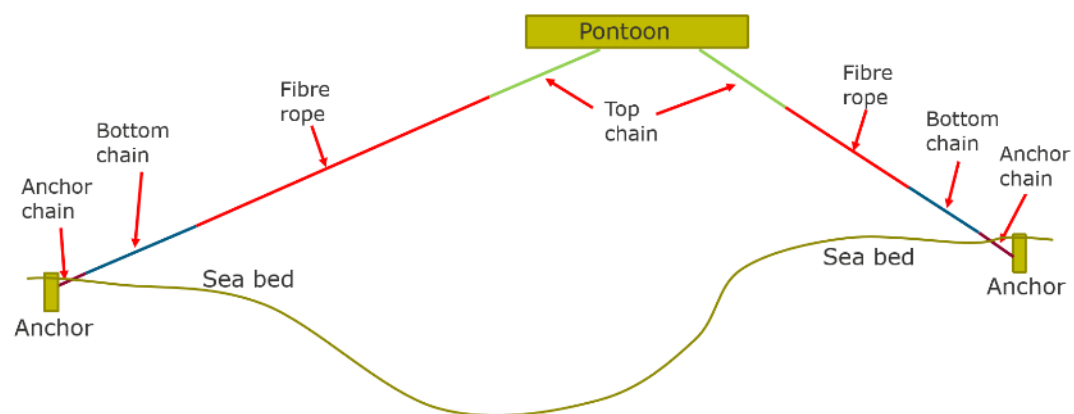


> Figure 2-3 Principle drawing (side view) of one pair of mooring lines.

In the figure above the different parts of the mooring line is shown. The lines mainly consist of a fibre rope, thus making the overall mooring response very linear. At the ends the lines consist of chain links and are especially dimensioned for fatigue and ground impact. Due to the stiffness requirement that ensures smoother dynamic behavior of the bridge, the line capacity, i.e. Minimum Breaking Load, is much higher than the governing loads acting on the mooring system.

The main goal of the anchor is to create a fixed point for the mooring line. Since the mooring line capacity is dimensioned with respect to stiffness and not capacity, dimensioning the anchors for MBL would be very conservative. Thus, the anchors are dimensioned for the governing dynamic and static loads according to the DNV rules.

An overview of the contributing components, and difference to the least robust concept, K13 (straight moored bridged) is shown in Figure 2-4. As can be seen from the figure, the mooring system contributes with a fair share to this uncertainty of K12. The concept was however deemed the most reliable and predictable among the other proposed concepts. Therefore, by reducing the uncertainty regarding geohazard and anchor holding capacity, one can greatly increase the robustness of the overall bridge concept.

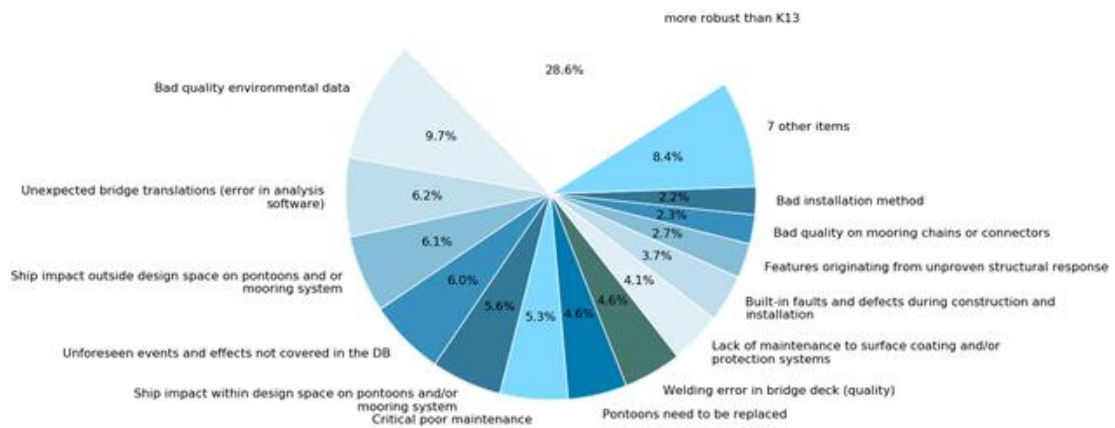


> Figure 2-4 Pie-chart of the contributing events to consequence for K12, ref. [1].

A short summary of the concept K12 given in Concept Selection and Risk Management report, ref. [1], is recited below.

The pros of K12 are the following:

- Redundant system with double horizontal load-carrying system.
- Largest potential for- and flexibility in designing a robust solution.
- Mooring reduces the response and increases design life compared to a bridge without a mooring system. Possible to increase design life further with small amount of additional steel.
- Fibre-rope mooring gives favorable interaction with bridge girder and Linear behavior of mooring without risk of successive mooring line failure for known load cases.
- Installation of complete assembled floating bridge, less work in Bjørnafjorden, simple mooring hook-up.
- Few and manageable anchor locations.
- No joints and bearings.

While the cons that must be addressed are:

- Mooring components needs replacement within design life. Complexity and costs related to this operation not sufficiently reflected and one has limited experience with taut mooring in shallow water.
- Challenging soil conditions with risk of underwater slides

## 3 RULES AND REGULATIONS

Generally, we refer to the Design Documents issued by the Client and the Design Brief prepared by OON, ref. Appendix A.

### 3.1 Abbreviations and definitions

SLS	Serviceability Limit State
ULS	Ultimate Limit State
ALS	Accidental Limit State
FAT	Fatigue limit state
CC	Consequence class
RC	Reliability class
FoS	Factor of safety
MBL	Minimum breaking load
PGA	Peak Ground Acceleration
$\gamma_m$	Soil material factor
OON	Olav Olsen and Norconsult AS joint work collaboration

### 3.2 Design basis documents

Main Design basis documents are:

SBJ-02-C4-SVV-02-RE-004\_0 Design Basis – Geotechnical design

SBJ-32-C4-SVV-26-BA-001\_3 Design Basis – Mooring and anchor

SBJ-32-C4-SVV-90-BA-001\_0 Design Basis – Bjørnafjorden floating brigdes

### 3.3 Rules and regulations

Most relevant rules and regulations listed as prioritized by the client are:

- Handbook V220: Geoteknikk i vegbygging (Guidelines for geotechnical design), 2018
- Handbook V221: Grunnforsterkning, fyllinger og skrånninger (Guidelines for Ground improvement, fillings and slopes), 2014
- NS-EN 1997-1:2004+A1:2013+NA:2016: Eurocode 7: Geotechnical design – Part 1: General rules
- NS-EN 1998-1:2004+A1:2003+NA:2014: Eurocode 8 Design of structures for earthquake resistance – Part 1: General rules seismic actions and rules for buildings
- NS-EN 1998-2:2005+A1:2009+A2:2011+NA:2014: Eurocode 8 Design of structures for earthquake resistance – Part 2: Bridges
- NS-EN 1998-5:2004+NA:2014: Eurocode 8 Design of structures for earthquake resistance – Part 5: Foundations, retaining structures and geotechnical aspects
- Forskrift om posisjonering – og ankringsystemer på flyttbare innretninger (Ankringsforskriften 09). FOR-2009-07-10-998

Additionally, the following offshore standards and recommended practice are followed for anchor design:

- DNVGL-OS-C101 Design of offshore steel structures, general LRFD method, 2016
- DNVGL-OS-E301 Position mooring, 2015
- DNVGL-RP-E303 Geotechnical design and installation of suction anchors, 2017
- NS-EN ISO 19901-7 Dynamisk posisjonering og forankring av flytende innretninger og flyttbare innretninger til havs, 2013

### 3.4 Project category

According to Design Basis - Bjørnafjorden floating bridges ref. [2], the bridge is categorized as CC3 and RC3 according to NS-EN 1990 Annex B, ref. [3]. The Design Basis allows for particular members of the structure to be categorized as CC2 and RC2. Furthermore, in Design Basis – Geotechnical design ref. [4] it is stated that the general consequence class for the project is CC3 and for other components which are not critical for the global stability of the bridge a lower consequence class can be assessed.

For the current concept K12 which relies on a mooring system, the individual components in the mooring system including anchors are regarded as CC3 and RC3 according to Eurocode. Furthermore, it is defined in the Design Basis for mooring and anchoring ref. [5], that the mooring system shall be designed for CC3 according to NS-EN-ISO 19901-7. Hence, the consequence class according to DNVGL standards is set to 2, where failure may lead to unacceptable consequences which is the strictest consequence class in the DNV-regulation.



### 3.5 Summary of design requirements

The table below presents the design requirements applied for this phase and for the recommended concept K12. Further description is given in the Design Brief Appendix A.

> Table 3-1 Summary of design requirements

Condition	Design requirement	Comment									
Local slope stability ULS-condition	Effective: $\gamma_m \geq 1.6$ Total: $\gamma_m \geq 1.6$										
Global slope stability ULS-condition	Effective: $\gamma_m \geq 1.4$ Total: $\gamma_m \geq 1.4$  For special cases: Effective: $\gamma_m \geq 1.25$ Total: $\gamma_m \geq 1.3$	Lower factor of safety may be used where no potential factors are identified to reduce the stability of the slope. This option will not be applied for this phase									
Earthquake (2750 years event) Seismic ALS-condition	<u>Pseudo-static analysis:</u> Fill materials: $\gamma_m \geq 1.2$ Clay and other materials: $\gamma_m \geq 1.1$  <u>Dynamic analysis:</u> Permanent shear strain $\gamma_p \leq 3\%$	A dynamic analysis will be performed if the pseudo-static criteria are not satisfied, ref. [4]  Rate effects and cyclic degradation are assumed to have no negative impact on strength parameters. The effect is assumed to be zero, ref. Appendix A.									
Holding capacity of anchors ULS- & ALS-condition	Soil material factor $\gamma_m$  <table border="1" style="margin-left: auto; margin-right: auto;"> <thead> <tr> <th>Anchor type</th> <th>ULS</th> <th>ALS</th> </tr> </thead> <tbody> <tr> <td>Gravity</td> <td>1.3</td> <td>1,0</td> </tr> <tr> <td>Suction</td> <td>1.2</td> <td>1.2</td> </tr> </tbody> </table>	Anchor type	ULS	ALS	Gravity	1.3	1,0	Suction	1.2	1.2	The different anchor types are defined in chapter 6.  Material factors for suction anchors are calibrated for undrained failure modes, ref. [6]. It's here deemed satisfactory for anchor design given that the net vertical load is in the gravitational direction during operational loading.  The soil strength degradation due to cyclic loading is assessed, and assumed to be neglectable, ref. Appendix A.
Anchor type	ULS	ALS									
Gravity	1.3	1,0									
Suction	1.2	1.2									
Landslide impact ALS-condition	Anchors will be evaluated for landslide impact.	Detailed calculations will not be performed.									
Settlements SLS-condition	Settlements will be checked in relation to allowable deformations in anchoring system. Lateral consolidation and creep deformation due to operational load, i.e. permanent horizontal pre-tension, shall be studied.	Allowable deformations will be decided based on global and mooring analysis.									
Effect of sedimentation on long-term stability of slopes	The effect of 30 cm sedimentation shall be studied with respect to slope stability.	30 cm is within the accuracy of the bathymetry information. The effect is assumed not to be critical and will not be performed in this phase.									

## 4 DESIGN PREMISES

### 4.1 Bathymetry and isopach

The fjord is asymmetrical with undulating seabed. On the southern side there is a steep inclination down to the basin. The basin itself stretches out almost two thirds of the crossing distance and has a depth of about -550 m. The last part in the north, which is shallower from about -150 m to -50 m depth, consists mainly of exposed bedrock as shown in Figure 4-1. The map below shows the bathymetry, prepared by NGI. ref. [7], coast line from "Felles KartdataBase" in red and height contours on land from Hoydedata.no [8].

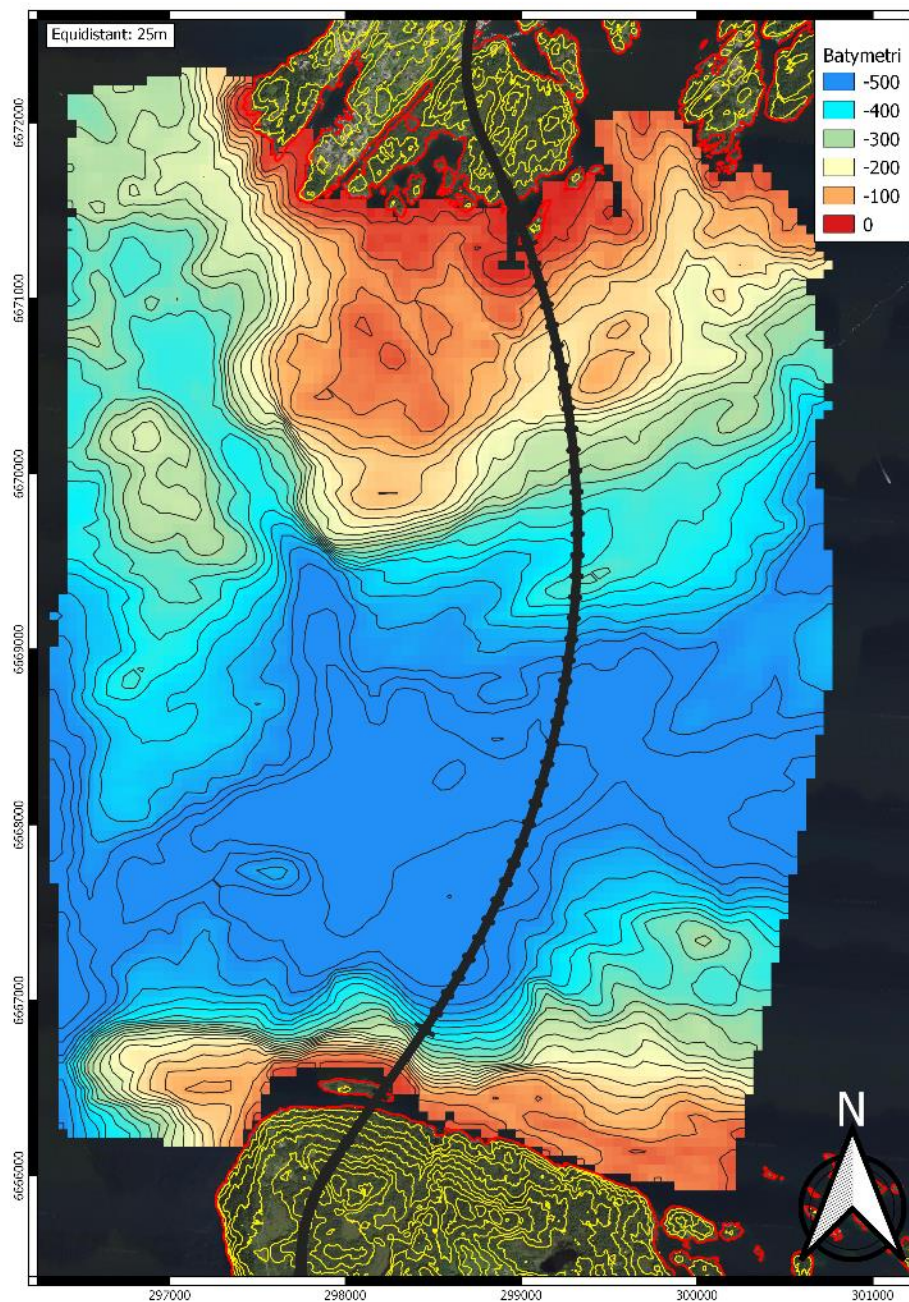


> Figure 4-1- Bathymetry of Bjørnafjorden.

Acoustic measurements were done in 2016 and 2018 by DOF SubSea. Figure 4-2 presents the post-processed data done by OON which includes data from 2018. Although deviation in depth to bedrock is expected, in this phase the isopach is assumed to be exact. The bedrock can thereby be calculated by subtracting the bathymetry with the isopach map which is shown in Figure 4-3. Profiles can thereby easily be viewed in QGIS. An example of this is illustrated in Figure 4-4.

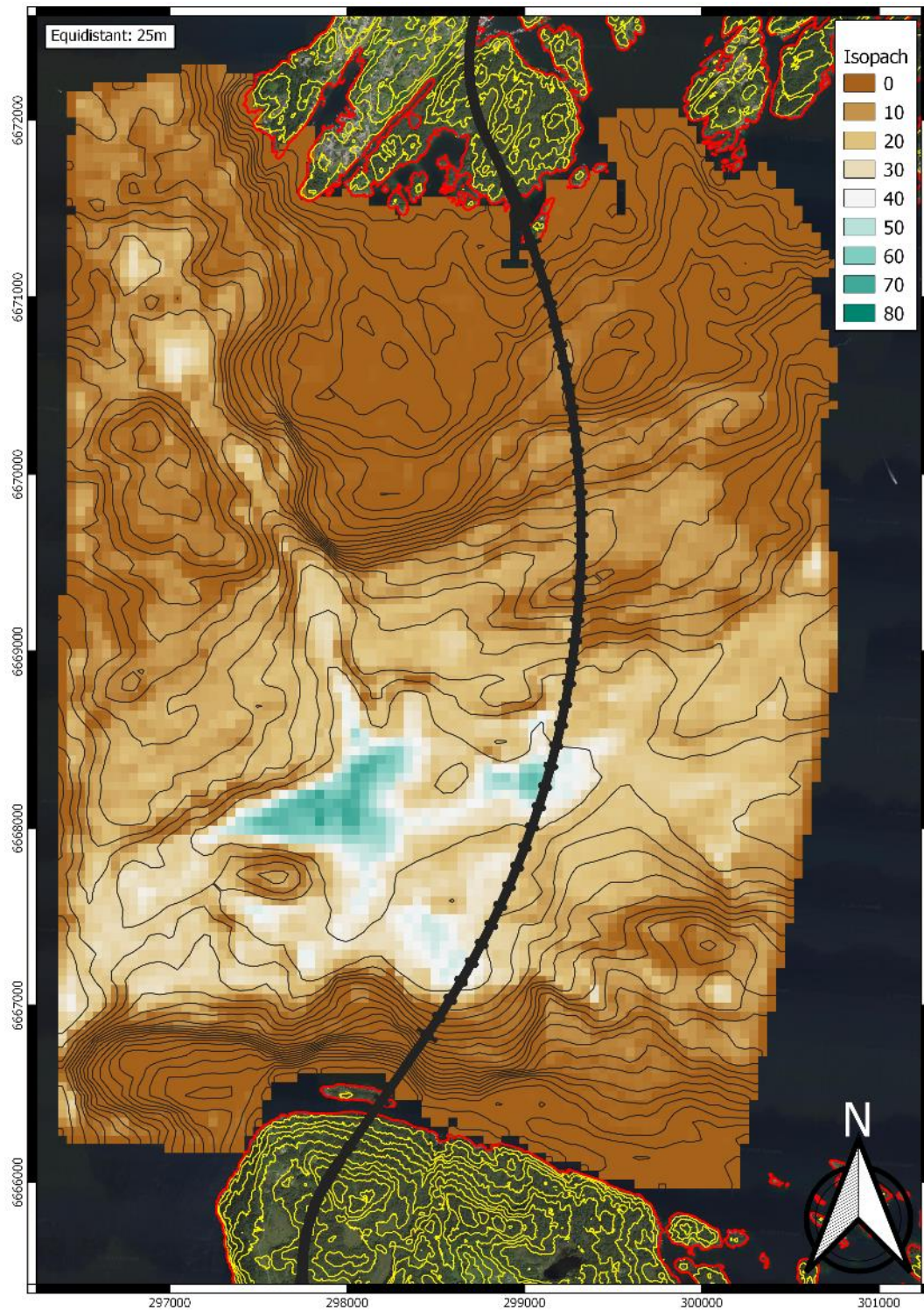


> Figure 4-2 - Interpolated isopach from data provided by DOF 2016 and 2018.

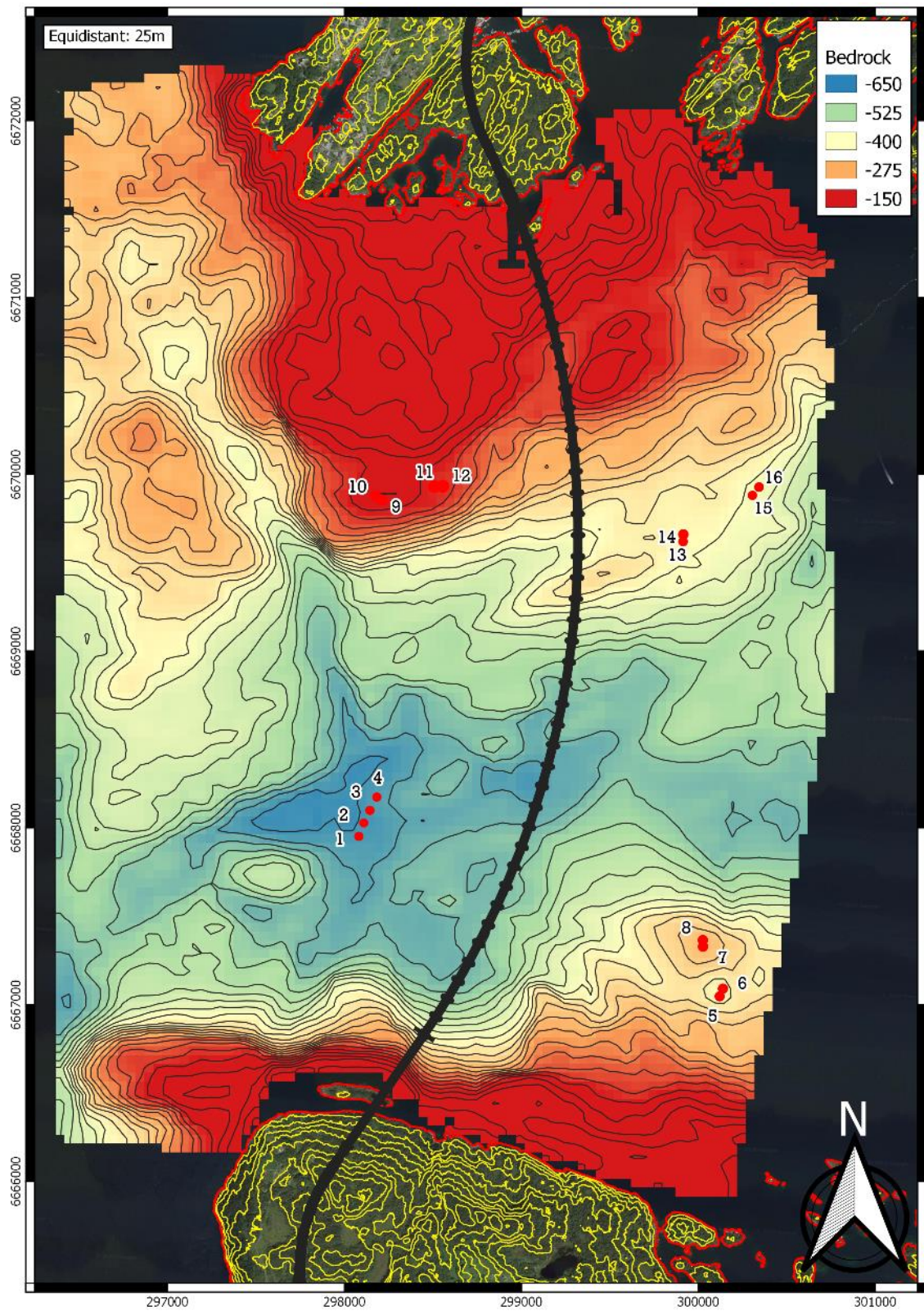


> Figure 4-3 – Calculated bedrock based on measured bathymetry and isopach.

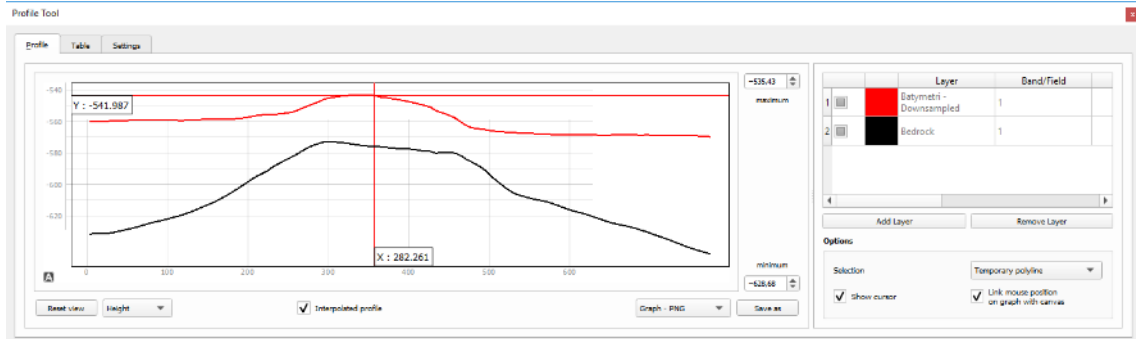


> Figure 4-4 – Profile view with seabed and calculated bedrock shown in QGIS.

## 4.2 Coordinate system

Most of the figures in this document are given with the following coordinate system:

Projection: UTM

Zone: 32N

Datum: EUREF89

Certain drawings are given in NTM projection for increased accuracy, as it's specified in the design basis for Bjørnafjorden, ref. [2].

Projection: NTM

Zone: 5

Datum: EUREF89

## 4.3 Soil conditions

Where soil is present, slightly overconsolidated clay is assumed. This is based on measured and derived parameters, ref. [9]. The clay is assumed to be homogeneous as the interpreted parameters do not verify specific layering of the soil. In-situ geotechnical data and soil samples are only collected at 5 locations, all of them taken in the central flat seabed basin.

> Table 4-1 Summary of representative soil parameters ref. [10].

z (m)	w (%)	$\gamma$ (kN/m <sup>3</sup> )	$\gamma_s$ (kN/m <sup>3</sup> )	$I_p$ (%)	FC (%)	CC (%)	OCR (-)	$S_t$ (-)	$S_{uD}/S_{uC}$ (-)	$S_{uE}/S_{uC}$ (-)
0 - 46	70 - 41	15.7 - 18.0	27.3	35	96	50	3.6 - 1.2	4	0.75	0.60

Note that the soil density increases linearly with depth. As a simplification a constant value will be used in calculations. In most cases 16 kN/m<sup>3</sup> will be used as an average. In special cases with deep failure zones the value may be increased and vice versa for shallow failure zones.

Additionally, CPTU results have been used to estimate undrained shear strength profiles with depth. In the design basis for mooring and anchor, ref. [5] it is stated that the characteristic undrained shear strength shall be taken as the mean value, accounting for soil variability. The mean characteristic shear strength is here taken as the average of the representative low and high estimates and reduced with 10% to account for variabilities. The mean characteristic shear strength will be used both for holding and penetration calculations, and for stability calculations.

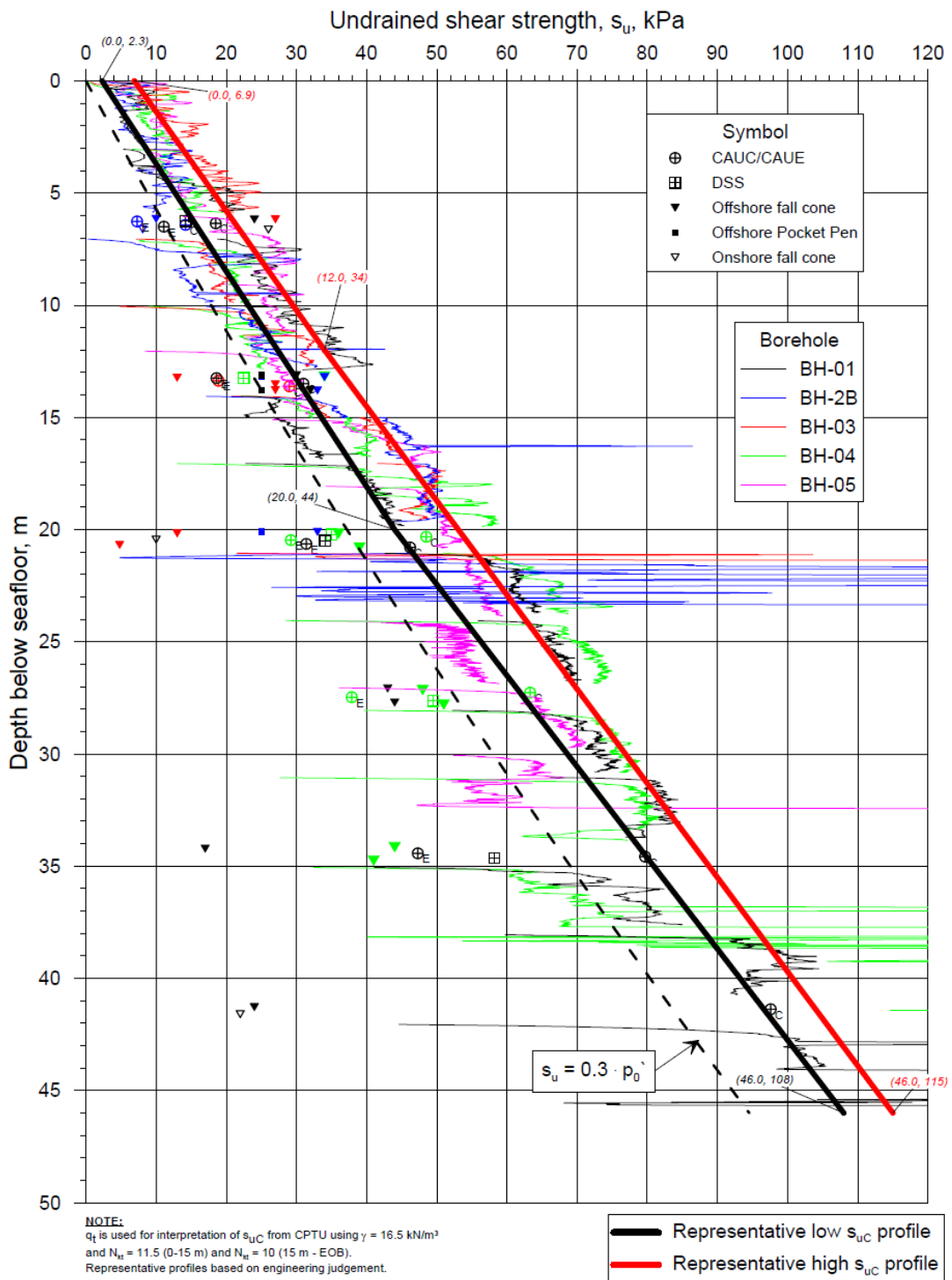


> Figure 4-5 - Active shear strength profiles with depth, ref. [11].

We are informed that supplementary soil investigations are performed and finished in 2019. The results from the investigations are not yet available. We are informed by the Client that the results confirm that clay is present in the slopes down to the central basin, and that the shear strength may be lower in the depth than assumed based on the introductory investigations. This is however not taken into account in the current calculations.

## 4.4 Softwares

### GIS TOOLS:

- QGIS 3.4.4
- SAGA GIS 2.3.2
- GRASS GIS 7.4.4
- Autodesk Civil 3D 2019

QGIS has mostly been used to compile together the different GIS data, file conversion and for map creation and presentation. For processing of raw GIS files, SAGA has been utilized. The software also allows for 3D presentation which has been used to visualize the high quality Bathymetry data. Grass GIS has been used to create watershed mapping of the bedrock. The programs are a part of the OSGeo4W and are open source which are freely available online.

Selected parts of the Bjørnafjorden has been exported to Autodesk Civil 3D. Here a terrain and bedrock surface has been generated. Profiles have afterwards been exported to GeoSuite Stability calculations.

### Static and dynamic slope stability calculations:

- GeoSuite V.16 Stability
- Plaxis 2D V.2018.01 with Dynamic VIP license

The limit equilibrium software GeoSuite Stability was initially used for calculating slope stability. Due to low obtained FoS for seismic loadings, Plaxis calculations has also performed both for static and dynamic conditions.

### Holding capacity of suction anchor:

- Plaxis 2D V.2018.01 with VIP license

Plane strain calculations, similarly as described in DNV RP-E303, ref. [6], has been performed in Plaxis 2D.

### Ground motion analysis:

- SeismoSignal 2018
- SeismoMatch 2018

A trial version of the SeismoSignal and SeismoMatch has been used for inspecting and analyzing the ground motions provided by NORSAR, ref. [12]. SeismoSignal has primarily been used to view the frequency content, pseudo-velocity and pseudo-displacement.

SeismoMatch has been used to compare the elastic response-spectra for the different ground motions together with the response spectra for Ground type A given in NS-EN 1998, ref. [13].

## 4.5 Seismic loads

The  $PGA_{2750Yr}$  calculated by NORSAR is  $1.30 \text{ m/s}^2$ , ref. [12], while according to Eurocode 8, ref. [12], it is  $1.33 \text{ m/s}^2$ . This was used in the previous calculations of Multiconsult and NGI and will therefore be used for pseudo-static slope stability. Furthermore, it's assumed that the elastic response analysis calculated in the previous phase is still valid and will be utilized where deemed relevant. The results from the elastic response analysis is presented in the table below where  $S_e = PGA \cdot S \cdot \eta$ , and  $\eta = 1.0$  (i.e. 5% viscous damping assumed).

> Table 4-2 Maximum accelerations from elastic response analysis, ref. [14].

Profile depth	$S_e$
[m]	[ $\text{m/s}^2$ ]
0 (Ground type A)	3.32
9	3.72
16	3.76
26	3.32
36	3.49

For the dynamic slope calculations, the time series provided by NORSAR, ref. [12], will be utilized. Since the recurrence period was set to 10.000 years, the provided time series has been modified as described in Appendix B. Only the earthquakes with vertical measurements will be used in the analysis, i.e. Whittier Narrows main shock, Whittier aftershock and Sierra Madre. A summary of the earthquake details provided by NORSAR are given in the table below.

> Table 4-3 Earthquake details for the ground motions provided by NORSAR, ref. [12].

Earthquake Name	Date	Hour	Min	Lat	Lon	Depth	Mag	Distance	Station	lat	lon	Chan	Orient
Whittier Narrows main shock	01.10.1987	14	42	34.0493	-118.081	15	6.1	20	Mt Wilson	34.224	-118.057	1	90
												2	up
												3	0
Whittier aftershock	04.10.1987	10	59	34.06	-118.104	13	5.3	19	Mt. Wilson	34.224	-118.057	1	90
												2	up
												3	0
Sierra Madre	28.06.1991	14	43	34.2591	-118.001	12	5.6	6	Mt. Wilson	34.224	-118.057	1	90
												2	up
												3	0
Chamoli aftershock	28.03.1999	19	36	30.315	79.387	10	5.4	15	Gopeshwa	30.24	79.2	1	20
												2	290



## 5 GEOHAZARD AND SLOPE STABILITY

### 5.1 Overall screening

The data provided by DOF SubSea, as described in Chapter 4.1, is given as a point cloud in .xyz file format. It has a resolution of 4 pixels per square meter. However, certain steep areas lack the specified resolution. Due to the large file size, the high-quality data is imported and handled in SAGA GIS. In most cases the derived maps are down sampled to 5 m x 5 m raster map to match the Isopach measurements and afterwards exported to QGIS.

By combining the bathymetry with hill-shading one can easily view the subsurface of Bjørnafjorden. An example of this is shown in Figure 5-1. The colors in the figure represent the elevation where purple being the deepest point and green being the highest point.

From the 3D model one can easily observe previous landslides that has occurred. In the figure below one can observe several scars from landslides, dimples in the subsurface and bedrock at the top. This information has been used to evaluate possible anchor sites with regards to run-out challenges, locate bedrock and possible issues with respect to anchor operation and installation.

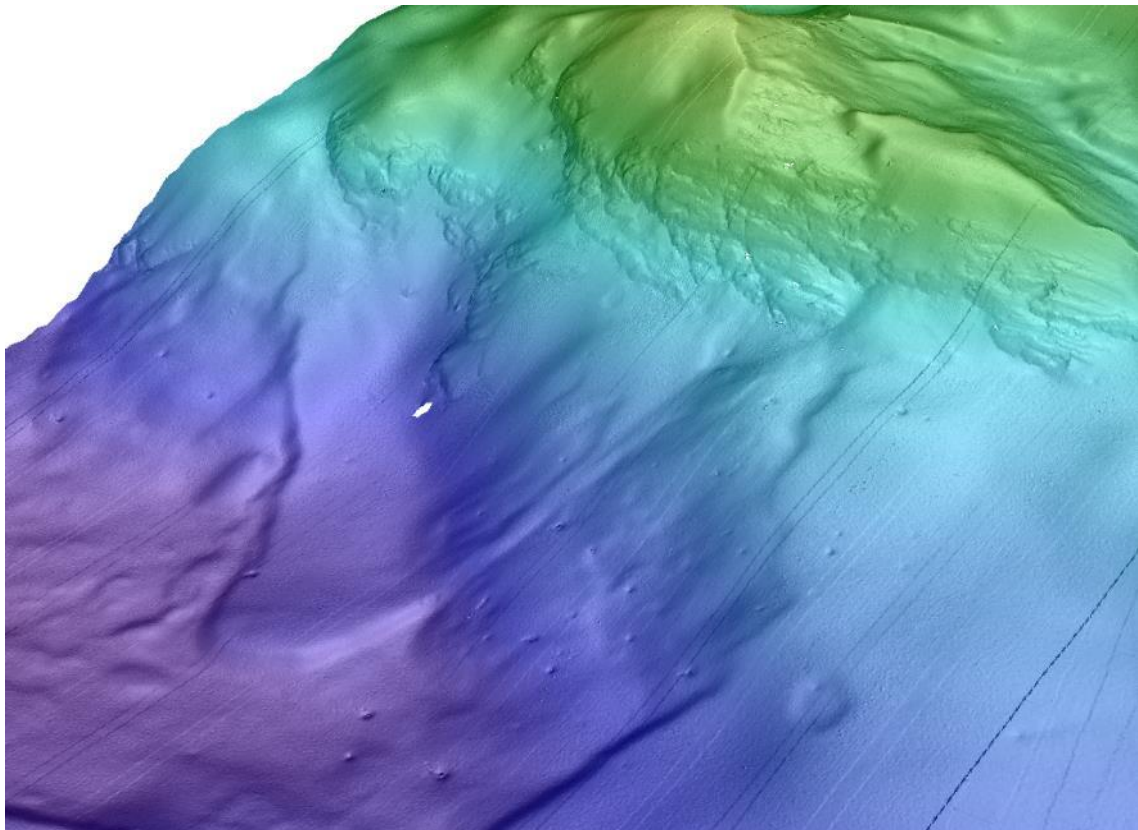


> Figure 5-1 High quality (4px per 1m<sup>2</sup>) 3D representation of bathymetry with hillshading.

A map showing the slope angle has often been utilized for geohazard and anchor site evaluation. The coloring is set such that angles below  $5^\circ$  are shown in beige and slope angle over  $45^\circ$  are shown in black. In between the color is from orange to dark purple. The benefit of this map is that bedrock and landslide debris can easily be viewed, as shown in Figure 5-2. It's also beneficial with respect to anchor site evaluation since most anchors of interest requires a relatively flat seabed.

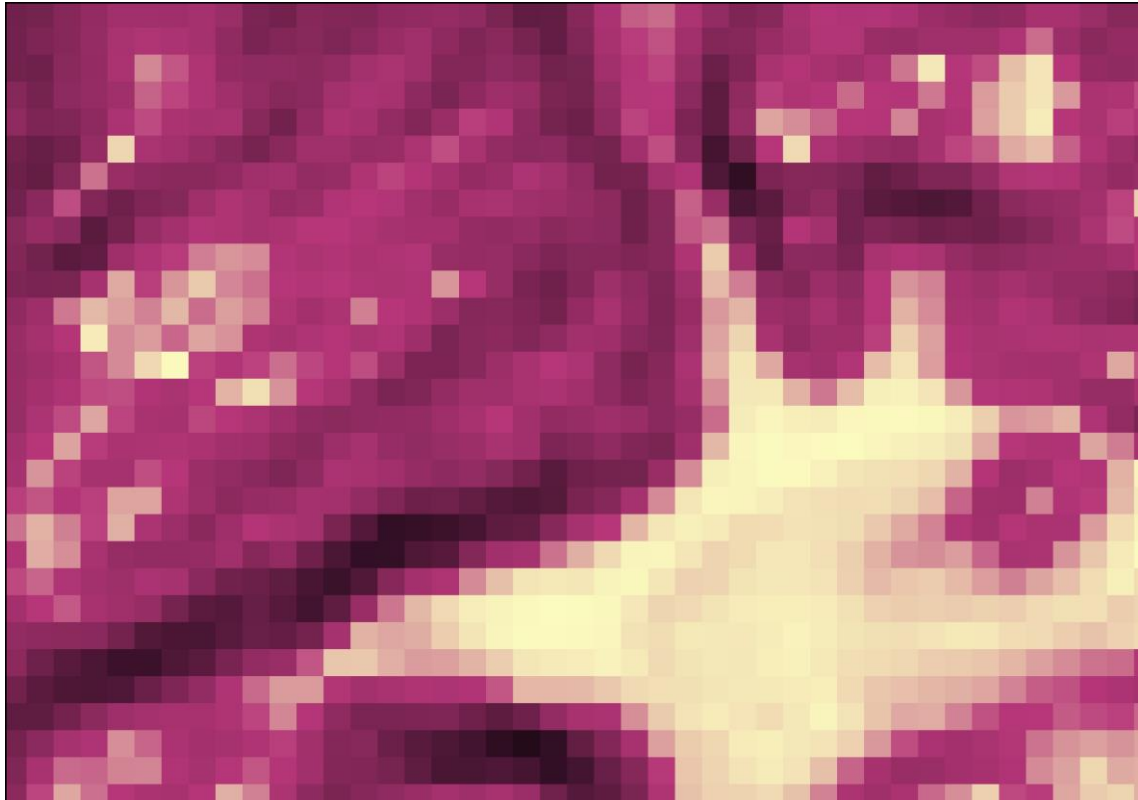


> Figure 5-2 Map of slope angle at the basin of Bjørnafjorden.

The figure above shows a close-up of the basin in Bjørnafjorden. The debris of a major landslide with ploughing depth of approximately 15 m, can be observed in the middle of the fjord, and minor debris are also visible in the north and to the west. An acoustic profile from Geoteknikkdagen 2017, ref. [15], is shown in Figure 5-3 and shows a horizontal soil layering, which is typical for Norwegian Fjords. Based on the isopach the sediment thickness is up to 80 m and on average about 60 m.

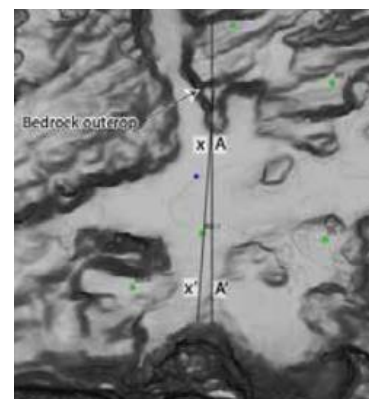
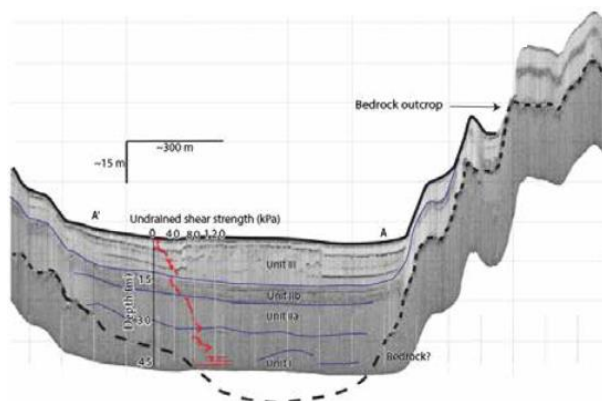


> Figure 5-3 Acoustic profiles in North-South direction in the basin, ref. [15].

Gravity core has been taken in front of the slide lobe and a summary is shown below in Figure 5-4 and is more thoroughly described in Geoteknikdagen 2017, ref. [15]. The samples have been analyzed with the goal of determining the frequency of slope failures and their likely ploughing depths. The interpretations show that more than one slide has occurred over the last 3850 years (estimated). It's also uncertain whether there have been several small landslides or one big landslide in sediment unit B. Considering an earthquake with a 2750-year recurrence period, one cannot rule out the possibility of future landslides. It's however uncertain how large the impact force will be and the likely ploughing depth. Since the soil is soft and the depth to bedrock is large, we assume that it may be possible to achieve sufficient capacity during and after landslides by ensuring that the anchors are deeply embedded.

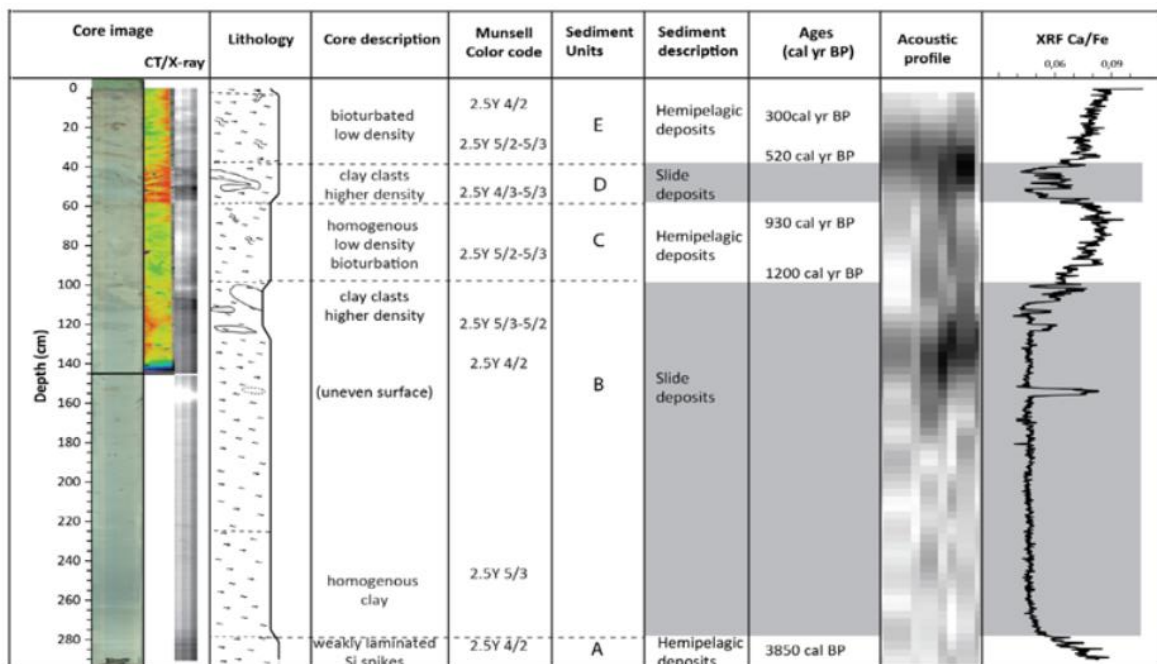


> Figure 5-4 Details and interpretation from gravity core samples.

Several hazard maps have been developed by NGI in the previous phase, ref. [10]. These have been used for preliminary anchor site evaluation. Most of the geohazard calculations are based on an assumption of infinite slope with undrained shear failure with linearly increasing weight and shear strength. It's observed that the results are closely tied to the slope angle both for the calculated static FoS and the estimated maximum transient shear strain for an earthquake with an annual exceedance probability of 2750 years recurrence period. This is due to increasing shear strength and increasing in-situ stress with depth. Figure 5-5 and Figure 5-6 indicates that several areas are unstable.

A similar static FoS has been calculated by OON using SAGA GIS. Drained, infinite slope failure is assumed with a constant value of friction angle, saturation, density and cohesion. The isopach is also included in the calculations, however the software does not distinguish between soil and rock, i.e. showing poor slope stability at steep areas where there is bedrock. Note that the friction angle has been scaled so that the FoS by OON matches the one calculated by NGI and is thus not representative for drained analysis. The purpose of the calculation was to extend the static FoS to the area that was measured by DOF SubSea in 2018.

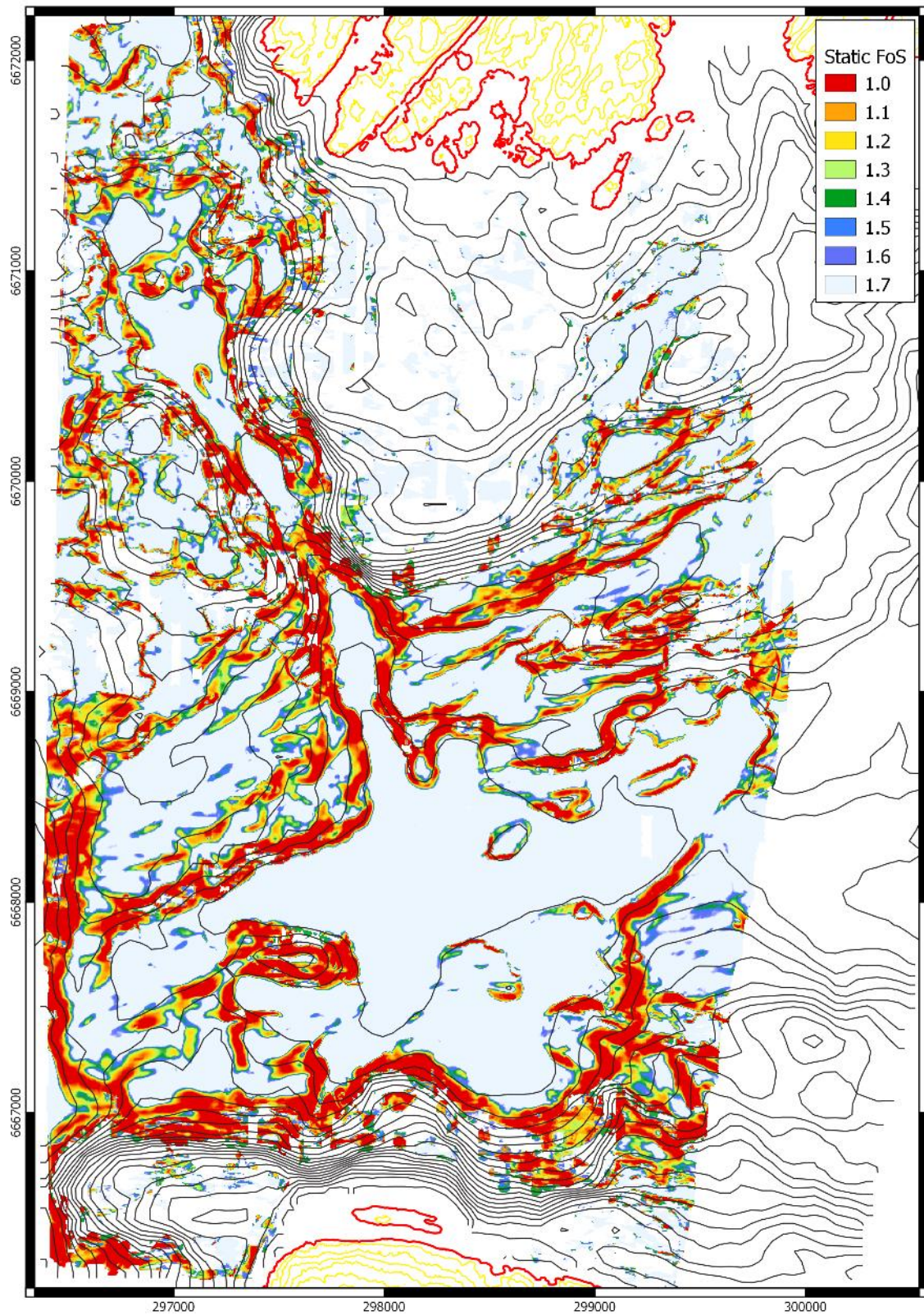


> Figure 5-5 Static Factor of Safety calculated by NGI, ref. [10].

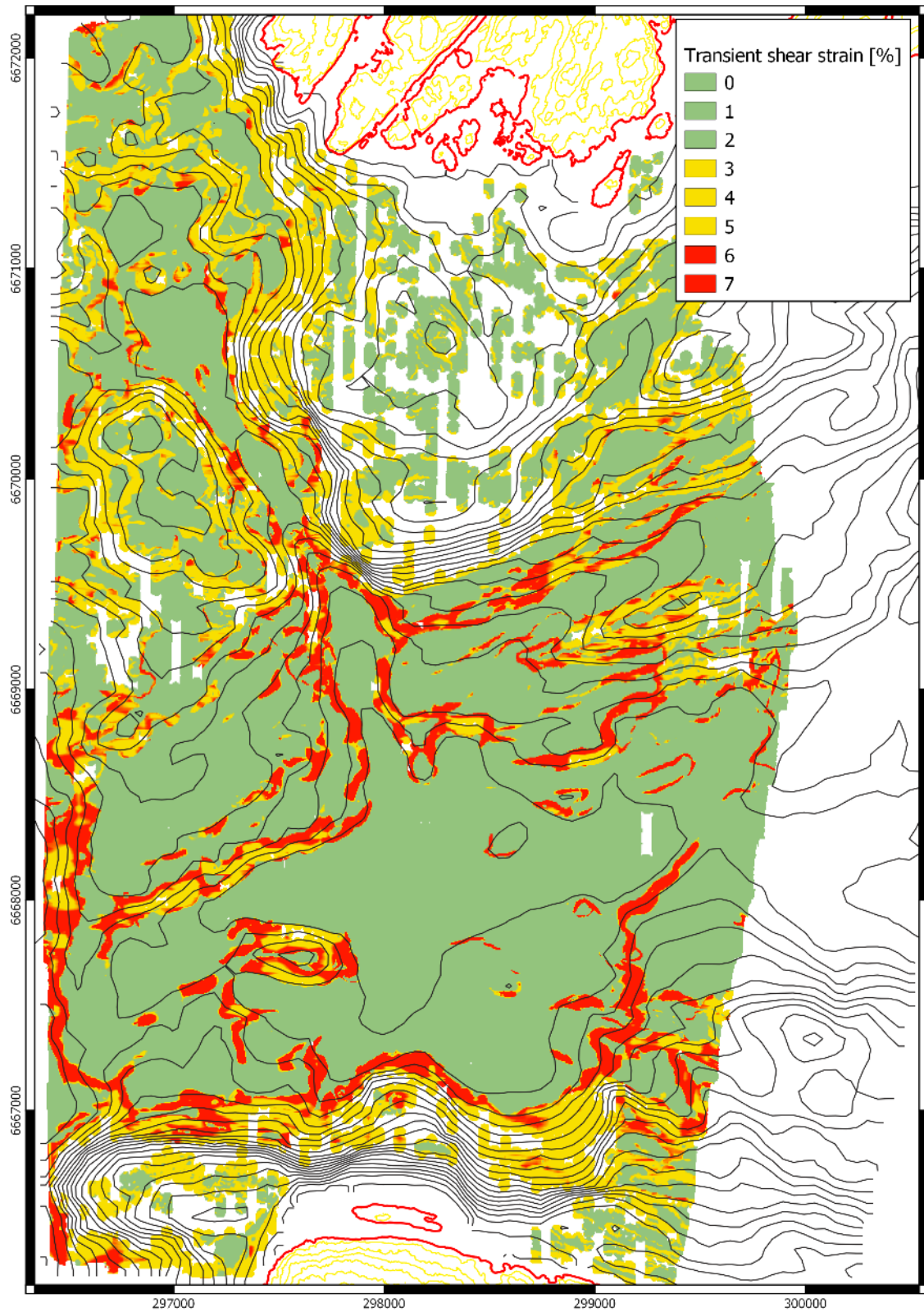
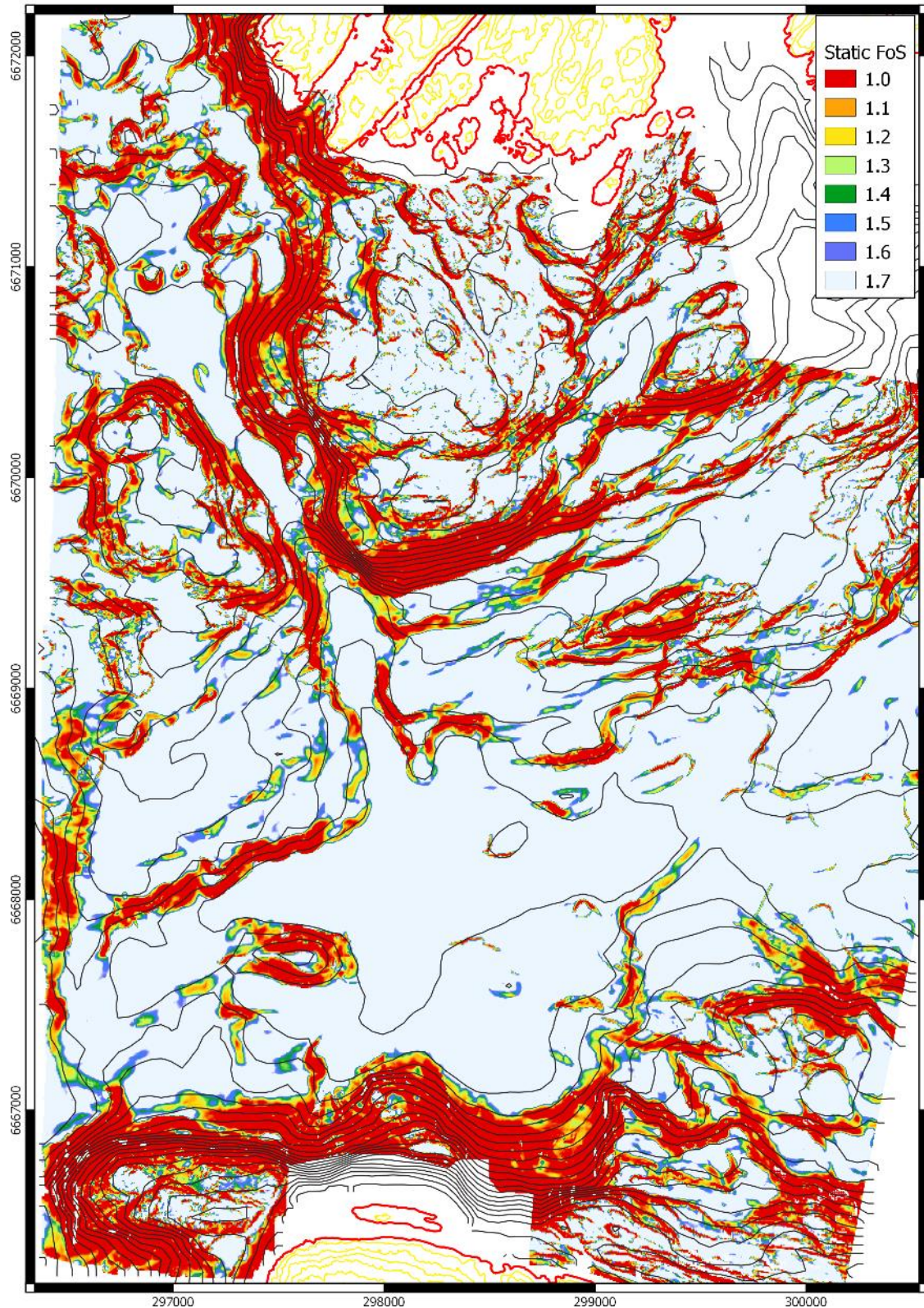


> Figure 5-6 Maximum transient shear strain [RP=2750 years] calculated by NGI, ref. [10].



➤ Figure 5-7 Static Factor of Safety calculated by OON using SAGA GIS. Friction angle is scaled to give similar results as shown in Figure 5-5.

Based on required holding capacity and installation requirements, certain criteria for anchor location has been defined. The proposed criteria given in the design basis for Mooring and anchor, ref. [5], has been used as a starting point. The maximum seabed slope is here restricted to  $7.5^\circ$  for suction and plate anchors and the maximum soil thickness for gravity anchors is restricted to 5 m. Furthermore, a distinction is made between areas with more than 15 m soil thickness, since here higher holding capacity can be achieved by embedding the anchor deeper.

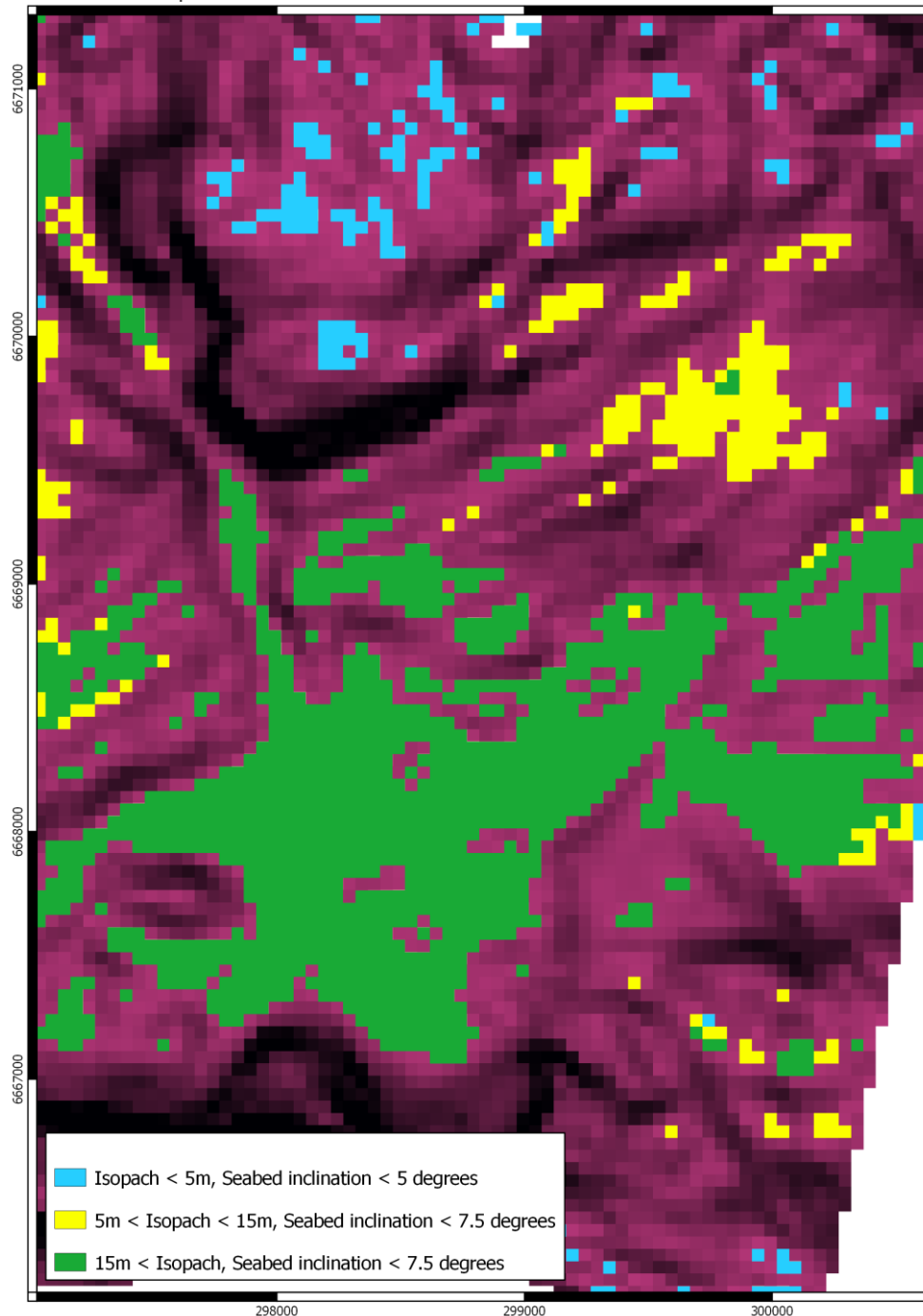


> Figure 5-8 Anchor criteria used when selecting and evaluating anchor locations.

## 5.2 Static global slope stability

### 5.2.1 GeoSuite Stability

The global slope stability is checked for what is regarded to be the most critical slopes near the anchor locations. See Figure 5-9. For anchor locations 7 to 12 no critical slopes are considered to affect the anchors. Stability calculations are carried out for Profiles shown in the figure below. Calculations for Profile G4 A-A are valid for a preliminary position of anchor 13 and 14.

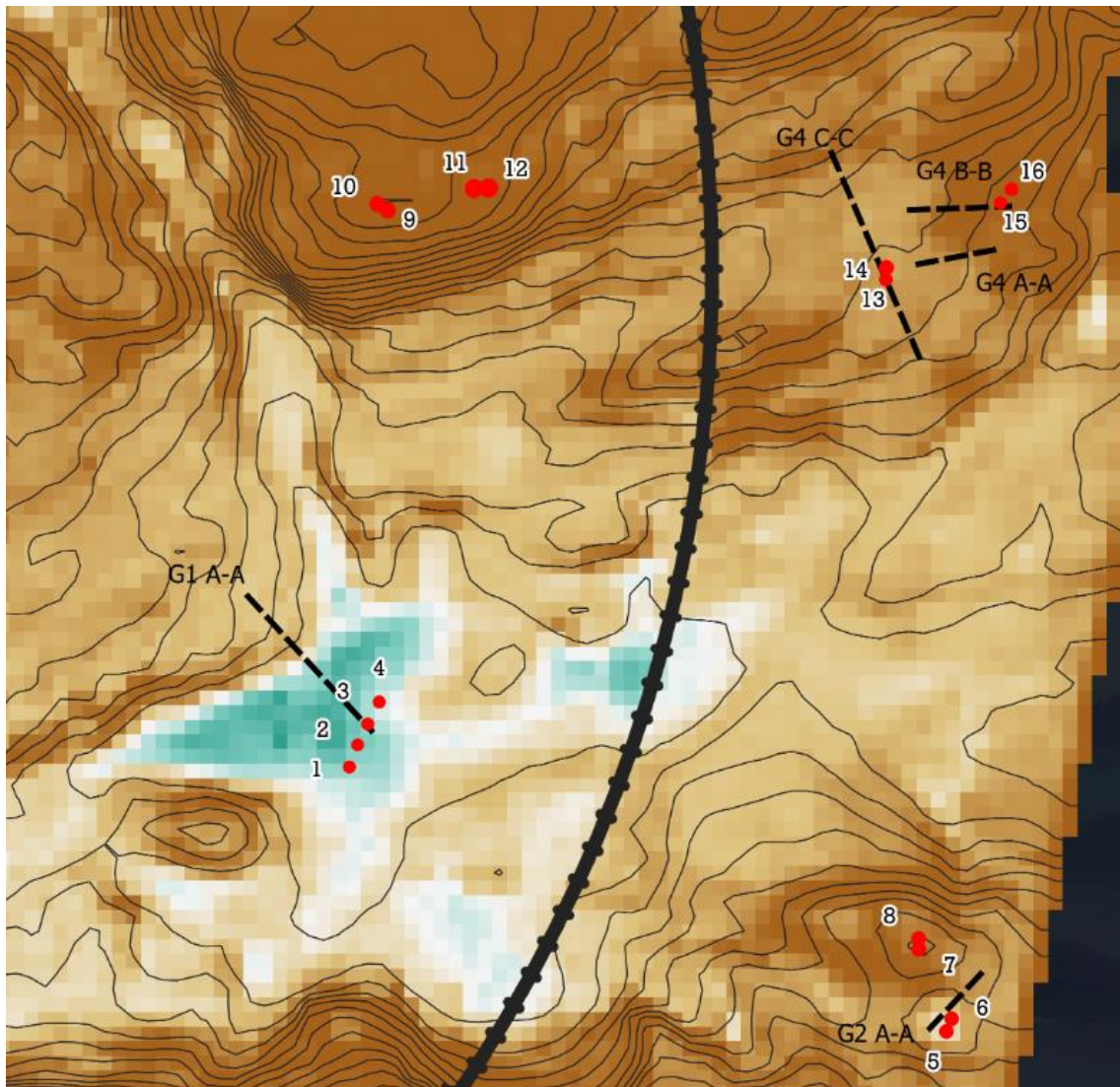


> Figure 5-9: Overview showing the profiles calculated in GeoSuite stability. The map show contours every 10 m, and the Isopach map is plotted in the background.

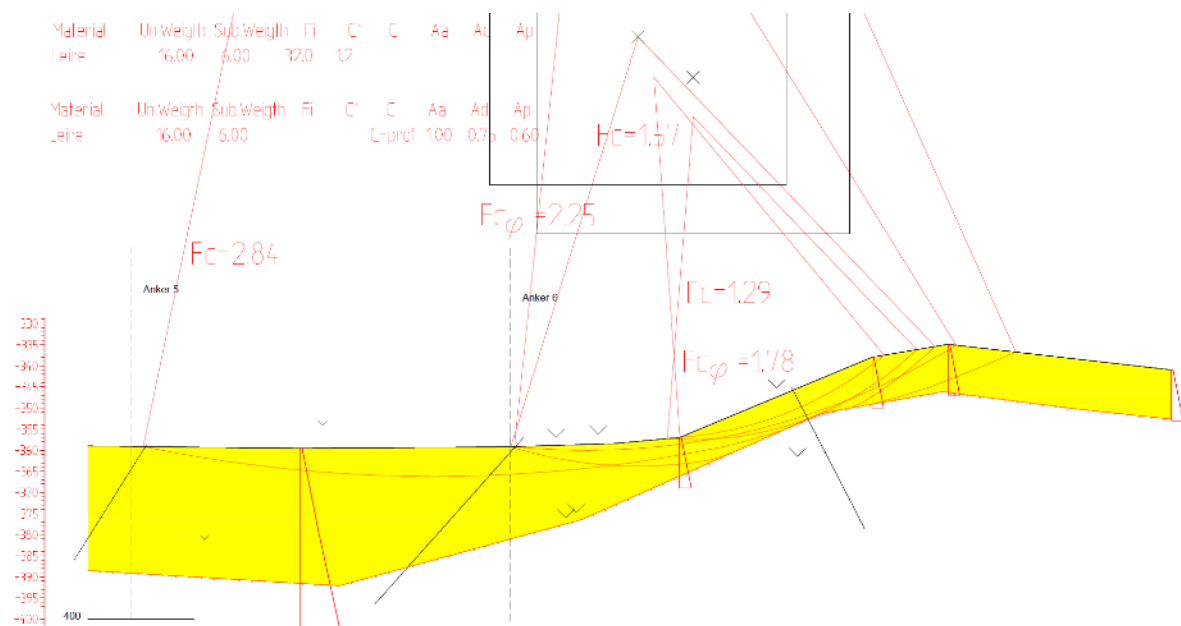
The stability calculations are performed with both undrained and drained parameters. Calculations are carried out with soil parameters as stated in chapter 4.3. The mean characteristic compression shear strength, reduced by 10 % to account for variabilities, are used for stability calculations:



$$S_{uC,avg}(z) = 0.9 \cdot \frac{S_{uC,high} + S_{uC,low}}{2} = \begin{cases} 4.14 + 1.96 \cdot z & \text{for } z < 12m \\ 3.52 + 2.01 \cdot z & \text{for } 12m \leq z < 20m \\ 0.15 + 2.18 \cdot z & \text{for } 20m \leq z \leq 46m \end{cases}$$

Furthermore, the ratio between the DSS undrained shear strength and the undrained shear strength in compression is  $s_{uD}/s_{uC} = 0.75$ , and the ratio between the undrained shear strength in extension and the undrained shear strength in compression is  $s_{uE}/s_{uC} = 0.60$ . For drained calculations the friction angle is set to  $32^\circ$  and the attraction to 2 kPa, which is the same as cohesion equal to 1.25 kPa. A constant value of 16 kN/m<sup>3</sup> is used for soil density in the stability calculations.

Results from the static GeoSuite Stability calculations for the profiles in Figure 5-9 are shown in Appendix C. In Figure 5-10, the results for profile G2 A-A are shown. Anchor locations are illustrated with vertical dashed lines in the profiles. In every profile, the safety factors for the most critical failure surfaces are shown. In addition, the lowest found safety factor for failure surfaces that reach the anchor locations are shown. For profile G2 A-A, the most critical failure surface in the profile has a safety factor of 1.29, while the lowest safety factor for failure surfaces that reach the anchors is found to be 1.57. See Figure 5-10. The undrained condition gives the lowest safety factors.



- > Figure 5-10: Calculated static slope stability for Profile G2 A-A, as shown in Appendix C.2.  $F_c$  is the safety factor for undrained analysis, and  $F_{c\phi}$  is the safety factor for drained analysis.

> *Table 5-1: Calculated factor of safety for the undrained static slope stability*

Profile	Appendix	Calculated safety factor for the most critical failures surfaces in the profile, $F_c$	Lowest calculated safety factor for failure surfaces that reach the anchor locations, $F_c$
G1 A-A	C.1	1.23	2.32
G2 A-A	C.2	1.29	1.57
G4 A-A	C.3	1.72	-
G4 B-B	C.4	2.39	-
G4 C-C	C.5	1.14	2.24

> *Table 5-2: Calculated factor of safety for the drained static slope stability*

Profile	Appendix	Calculated safety factor for the most critical failures surfaces in the profile, $F_{c\phi}$	Lowest calculated safety factor for failure surfaces that reach the anchor locations, $F_{c\phi}$
G1 A-A	C.1	1.76	4.73
G2 A-A	C.2	1.78	2.25
G4 A-A	C.3	2.18	-
G4 B-B	C.4	2.69	-
G4 C-C	C.5	2.22	6.27

Table 5-1 summarize the calculated safety factors for the undrained static slope stability.

As stated in Table 3-1, the design requirement for global slope stability is  $\gamma_m \geq 1.4$  for both drained and undrained analysis. For failure surfaces that reach the suggested anchor locations, the calculated factor of safety is acceptable for all the slopes considered. However, the calculated safety factors for the most critical failure surface in the profiles, are below the requirements for global slope stability for profile G1 A-A, G2 A-A, and G4 C-C. Thus, it is necessary to evaluate if run-outs from these failure surfaces can affect the anchors.

The calculated safety factors for the drained static slope stability are summarized in Table 5-2. The calculated safety factors for the drained static slope stability are well above the requirements for all the slopes considered.

### 5.2.2 Plaxis slope stability

In conjunction with dynamic slope performance, static slope stability has been calculated for 15 different profiles in Plaxis 2D. Thus, the same Plaxis models is used for dynamic and static analysis with different loading and boundary conditions. The profiles are shown in Figure 5-11.

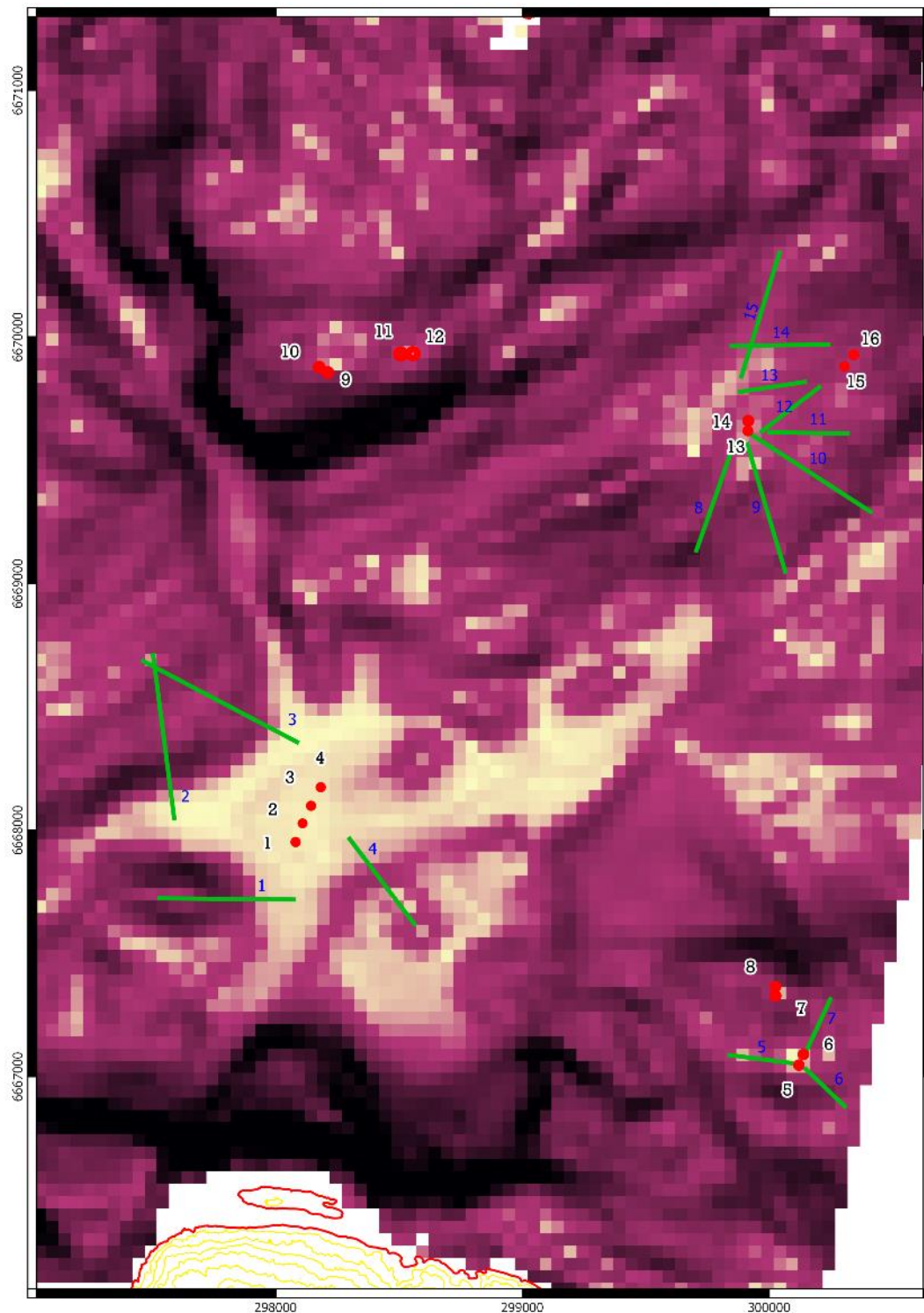


> Figure 5-11 Profiles calculated in Plaxis 2D.

The profiles are taken directly from QGIS with the down-sampled bathymetry data and the estimated bedrock. The profiles are afterwards smoothed out by removing excess points for improved meshing. Special care is taken at the boundaries which is described in 5.3.2.

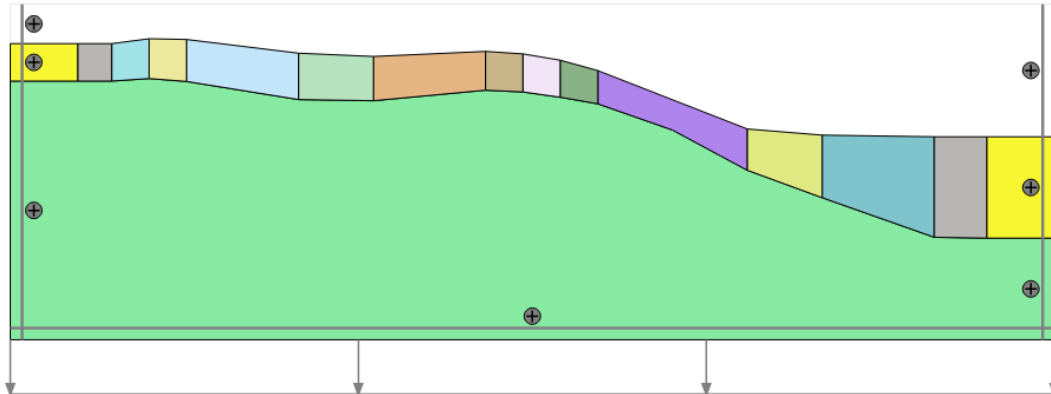


> Figure 5-12 Model of profile 7 with undrained material.

Property	Unit	Value
<b>Material set</b>		
Identification		Drained Clay
Material model		Mohr-Coulomb
Drainage type		Drained
Colour		RGB 228, 216, 161
Comments		
<b>General properties</b>		
$\gamma_{\text{unsat}}$	kN/m <sup>3</sup>	16,00
$\gamma_{\text{sat}}$	kN/m <sup>3</sup>	16,00
<b>Stiffness</b>		
$E'$	kN/m <sup>2</sup>	22,40E3
$\nu'$ (nu)		0,4000
<b>Alternatives</b>		
$G$	kN/m <sup>2</sup>	8000
$E_{\text{oed}}$	kN/m <sup>2</sup>	48,00E3
<b>Strength</b>		
$c'_{\text{ref}}$	kN/m <sup>2</sup>	1,250
$\phi'$ (phi)	°	32,00
$\psi$ (psi)	°	0,000
<b>Velocities</b>		
$V_s$	m/s	70,04
$V_p$	m/s	171,6
<b>Advanced</b>		
Set to default values		<input checked="" type="checkbox"/>
<b>Stiffness</b>		
$E'_{\text{inc}}$	kN/m <sup>2</sup> /m	0,000
$\gamma_{\text{ref}}$	m	0,000
<b>Strength</b>		
$c'_{\text{inc}}$	kN/m <sup>2</sup> /m	0,000
$\gamma_{\text{ref}}$	m	0,000
Tension cut-off		<input checked="" type="checkbox"/>
Tensile strength	kN/m <sup>2</sup>	0,000

Drained slope stability is calculated using the elasto-perfectly plastic Mohr-Coulomb. The same material model is also used to generate the in-situ stresses utilizing "Gravity loading" in Plaxis. Since most of the soil is sloping, i.e. increased horizontal stress, the Poisson ratio ( $\nu$ ) is set to 0.4 for increased confining pressure.

The depth is limited by the bedrock, thus a constant soil weight of 16 kN/m<sup>3</sup> is justified and therefor used in the calculations. The strength characteristics is as described in the Design Brief, ref. Appendix A. Zero dilatancy is assumed in the calculations.

Since homogenous soil with depth is assumed, the stiffness is of little importance when regarding critical failure modes. The shear stiffness is for simplification set to 8000 kPa such that the possible heaving which occurs from changing material model is minimized. The material parameters are summarized in Figure 5-13.

After "Gravity loading" a NIL-step is performed both for drained and undrained material, thereby allowing for plastic redistribution of stresses. The slope stability is afterwards calculated using the c-phi-reduction method in Plaxis. The "phases" used in calculation are presented in Figure 5-14.

> Figure 5-13 Drained material parameters used in calculations.

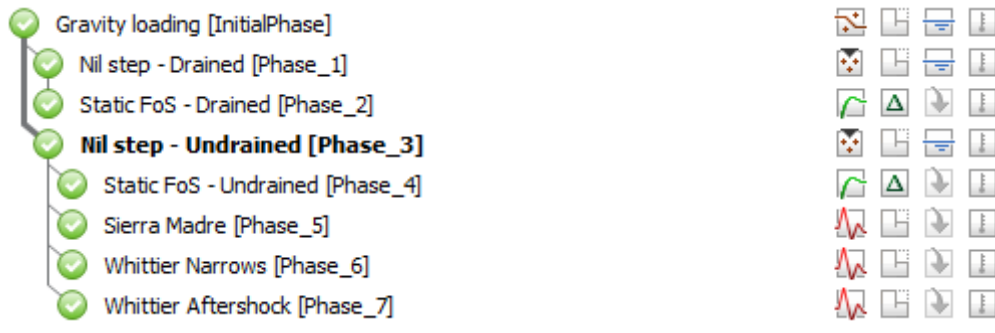


> Figure 5-14 Phases used for static and dynamic slope stability in Plaxis 2D.

Property	Unit	Value
<b>Material set</b>		
Identification		Clay_1
Material model		NGI-ADP
Drainage type		Undrained (B)
Colour		RGB 161, 226, 232
Comments		
<b>General properties</b>		
$\gamma_{unsat}$	kN/m <sup>3</sup>	16,00
$\gamma_{sat}$	kN/m <sup>3</sup>	16,00
<b>Stiffness</b>		
$G_{ur}/s_u^A$		200,0
$\gamma_f^C$	%	3,300
$\gamma_f^E$	%	10,00
$\gamma_f^{DSS}$	%	5,000
<b>Strength</b>		
$s_{u,ref}^A$	kN/m <sup>2</sup>	4,000
$s_{u,C,TX}/s_u^A$		0,9900
$\gamma_{ref}$	m	-331,7
$s_{u,inc}^A$	kN/m <sup>2</sup> /m	2,000
$s_{u,P}/s_u^A$		0,6000
$\tau_0/s_u^A$		0,3000
$s_{u,DSS}/s_u^A$		0,7500
<b>Advanced</b>		
$\nu'$ (nu)		0,3000

> Figure 5-15 Undrained material parameters used in calculations.

A drained, linear elastic material is used to model the bedrock. The unit weight is set to  $27 \text{ kN/m}^3$ ,  $\nu = 0.2$  and the shear stiffness  $G = 4.0E6$ . The shear modulus is chosen such that the shear wave velocity of the bedrock is approximately 1200 m/s. It's assumed that the bedrock is intact and no increasing stiffness with depth.

The undrained material is modeled using the standard NGI-ADP in Plaxis. The failure strains are calibrated using soil test and compared with lab-results, as presented in Figure 5-16. The depth 13.5 m was primarily used in calibration for CAUC and CAUE. The DSS failure strain was chosen in-between  $\gamma_f^C$  and  $\gamma_f^E$  to fit better at 20 m. The large deviation in the deeper soil test is believed to be caused by incorrect consolidation stress, ex. 192.4 kPa instead of 174 kPa at 27.27 m.

For simplicity the active undrained shear strength is modelled as  $S_u^C = 4 + 2 \cdot z$ . By using one soil layer one avoids issues with respect to meshing & calculations errors.

The hidden parameter 'verticalinc' in Plaxis is utilized, and together with an appropriate  $\gamma_{ref}$  one can ensure that the undrained shear strength varies linearly with depth from terrain as shown in Figure 5-17. The ADP factors are set to the interpreted values given in ref. [11]. The mobilization is set low such that plastic deformation is forced to occur during the NIL-step when changing materials. The idea behind this is to simulate approximately NC-clay in the model.

The stiffness ratio is defined with respect to cyclic degradation caused by earthquake and is further described in 5.3.2. Since the soil is assumed to be homogenous, the stiffness is of little importance when calculating critical failure mode.

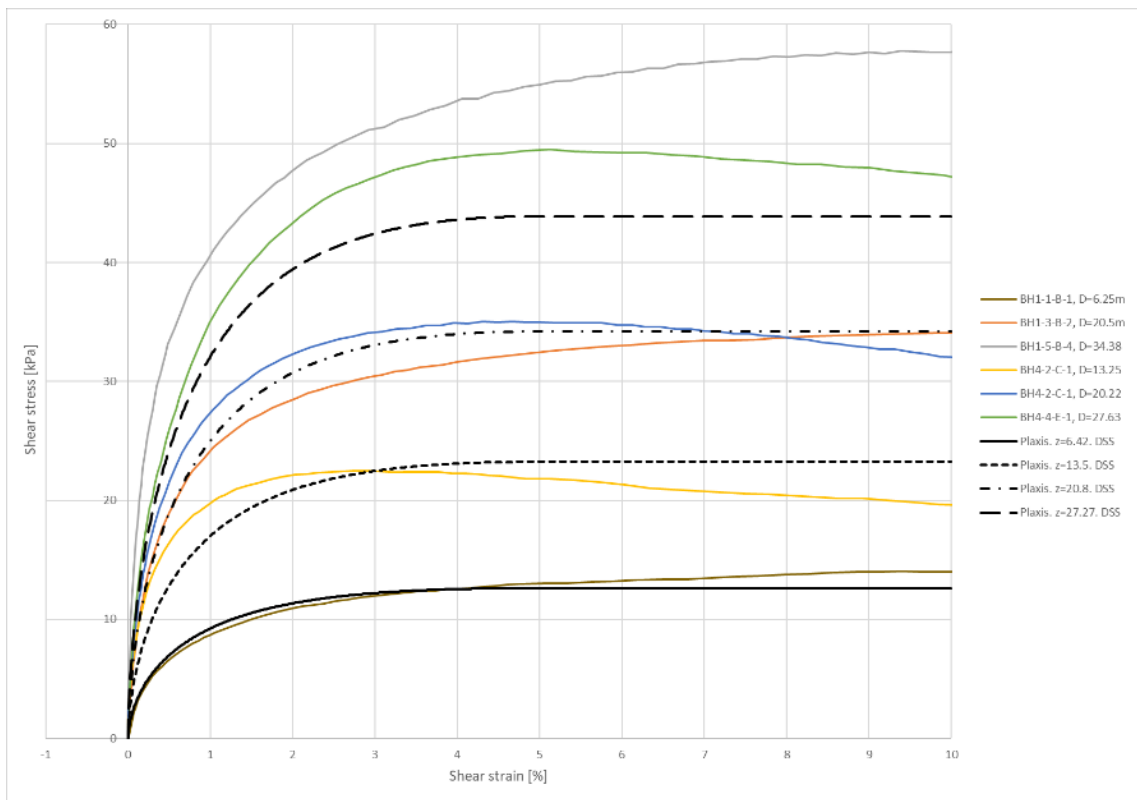
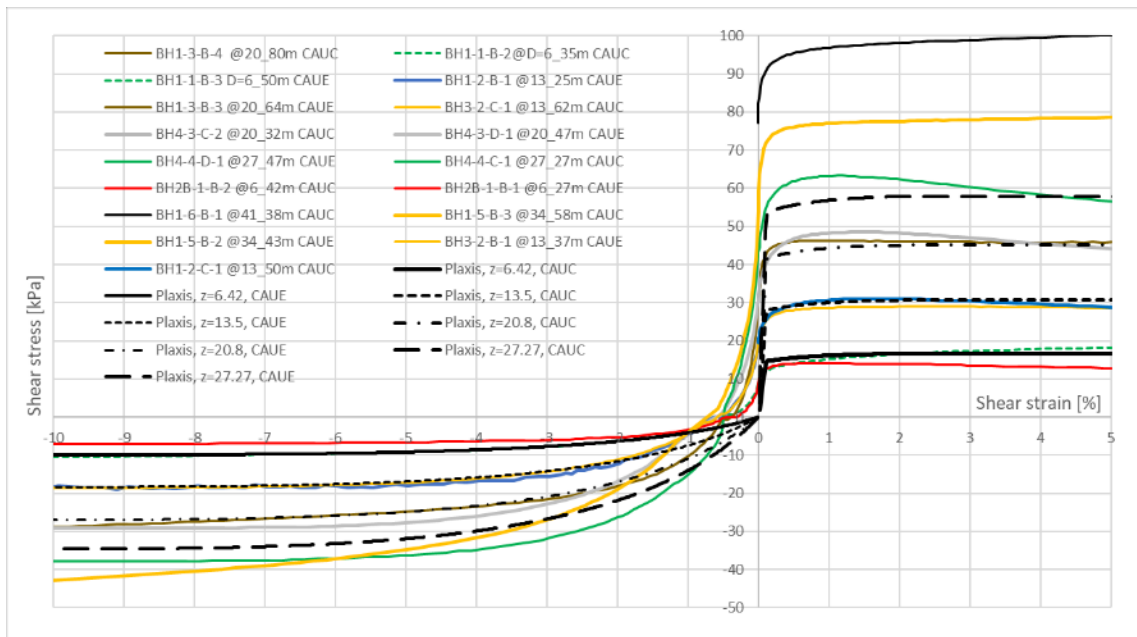


> Figure 5-16 Calibration of shear strain failure for NGI-ADP.

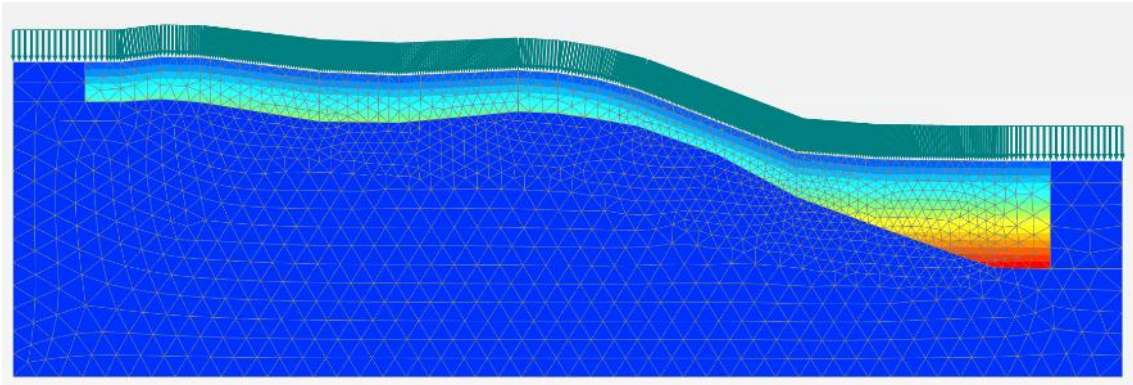


> Figure 5-17 Increasing undrained shear strength from terrain,  $S_u^c$  from 4 to 64 kPa.

Typical slope stability is presented in Figure 5-18 and Figure 5-19. It's observed that the undrained failure mode is often deeper than for drained conditions, which is to be expected. Furthermore, the failure mode is often limited by the bedrock, thereby influencing the failure mechanism.

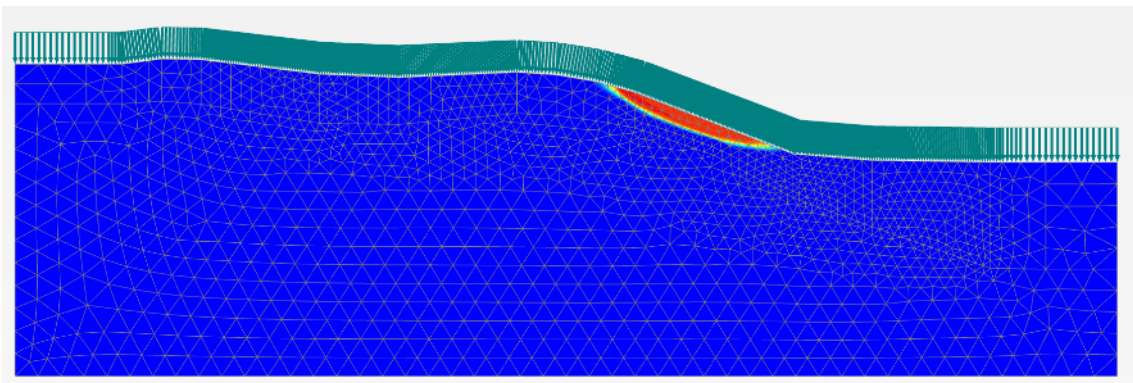


> Figure 5-18 Critical slope stability for drained conditions,  $FoS = 1.829$

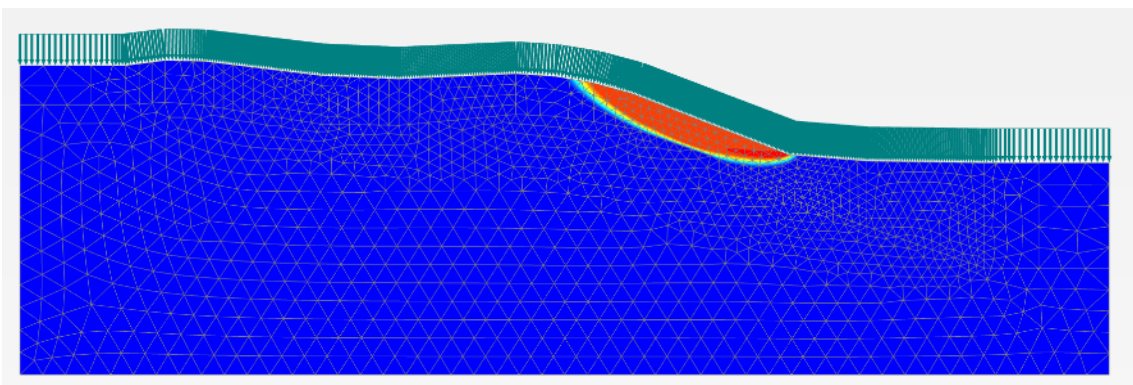


> Figure 5-19 Critical slope stability for undrained conditions,  $FoS = 1.329$

The results from static slope stability are summarized in the table below. The drained safety factors are generally higher than the undrained safety factors. Since none of the anchors are placed directly in the vicinity, and no additional measures are planned for the slopes, the only likely trigger mechanism at this depth is assumed to be seismic loadings, which is evaluated in the next section.

For some of the profiles, additional failure modes have been calculated to determine whether there are other (independent) critical shear surfaces in the slope. This is done by suppressing the c-phi reduction in the soil clusters where the first failure mode occurs. The idea behind this is to investigate if there are any other failure modes with similar safety factor in the same profile.

> *Table 5-3 Plaxis results of drained and undrained slope failure.*

Profile	FoS of critical failure mode		FoS of second critical failure mode
	Drained	Undrained	Undrained
1	1.316	1.127	-
2	1.288	1.037	1.717
3	1.902	1.318	1.357
4	2.251	1.584	-
5	5.103	3.111	-
6	1.545	1.212	-
7	1.829	1.329	-
8	2.232	1.505	-
9	1.418	1.259	1.346
10	1.285	1.126	1.512
11	1.458	1.274	-
12	1.944	1.603	-
13	1.976	1.730	-
14	1.977	1.625	-
15	2.089	1.539	-

The deviation of the results in Table 5-2 and Table 5-3 are assumed to be caused by using different cross-sections and are therefore deemed acceptable. The results show that several of the slopes does not satisfies the requirement for drained and undrained stability. Although one might obtain higher safety factor from additional soil investigation, it's here assumed to not be the case as indicated by the client, ref. 4.3. Thus, the overall philosophy is that anchors 1-6 and 13-14 are vulnerable to possible landslide debris and should be considered in anchor design.



## 5.3 Seismic slope stability

### 5.3.1 Pseudo-static analysis

Calculations for seismic conditions are carried out with pseudo-static analysis in GeoSuite Stability. Calculations are performed for the profiles shown in Figure 5-9. In the pseudo-static analysis, as presented in [16], seismic loading is defined as additional static loads with a horizontal ( $F_H$ ) and vertical component ( $F_V$ ) defined as:

$$F_H = 0.5 \cdot \alpha \cdot S \cdot W$$

$$F_V = \pm 0.33 \cdot F_H \text{ (put in the most unfavorable direction)}$$

$$\alpha = \frac{\alpha_g}{g}$$

$$\alpha_g = \gamma_I \cdot 0.8 \cdot a_{g,40\text{Hz}}$$

Where:

- 0.5 is the pseudo-static reduction factor
- $a_{g,40\text{Hz}}$  is the ground acceleration on rock at 40 Hz. The acceleration is set as 0.83 m/s<sup>2</sup> based on Figure NA.3(901) in [13] and a return period of 475 years.
- 0.8 is a factor to convert from acceleration at 40 Hz to the peak ground acceleration
- $\gamma_I$  is the importance factor of the structure, which equals 2.0 for seismic class 4 according to Table NA.4(901) in [13]
- S is the soil factor. For seismic soil category E the soil factor,  $S = 1.65$ . Seismic soil category E is chosen based on the  $s_u$  and shear wave velocity  $v_s$  profile, and assuming that its generally 5 to 20 m of soft clay over a stiffer material [13].
- g is acceleration of gravity (9.8 m/s<sup>2</sup>)
- W is weight of the potential gliding soil mass

This gives the following additional static loads components:

$$\alpha_g = 2 \cdot 0.8 \cdot 0.83 = 1.328$$

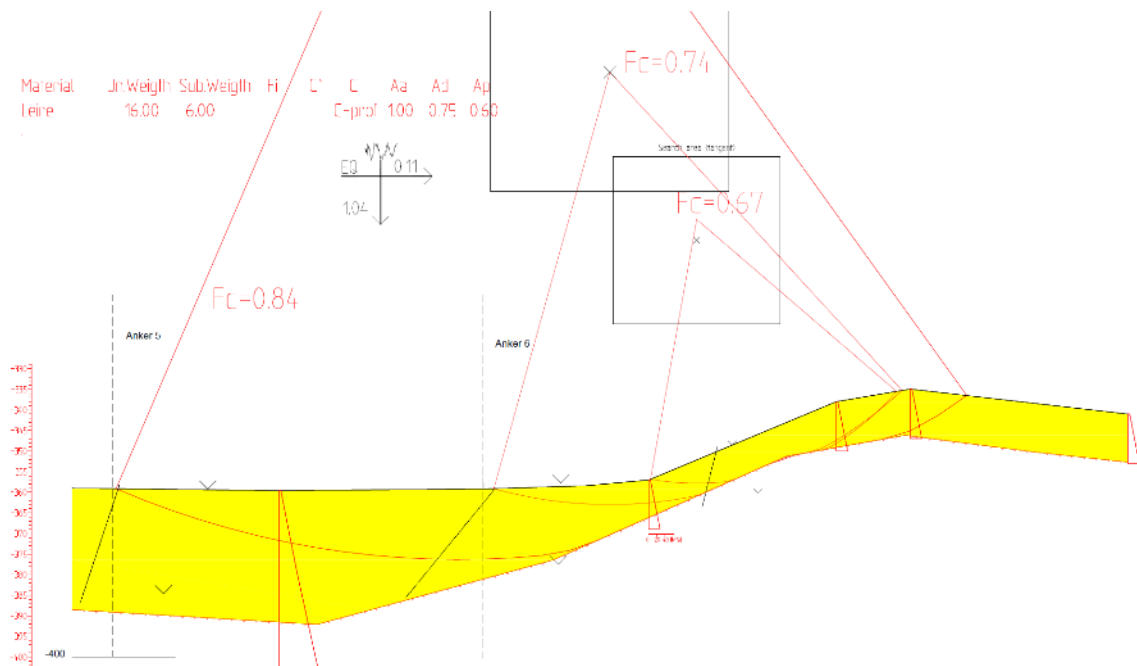
$$\alpha = \frac{1.328}{9.8} = 0.136$$

$$F_H = 0.5 \cdot 0.136 \cdot 1.65 \cdot W = \mathbf{0.11}$$

$$F_V = \pm 0.33 \cdot 0.11 = \pm \mathbf{0.04}$$

The calculated  $F_H$ -factor is the same value as NGI used when calculating 1D infinite pseudo-static slope stability in the initial screening of Bjørnafjorden in report [7].

In the Design Basis [4] the required safety factor for pseudo-static stability is set to be  $\gamma_m = 1.1$  for clays. Results from the pseudo-static stability calculations are shown in Appendix D. The calculations carried out in GeoSuite Stability shows that the required safety factor for pseudo-static stability is far from met. In fact, for all the slopes investigated the calculated factor of safety is below 1.0 for the pseudo-static calculations. In this regard it is important to remember that the calculations carried out are based on a simplified pseudo-static approach to a dynamic problem, and that the calculations are for an earthquake with a return period of 2750 years. A return period of 2750 years corresponds to adding a seismic factor of 2.0 on the  $a_{g,40\text{Hz}}$  value for a 475 year return, as stated by NGI in report [7].



- > Figure 5-20: Calculated pseudo-static slope stability for Profile G2 A-A, as shown in Appendix D.2. The calculated pseudo-static safety factor is far below the requirement of  $F_c = 1,1$ .

As the safety factor for the pseudo-static stability is not satisfactory, it is necessary to perform dynamic analysis to see if the criteria for maximum transient shear strain in the seismic condition can be met.

### 5.3.2 Dynamic analysis

Dynamic slope calculations have been carried out for the same profiles as for static slope stability. Since the profiles are long, special care has been taken when modeling the profiles. As previously stated, excess points on the seabed are trimmed away such that overall seabed profile is kept and thereby reducing the amount of soil clusters.

The NGI-ADP has been used to model the undrained response during earthquake loading. The material parameters are as described in 5.2.2. However, the model cannot simulate hysteresis, i.e. loss of energy with cycles, and is linear elastic upon unloading. Furthermore, the model does not soften with increasing cycles, which is commonly observed in real soils. Since the stiffness ratio can heavily influence the overall response, a sensitivity study is recommended for further verification. A shear modulus 200 times the peak undrained compressive shear strength has been used in model, as suggested by NGI, ref. [10]. Rayleigh damping has also been introduced in the model with the same target damping ratios as was used by NGI in the last phase, i.e. 5% damping at 0.97 and 4.87 Hz. Note that ideally the damping ratio would vary with increasing shear strain.

The boundary conditions are vital to the analysis and extra measures has therefor been taken to improve the calculation. As recommended by Plaxis, the compliant base and free field dampers have been used at the boundaries. This allows for input ground motions at the bottom and traveling waves at the boundary will be absorbed. Note that a drained material is recommended at the boundaries for better wave-absorption, especially with respect to body/p-waves. An undrained soil cluster is placed in-between the drained soil and the profile to act as a buffer zone. The top surface is also flat to reduce the risk of singularities due to compatibility issues. Default coefficient are used for the viscous dampers at boundaries. The profiles are shown in Figure 5-11.

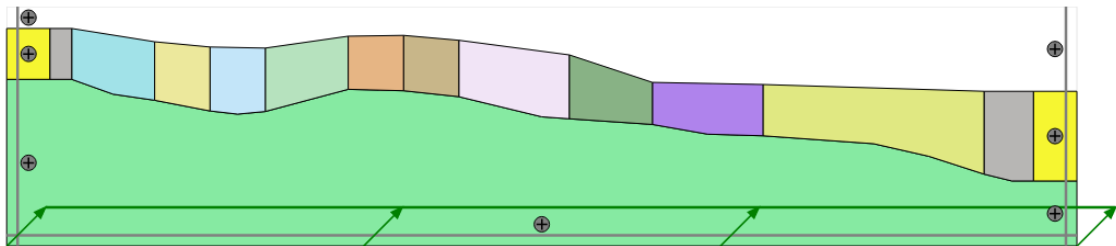


> Figure 5-21 Model of profile 4 with earthquake loading.

Since the shear velocity is dependent on the stiffness, which again is dependent on the shear strength, the shear velocity will thus increase with depth. This can be determined from calculating  $V_s = \sqrt{\frac{G_{ur}}{\rho}}$ , where  $G_{ur} = 200 \times S_u^C(z)$ . In Plaxis output one can view the Youngs modulus which is related to the shear stiffness by  $E = 2G_{ur}(1 + \nu)$ . The benefit with such a model is that the eigenfrequency of the soil, which is stiffness dependent, and slope topography will automatically be included in the calculations. The shear strength and stiffness for model 4 is shown in Figure 5-22 and Figure 5-23.

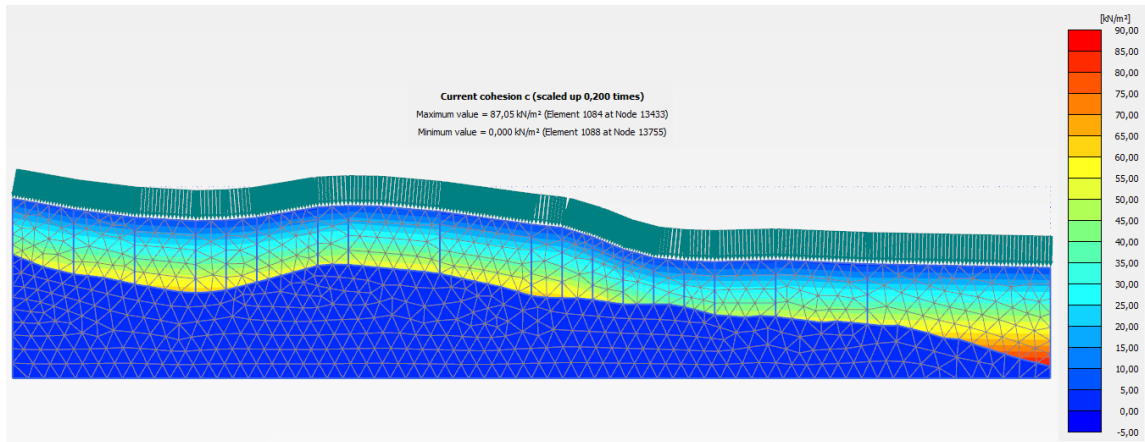


> Figure 5-22 Active undrained shear strength of profile 4.

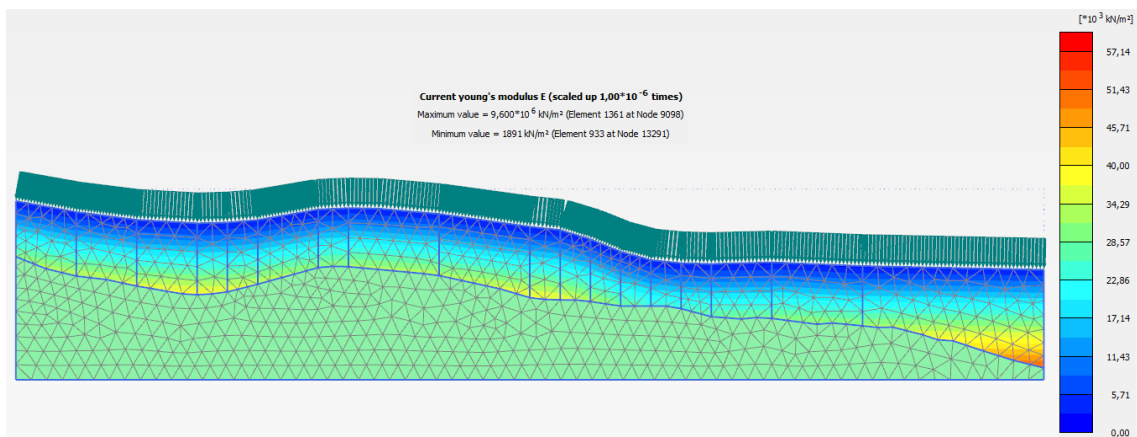


> Figure 5-23 Elastic young's modulus of profile 4.

The earthquake motion is applied at the bottom boundary as an acceleration with drift correction. Time series provided by NORSAR has been scaled and normalized to g-forces. Since it's not known whether the recording was done at an outcrop or bedrock, it's conservatively assumed that it was measured at bedrock. Hence the scaling factor in the calculation is set to 9.81 m in both directions. The vertical ground motion is applied as a dynamic multiplier in the vertical direction and vice versa for the horizontal ground motion. Examples of ground motion is shown Figure 5-24.

Displacements are reset to zero and the max steps is set to the same number as the sample points in the recording. The time step determination is set to manual, where the number of sub steps is determined by Plaxis. Note that this will heavily depend on the mesh, and acute angles should therefore be avoided. The dynamic time is equal to the entire duration of the record, and default parameters are otherwise used.

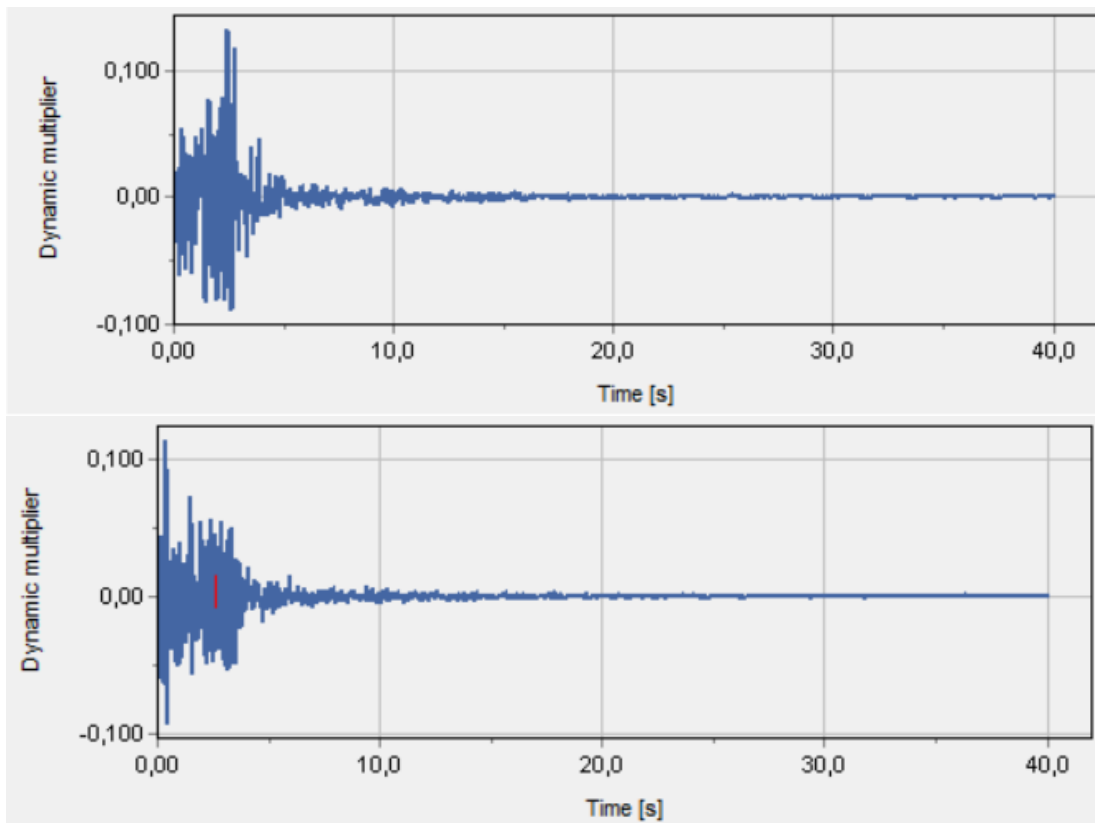


> Figure 5-24 (a) Horizontal Sierra Madre – Ch01, (b) Vertical Sierra Madre – Ch02

Traveling waves from the bedrock will pass the soil-bedrock interface and afterwards rebound at the free surface as illustrated in Figure 5-25. Depending on the soil thickness this may give varying results. In general, it's observed that typically two shear surfaces are formed – one at the bedrock and one near the free surface. Given steep enough slope and sufficient soil one can get similar failure zones as for the static slope stability. This is illustrated in Figure 5-26.

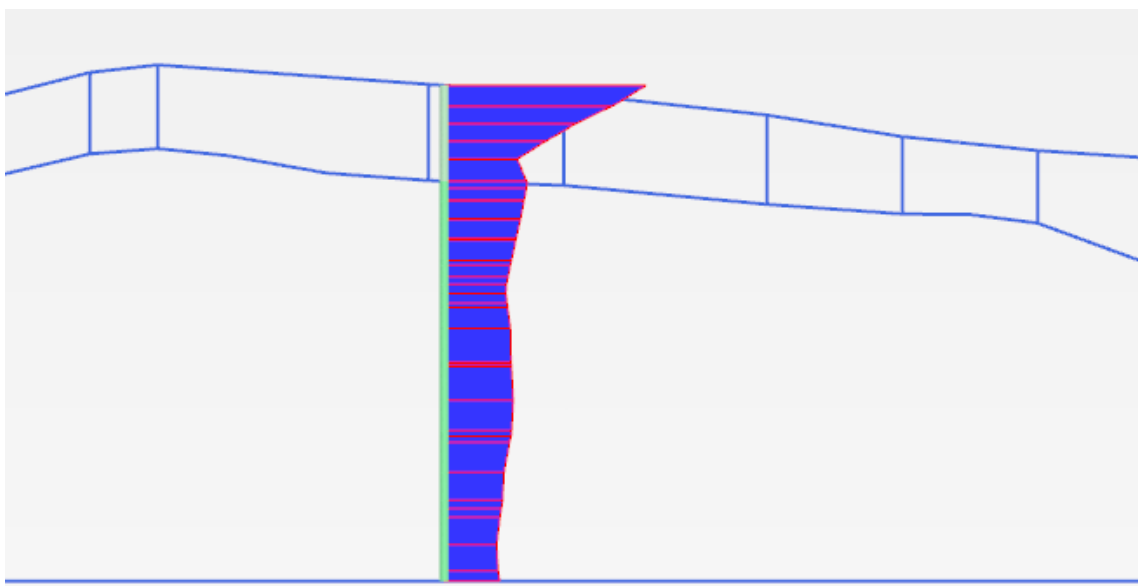


> Figure 5-25 Max acceleration from bedrock to surface.

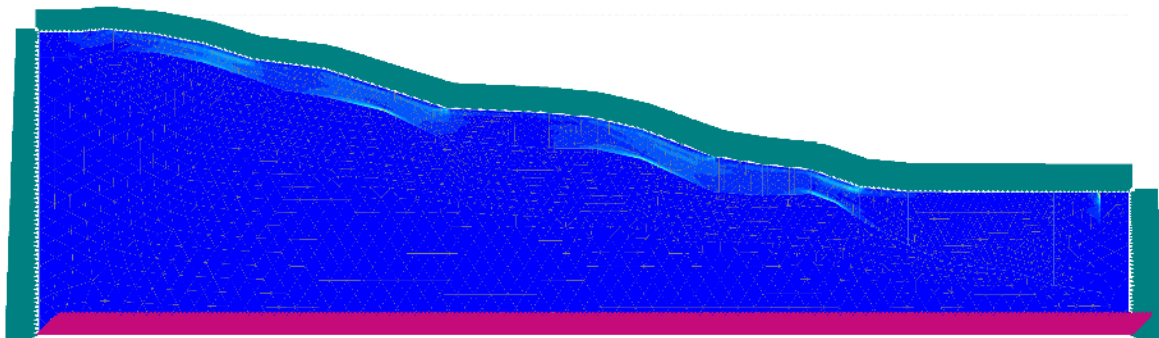


> Figure 5-26 Example of permanent deviatoric shear strain in a slope

The requirement for permanent shear strain  $\gamma_p$  is assumed to be related to the deviatoric shear strain. As one can see in Table 5-4, several of the slopes does not satisfy the criteria for all ground motions. The results correspond well with the profiles with low static safety factor in Table 5-3 and is partially confirmed by section 5.3.1. The static and dynamic thus shows that there is a possibility for slope failure and should be considered in design of exposed anchors.

> Table 5-4 Maximum permanent deviatoric shear strain in slope.

Profile	Sierra Madre	Whittier Narrows main shock	Whittier aftershock
1	~ 6.4%	~ 5.2%	~ 3.2%
2	~ 9.1%	~ 8.2%	~ 4.6%
3	~ 2.0%	~ 1.3%	~ 1.0%
4	~ 2.0%	~ 1.0%	~ 0.58%
5	~ 0.5%	~ 0.3%	~ 0.2%
6	~ 6.4%	~ 3.6%	~ 1.9%
7	~ 3.8%	~ 2.9%	~ 2.0%
8	~ 2.3%	~ 1.2%	~ 1.0%
9	~ 8.1%	~ 6.3%	~ 4.3%
10	~ 5.7%	~ 3.7%	~ 2.5%
11	~ 5.8%	~ 5.0%	~ 3.0%
12	~ 2.0%	~ 1.2%	~ 0.72%
13	~ 1.9%	~ 1.0%	~ 0.95%
14	~ 2.1%	~ 1.1%	~ 0.98%
15	~ 2.1%	~ 1.2 %	~ 0.76%

## 5.4 Run-Out evaluations

For several of the proposed anchor locations the soil thickness is less than 15 m. In Figure 5-27 the areas where the soil thickness is between 1 and 15 meters is shown. Based on stability calculations the critical failure surface is at the interface with bedrock. Other failure modes may be critical, but they are not identified in the stability calculations, and therefore not included in the Run-Out evaluations. The current watershed provided by NGI is based on the bathymetry and can thus be misleading in terms of slab avalanches. In order to evaluate the risk of potential run-out volume, a watershed based on the assumed bedrock is calculated using GRASS GIS 7.4.4.

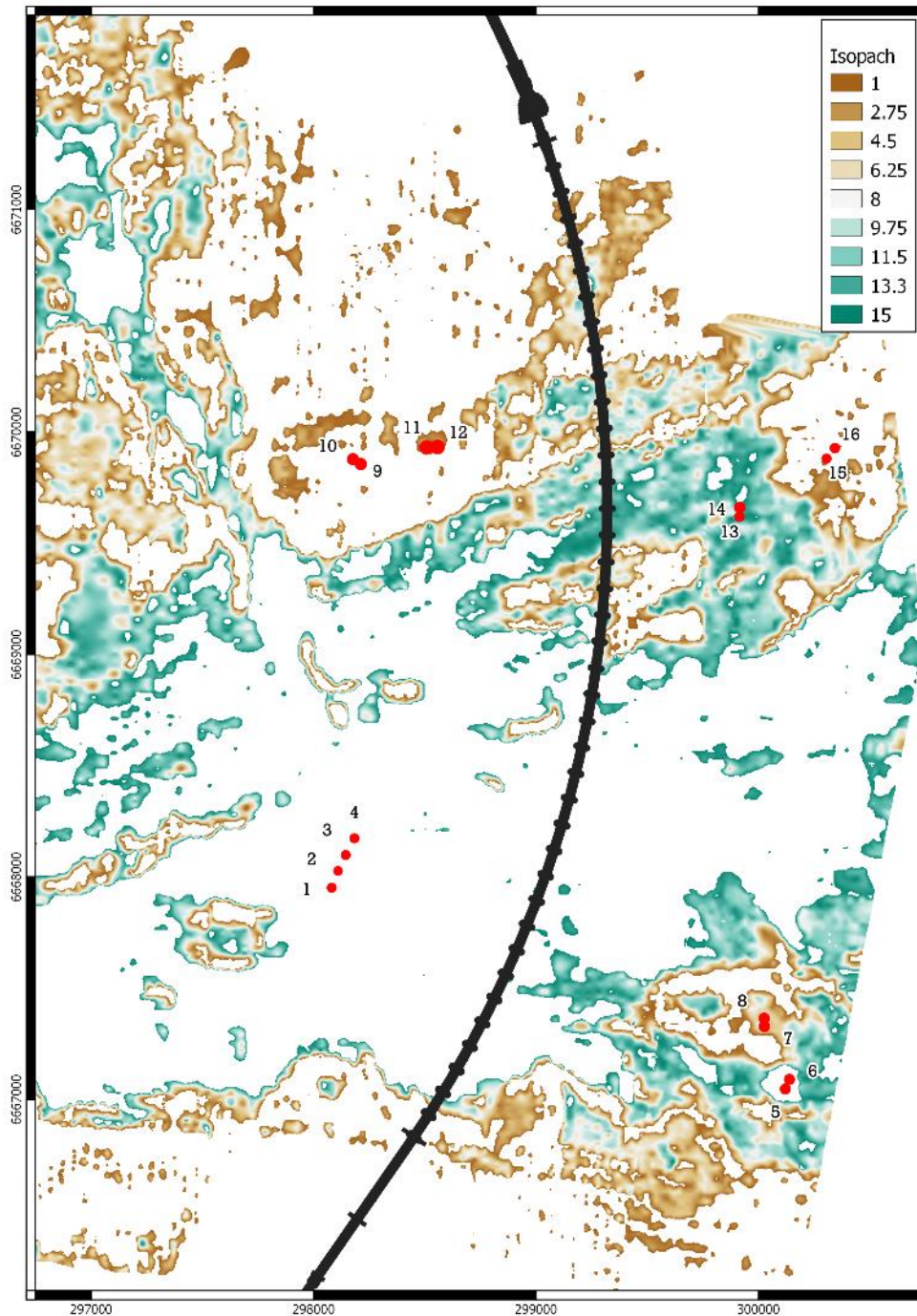


> Figure 5-27 Map showing the areas where the soil thickness is between 1 and 15 m.

The calculated bedrock was used as input in the watershed analysis together with the default parameters. The results are shown in the Figure 5-28 below. The white colour indicates that an area is on a local hill, while the blue areas can be thought of as hypothetical rivers. The green areas represent the transition zones, between ridges and rivers. It can also be seen that the watershed analysis done in GRASS corresponds well with the ridges and stream lines calculated in the last phase by NGI, ref. [10].



> Figure 5-28 Flow accumulation from watershed calculation of bedrock, overlain with ridges and streams calculated by NGI, ref. [10].



### 5.4.1 Group 1

The anchor group is located approximately in the centre of the basin. Since the anchors are placed at the lowest point, they are exposed for landslide debris in all directions. This is confirmed by the stream lines calculated by NGI and the flow accumulation calculated in GRASS GIS. The latter is shown as blue rivers in the Figure 5-29, overlaying the slope angle map.

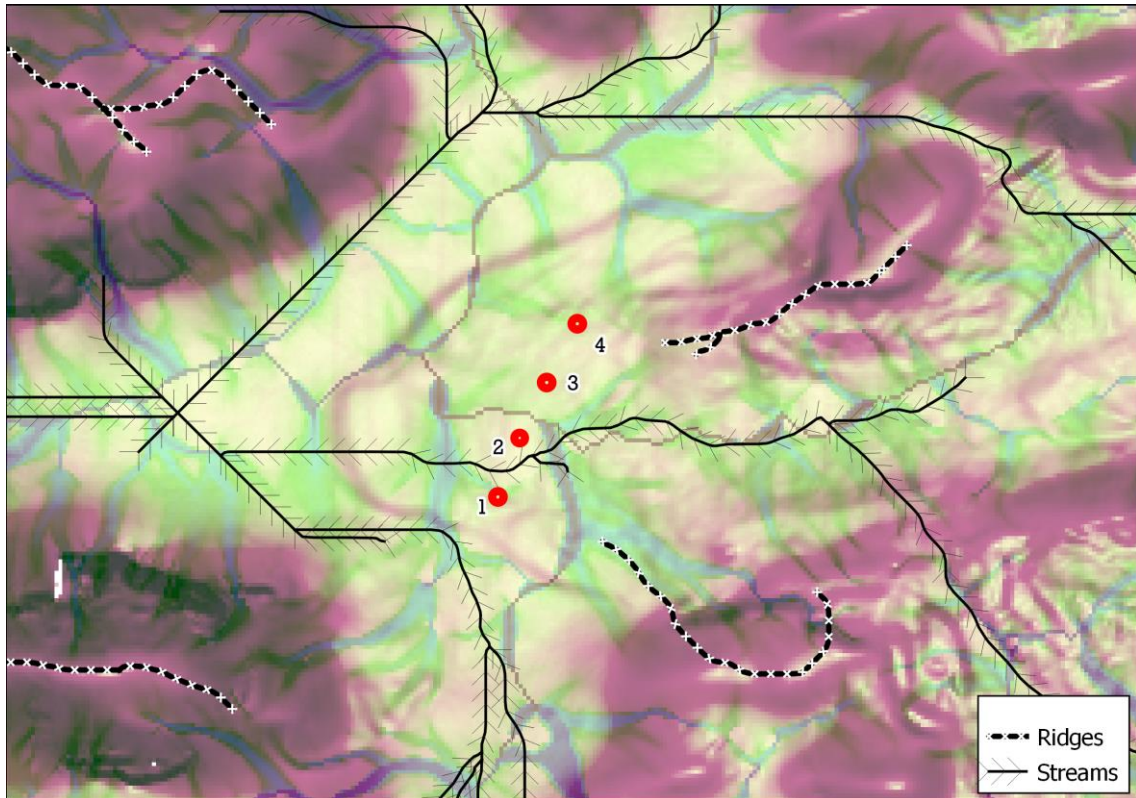
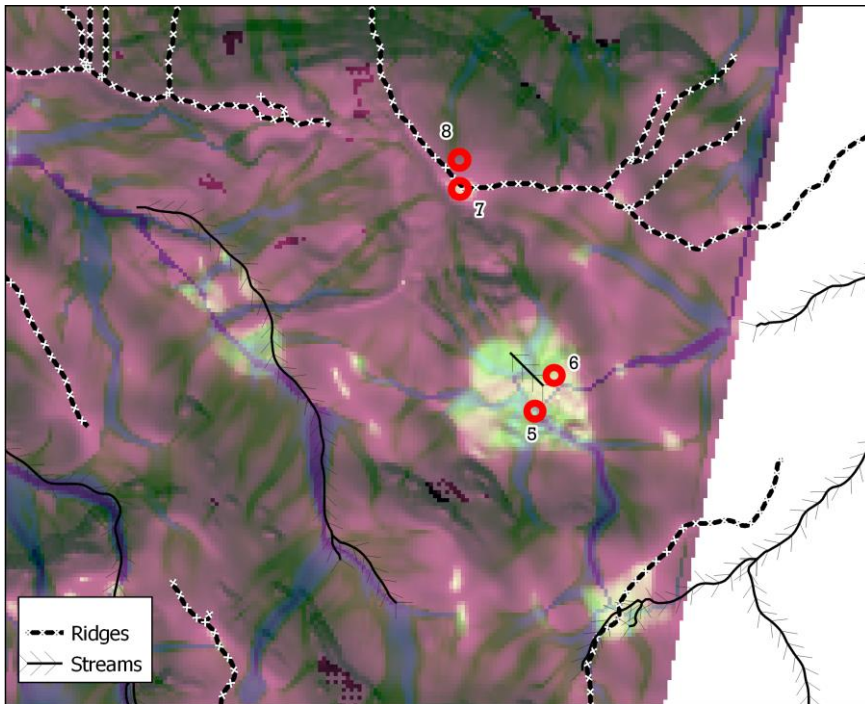


> Figure 5-29 Map showing flow accumulation (calculated at bedrock) together with ridges and streams calculated from the bathymetry of anchor group 1.

### 5.4.2 Group 2

Anchors 5 and 6 are placed in a local pit with a large sediment thickness, while anchors 7 and 8 are placed on top of a hill. The soil thickness on the hill is roughly 5-7 m thick and it's assumed that the soil consists of clay which can be removed, thus avoiding any risk of landslides from above.

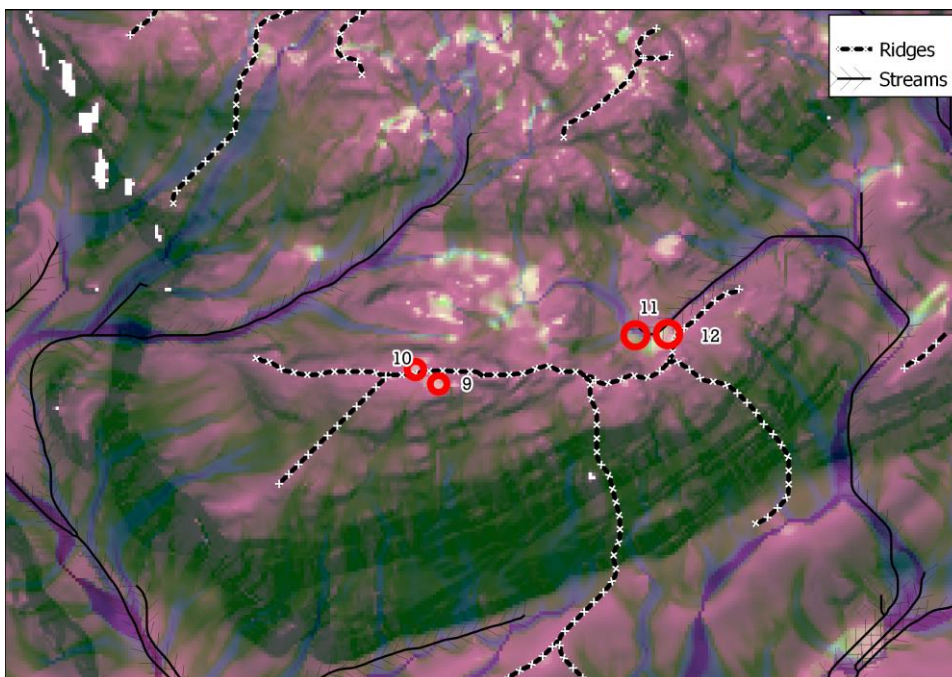
As shown in Figure 5-27 the anchors 5 and 6 in the pit is surrounded by a soil thickness of around 10 to 15 m with a differential height variation of about 20 m in the near vicinity. By examining the slope angle map and the high-quality 3D bathymetry one can observe bedrock in the north-west and south-west. Furthermore, the flow accumulation shown in Figure 5-30 indicates the possible run-out sources are fairly limited compared to anchor groups 1 and 4. This has also been confirmed in QGIS using the profile addon. Based on the above observations, it's believed that in case of a landslide, the volume and kinetic energy will be finite and manageable by embedding the anchors deeper.



- > Figure 5-30 Map showing flow accumulation (calculated at bedrock) together with ridges and streams calculated from the bathymetry of anchor group 2.

#### 5.4.3 Group 3

All the anchors in group 3 is placed directly on bedrock. As can be implied from Figure 5-27 and Figure 4-2, the soil thickness is very limited. Based on this information run-out is evaluated to not be relevant in this area.



- > Figure 5-31 Map showing flow accumulation (calculated at bedrock) together with ridges and streams calculated from the bathymetry of anchor group 3.

#### 5.4.4 Group 4

Anchors 13 and 14 were previously at the same ledge together with anchors 15 and 16. Initial pseudo-static calculations gave low factor of safety, and therefore the anchors were moved further west as can be seen in Figure 5-29. Later on, several slopes were calculated for stability and the corresponding run-out debris was evaluated.

It can be seen from the calculations, ref. 5.2.2, that the static slope stability is poor for the slopes near anchor 13 and 14. Additionally, one can observe in Figure 5-32 that the current anchor positions are located at the centre of a stream line, which also corresponds well with the calculated watershed at bedrock. This suggests that if a retro progressive slide were to occur, the surrounding soil masses could disappear. In fact, it's assumed this have been the case for the area where anchor 15 and 16 is currently located. The static and dynamic slope stability up stream is deemed to be satisfactory for anchors 13 and 14, ref. 5.2.2 and 5.3.2.

Anchors 15 and 16 are placed in a previous landslide area. They are partially shielded from potential run-out debris in the north, and the slope calculations in the west indicate satisfactory safety factors. Due to the limited amount of potential run-out debris and slope stability results the anchors are deemed to be well secured.

A ridge line can be seen between the previous and the current anchor location in Figure 5-32. Assuming a retro progressive slide occurs at the profiles with the lowest FoS, this will imply that the debris flow will mostly go towards the south. This also implies that the debris flow in the easterly direction will be fairly limited. These assumptions indicate that perhaps a better anchor location can be achieved at the bedrock to the east.

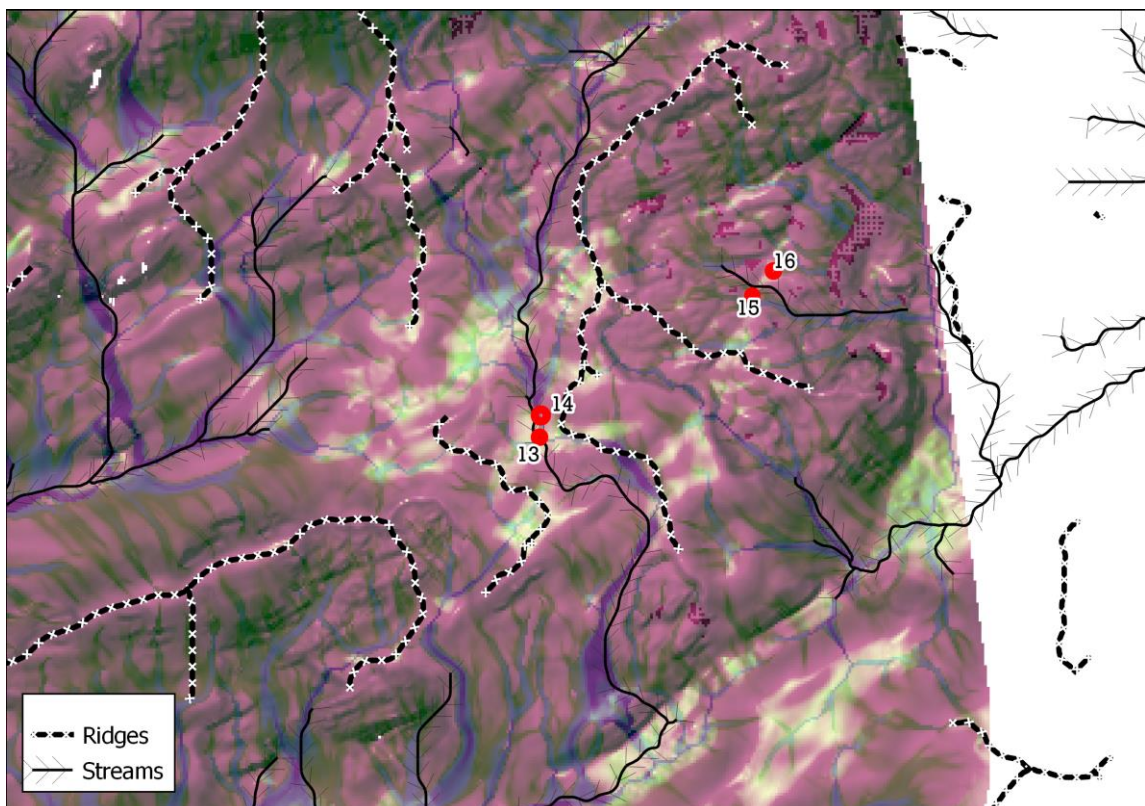


> Figure 5-32 Map showing flow accumulation (calculated at bedrock) together with ridges and streams calculated from the bathymetry of anchor group 4.

Profile of the lines shows that there is sufficient clearance between the seabed and the mooring line. Further description is in Design of mooring and anchoring, ref. [17], for all of the mooring lines. An example is shown below in Figure 5-33.

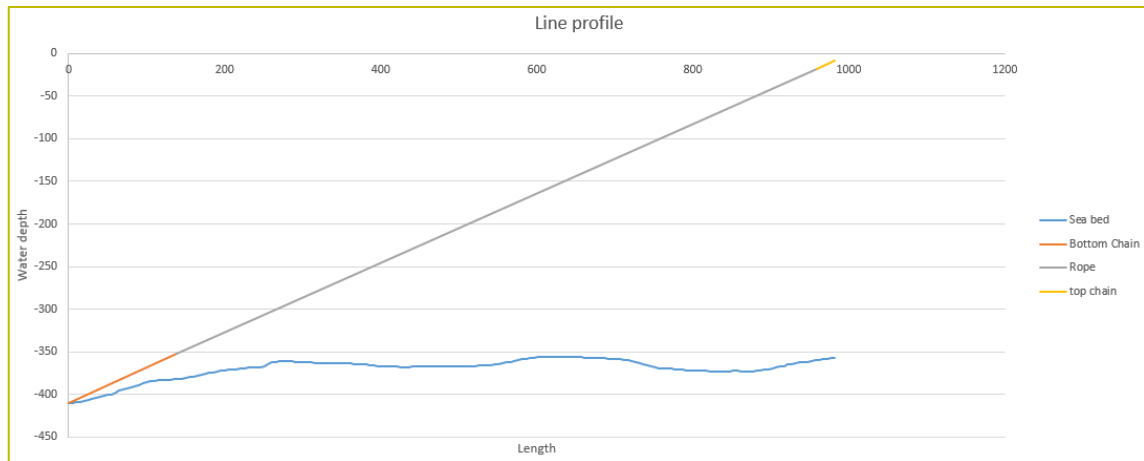


> *Figure 5-33 Profile of mooring line 15.*

Based on the considerations described above, and since scars from previous landslide can be readily observed in the surrounding surface, it's recommended to do further soil investigation to determine the optimal anchor location in this group.

## 5.5 Recommended anchor locations

The anchor clusters are placed such that the overall bridge response is reduced and thereby also reducing the mooring load. The anchor locations have been chosen based on a geohazard assessment, maximum attainable holding capacity and installation requirements. The last requirement involves keeping the lines as normal as possible to the arc of the bridge.

Gravity anchors are here considered to be the most reliable and predictable type and have therefor been prioritized when considering possible anchor locations. In total 8 locations have been found to be suitable for using gravity anchors.

For the rest of the anchors, the anchors are placed at areas where the soil thickness is the highest. The reasoning behind this is that the anchors can be embedded further down to achieve higher holding capacity if required. Based on previous experience and the surrounding terrain, it is proposed to use suction anchors for the 8 remaining anchors with varying skirt lengths. The anchor locations are shown in Figure 5-34 and Figure 5-35.

> *Table 5-5 Summary of proposed anchor locations in UTM32N and NN2000 coordinates.*

Group	ID	East	North	Elevation [m]	Isopach [m]	Seabed inclination [°]	Anchor type
1	1	298080.6	6667952.1	-561.5	58.6	1.2	Suction
	2	298108.5	6668027.6	-561.2	57.4	0.3	Suction
	3	298143.2	6668098.9	-561.1	54.2	0.4	Suction
	4	298182.4	6668174.3	-561.2	47.1	0.8	Suction
2	5	300120.3	6667047.1	-359.3	35.1	0.7	Suction
	6	300144.4	6667092.3	-359.2	30.0	1.0	Suction
	7*	300025.7	6667328.3	-291.7	5.6	1.6	Gravity
	8*	300025.2	6667365.1	-296.5	6.5	16.4	Gravity
3	9	298210.9	6669856.1	-123.2	0	2.5	Gravity
	10	298176.0	6669878.1	-123.5	0	2.4	Gravity
	11	298508.3	6669930.0	-167.2	1.9	3.2	Gravity
	12	298557.6	6669931.8	-158.1	1.8	3.0	Gravity
4	13	299914.0	6669620.5	-382.2	15.5	0.8	Suction
	14	299916.4	6669660.5	-380.5	13.7	3.1	Suction
	15	300305.9	6669880.9	-410.3	0.8	3.4	Gravity
	16	300344.5	6669926.1	-411.8	1.3	2.7	Gravity

\* The values are measured at the seabed, and thus not representative since the soil will be dredged and partially exchanged with crushed rock prior to anchor installation.

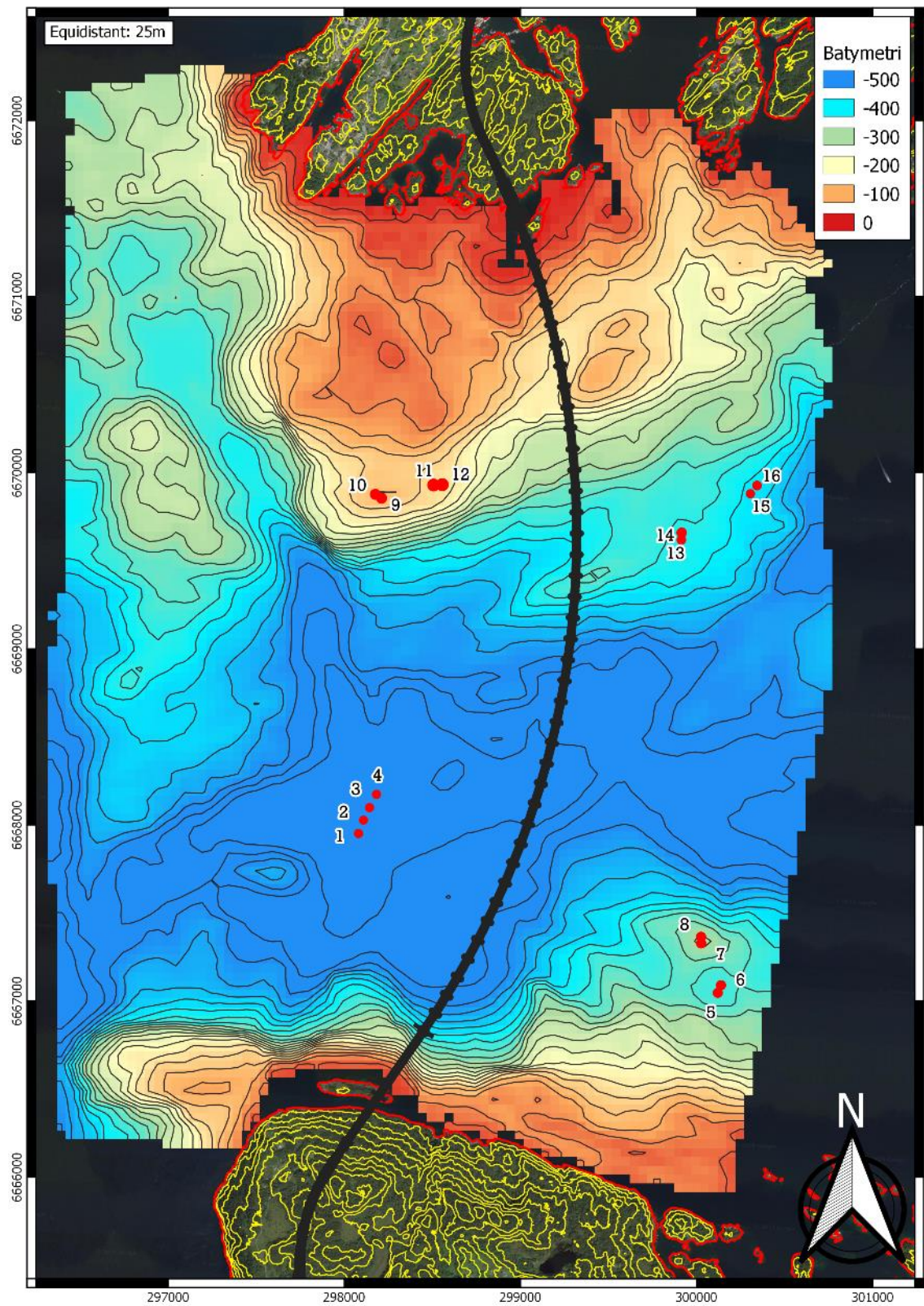


> Figure 5-34 Bathymetry of Bjørnafjorden shown together with proposed anchor locations.

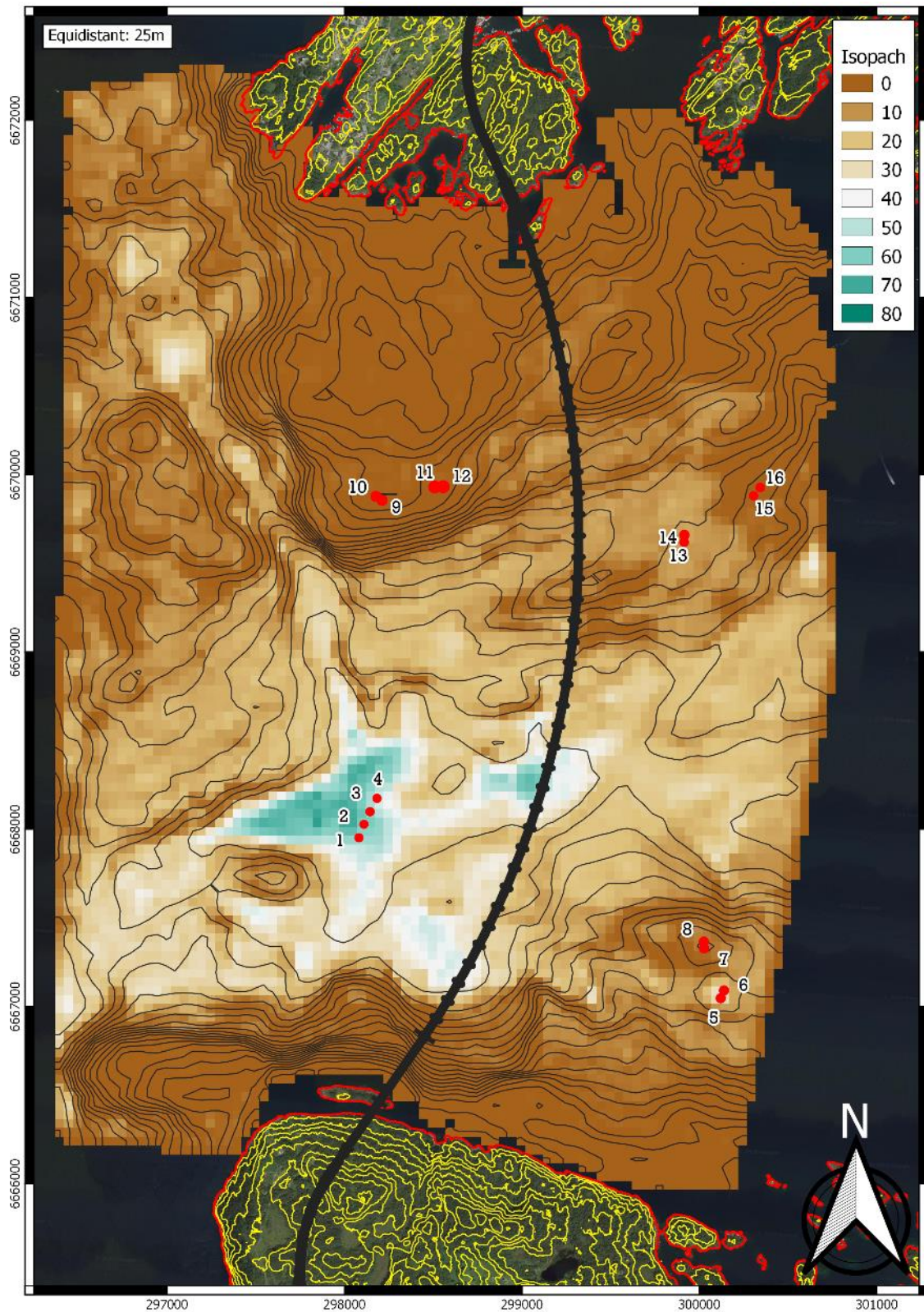


> Figure 5-35 Isopach of Bjørnafjorden shown together with proposed anchor locations.

## 5.6 Risk assessment for anchor groups

### 5.6.1 Group 1

As previously stated in Chapter 5.4.1, the anchors are exposed for possible landslide run-out sources in all directions. Even though calculations may show adequate FoS and performance to earthquake, the uncertainties related to this are high. By doing additional soil investigation and advanced numerical analysis of run-out dynamics one might be able to predict the likelihood and impact from possible run-out sources. However, due to the nature of soil variability and behavior, this will be a challenging and demanding task. Another possibility could be to do similar calculation to a PSHA for earthquakes. By quantifying possible sources, doing flow calculations based on flooding and combining the FoS to a given probability of failure, one could perhaps estimate the impact force for a given probability.

As a simplified approach to the challenge with landslide run-outs for this phase of the project, it is proposed to assume remoulded shear strength in the top meters, due to possible landslide ploughing. The additional load from debris flow forces is not accounted for, as they are assumed to be small due to energy dissipation over large distances. It's also assumed that global failures involving the anchors are highly unlikely. Based on Figure 5-4 a 3 m deep zone with remoulded clay is conservative when included in the holding capacity calculations for peak design load with loss of two mooring lines when calculating the holding capacity. It's however unknown how deep the landslide will plough, thus further soil investigation is needed to assess the likely ploughing depth from possible landslides.

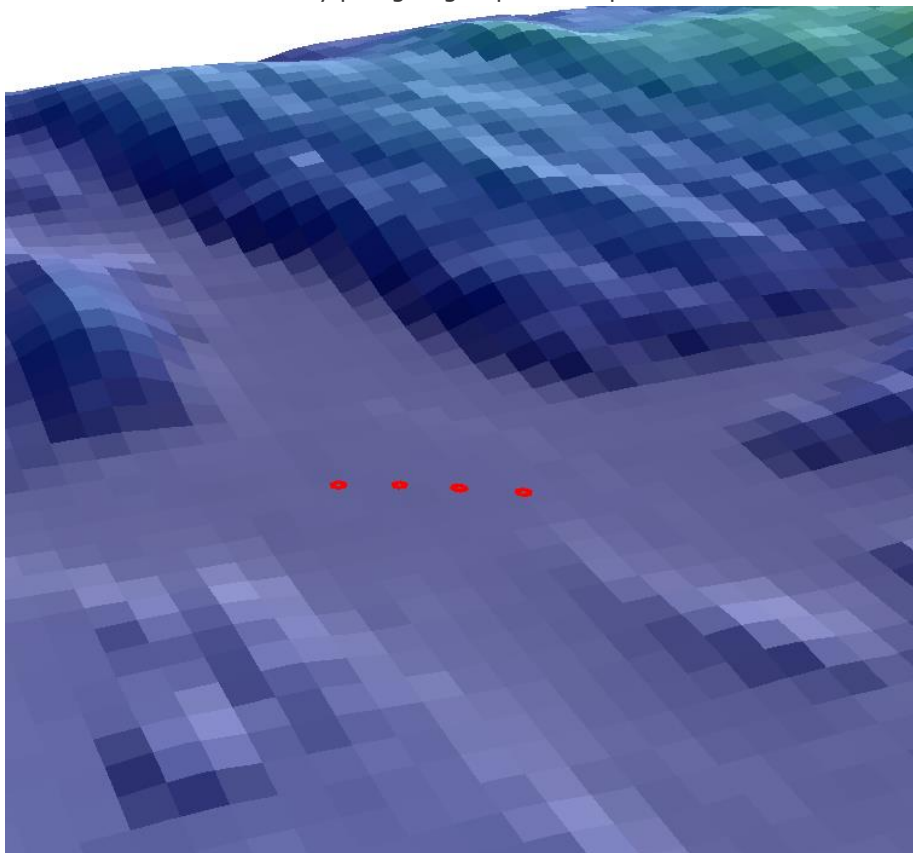


> Figure 5-36 3D bathymetry of anchor group 1.



### 5.6.2 Group 2

Anchors 7 and 8 are placed on top of the hill and are therefore regarded as safe with respect to run-out debris. The only issue tied to this location is increased seismic acceleration due to topography layout.

As described in 5.4.2 the amount of possible run-out debris for anchor 5 and 6 is limited, as can be partially observed in Figure 5-37. One can therefore similarly to group 1 assume remolded shear strength in the upper 3 meters to determine the required skirt length to achieve sufficient holding capacity. This value can be reduced depending on further soil investigation.

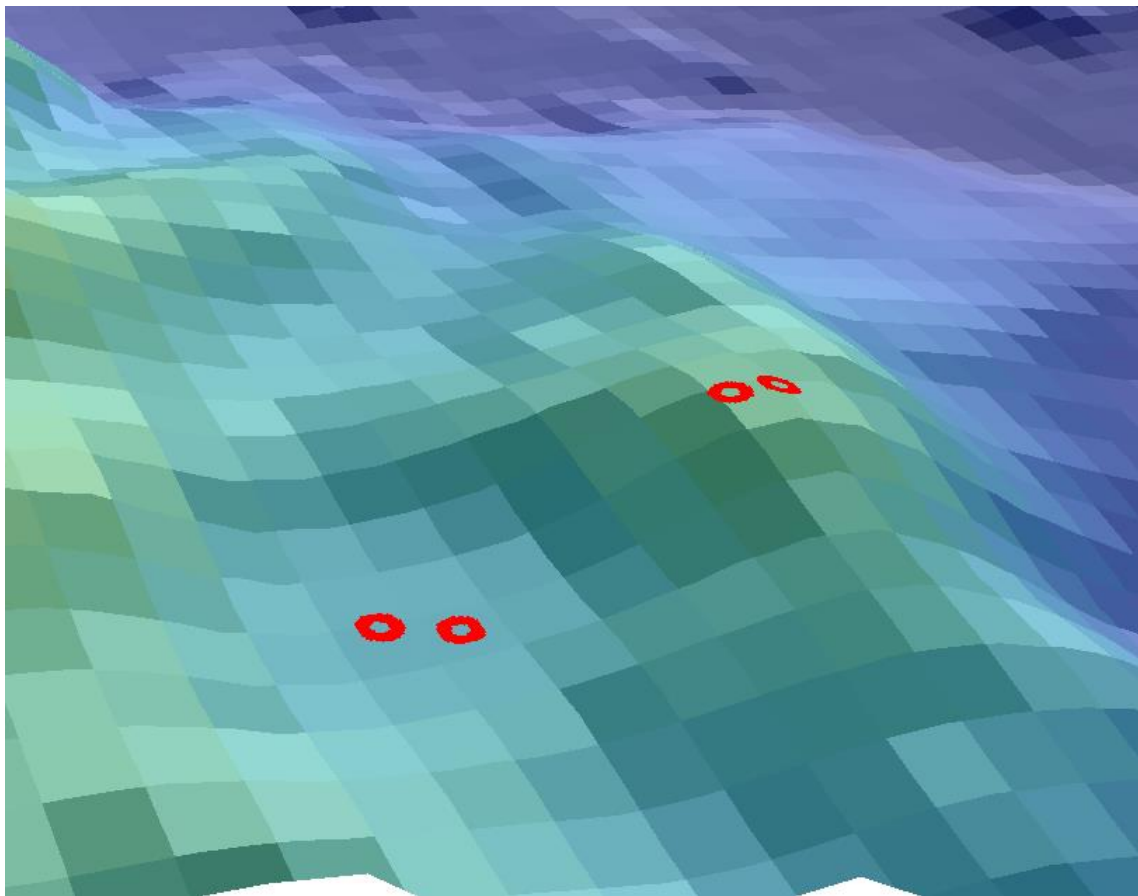


> Figure 5-37 3D bathymetry of anchor group 2.

### 5.6.3 Group 3

No issues with respect to geohazard and anchor capacity are identified at this location. Ideally the anchors would be placed more normal on the bridge, but this is not possible due to the steep slope which can be seen in Figure 5-38.

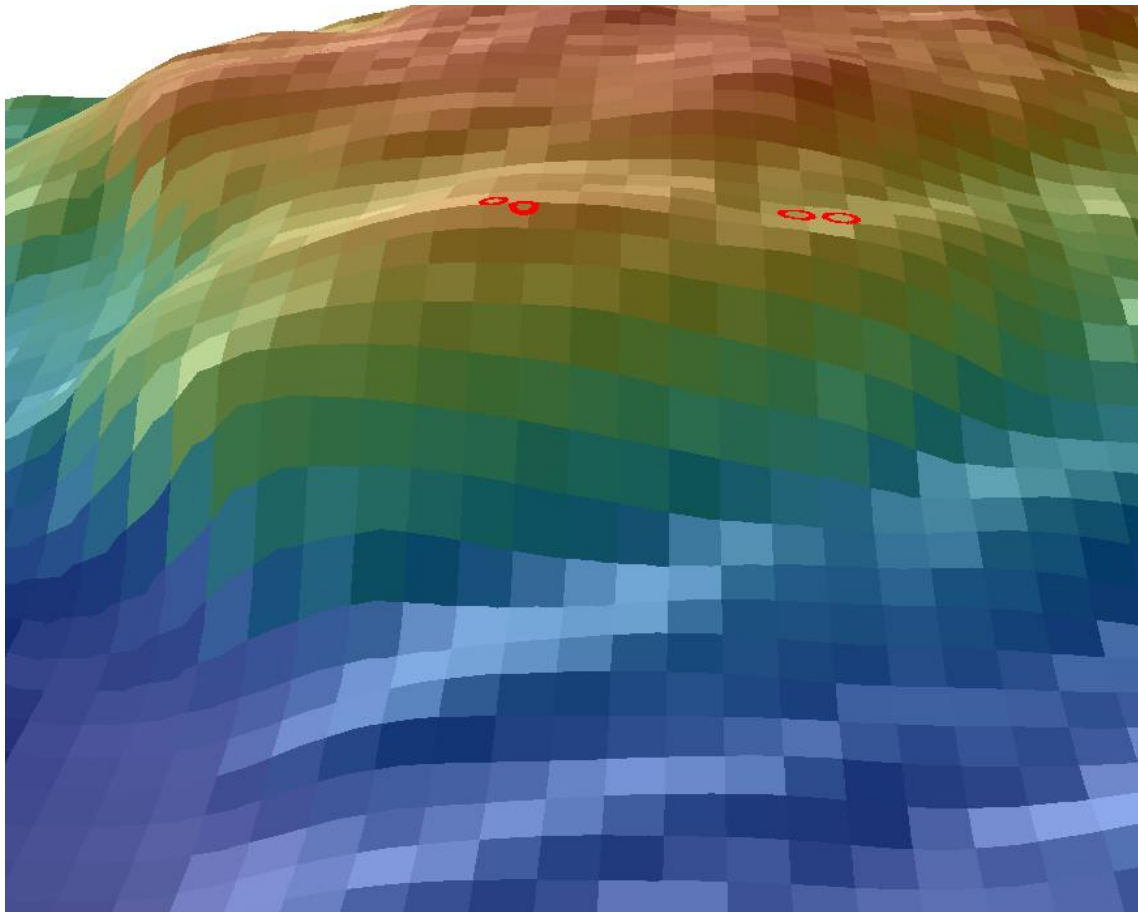


> Figure 5-38 3D bathymetry of anchor group 3.

#### 5.6.4 Group 4

Anchors 15 and 16 are placed firmly on bedrock and is partially shielded in the north from run-out debris. The slope stability towards west has been calculated to be adequate, ref. Table 5-3, and Figure 5-32 indicates that the potential debris volume is fairly limited. It's thus concluded that these anchors have a safe position.

The slope stability calculations for anchor 13 and 14 indicates that the safety factors inadequate with respect to the criteria given in design basis, ref. [4]. One can also observe scars from previous landslide in Figure 5-39.

The area for anchor 13 and 14 may thus be troublesome with regards to landslides, both from north and in the southern direction. Landslides towards south can lead to loss of soil, as the anchors are located at a streamline. It is not possible to design the anchors for a complete loss of the soil. At this stage the challenges caused by possible landslides, are solved by having spare capacity, assuming 3 m of remoulded soil in the top, taking slides from the north. For worst case scenario, with slide towards south, the anchors may be lost. As the bridge is designed to be intact for this case, it is regarded to be acceptable. Additional soil investigations in this area is recommended to determine the optimal anchor position with respect to retro-progressive slides and possible run-out debris.

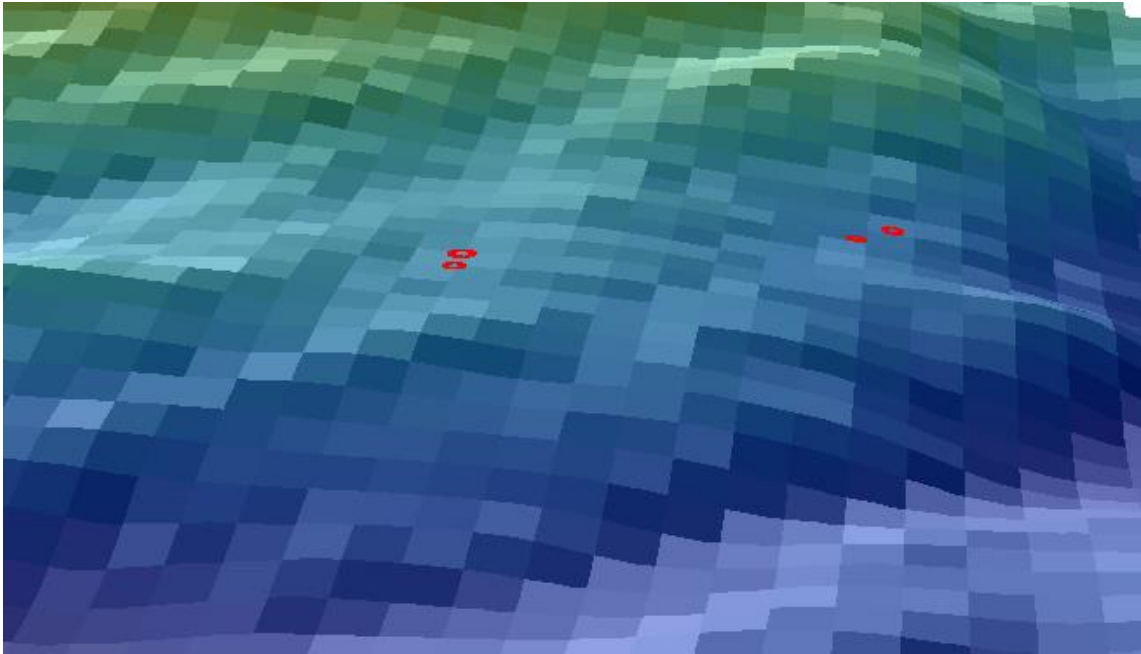


> *Figure 5-39 3D bathymetry of anchor group 4.*

## 6 ANCHOR DESIGN

### 6.1 Anchor types considered

For the bridge concept evaluation of Bjørnafjorden, several anchor types have been considered and evaluated. A short summary from the design brief, Appendix A, is given here.

Although a high cost is assumed associated with gravity anchors, it's here considered to be the most robust anchor type and have thus been prioritized over other anchor types. It's assumed that the gravity anchor is placed close to bedrock and is generally less exposed to runout debris.

Plate anchors were earlier considered to be a very likely candidate as an anchor type in Bjørnafjorden. Due to previous experience and overall total cost it has not been included in the current mooring configuration. The issues were mainly tied to installation challenges and strict tolerance requirements, example anchor 5 and 6. The plate anchor response is also assumed to be less predictable compared to other anchor types and have thus been disregarded.

Several of the team members have had good experience with suction anchors with respect to installation and design calculations. It's also assumed that the suction anchor response is more predictable compared to the plate anchor response. Another benefit is that the global dimensions can easily be adjusted with respect to bedrock, soil and loading conditions.

For areas with scarce soil thickness, i.e. between 10 and 15 m it was proposed to use mixed or combined anchor types. The mixed anchor is essentially a short and wide suction anchor, while the combined anchor is similar to a gravity anchor, but specially designed to be placed on soft soil. Further description is given in Appendix A. One should note that these anchor types are not desirable for the mooring configuration due to increased complexity. It was however considered to have possible alternatives in case anchor capacity could not be achieved with the other anchor types.

Grouted bedrock anchors have been considered, but it has been specified by the client that this anchor type shall not be evaluated at this stage.

In summary the anchors in the mooring system only consists of gravity and suction anchors. However, for the current mooring configuration it's believed that the gravity anchors can be exchanged with grouted bedrock anchors.

### 6.2 Anchor loads

The restraining loads in each mooring line is taken from the global bridge analysis and afterwards adjusted for prestressing. The loads from the current model is presented below in Figure 6-1 and the load composition is shown in Figure 6-2. The max unfactored load for the mooring line connected anchor 1 is roughly 3.3 MN, where the prestressing contribution is 2.3 MN unfactored, i.e. 70% of the total load. Note that ALS results for the different limit states are currently unavailable, but it's estimated to be non-governing for anchor design when compared to the redundancy requirement given in the design basis for mooring and anchor, ref. [5].

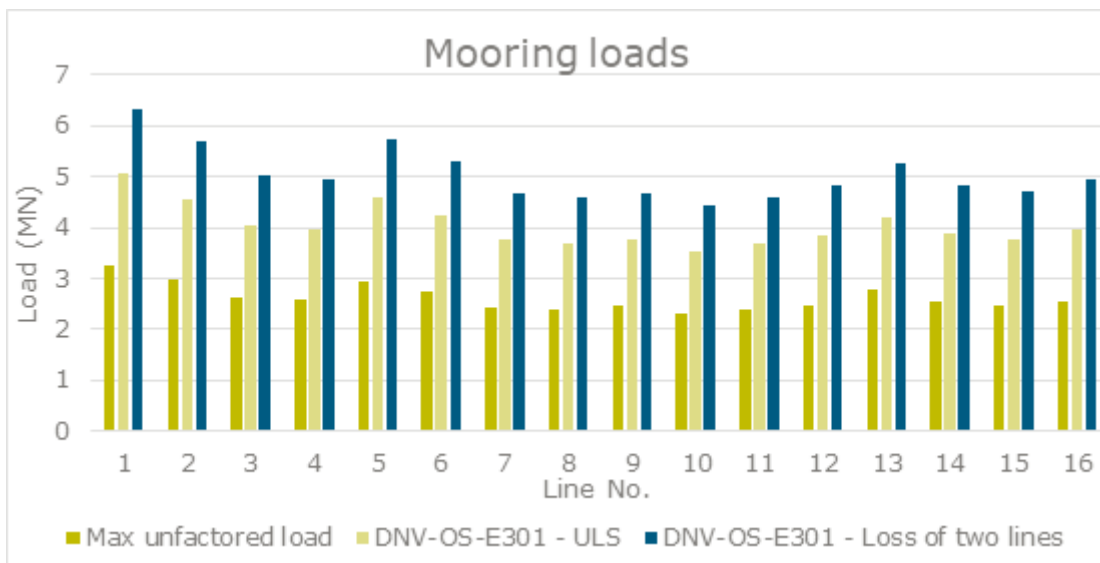


> Figure 6-1 Line loads used for anchor design, K12 - model 20.

The operation load is defined in the design basis for mooring and anchor, ref. [5]. It's stated that the mooring system shall be intact and characteristic loads from line tension and environmental loads shall be included. The max unfactored load, which includes 100 years return period for environmental loads, is here defined as the operation load and used in anchor design. From Table 3-1 it's defined that the vertical load component of the operation load shall not exceed the submerged anchor weight and is thus a limit state in anchor design.

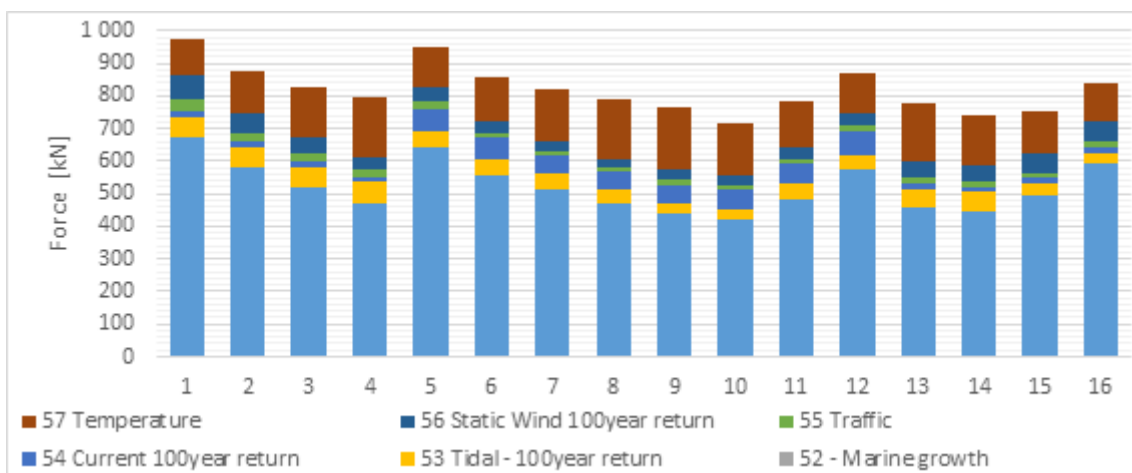


> Figure 6-2 Load composition for tensile loads, without pretension.

According to the design basis for mooring and anchor 2.22.2, ref. [5], the soil design shall be carried out according to DNVGL-OS-E301, ref. [18], with load factors from DNVGL-OS-C101, ref. [19]. Note that different load factors from NS-EN ISO 19901-7, ref. [20], is used for mooring design. It's also specified that the bridge shall be able to withstand the loss of two arbitrary mooring lines. The increase due to stiffness and load distribution is estimated to be about 25% for ULS and 55% for ALS. Recent calculation with loss of line 3 and 4 has been calculated and indicates that the load increase is lower (~12%) than previously estimated. Further calculations are thus required to determine the actual mooring loads with respect to line loss.

The design for anchor loads is here defined as the ULS condition with the loss of two mooring lines. Furthermore, it's assumed that the mooring system is linear which implies that the angle at dipping point (or padlock for gravity anchor) can easily be determined from anchor and pontoon positions. The angles used in calculations are presented in Table 6-1. Line-soil interaction is neglected which is conservative for ULS calculations since the effect is increased load angle and reduced load, and the vertical capacity is generally higher than the horizontal capacity. The effect is also assumed to be small since the clay is soft and the pretension load is large. Lastly the peak load is assumed to occur over a short duration such that suction will occur in the soil.

> *Table 6-1 Dip-point angle assumed to be the same at padlock angle.*

#	1	2	3	4	5	6	7	8	9	10	11	12	13	14	15	16
$\alpha_p$	32.5	32.5	32.8	32.9	14.8	14.8	14.3	14.8	6.1	6.0	11.4	12.4	33.2	32.8	22.7	21.8

A summary of the limit states and the maximum and average loads are summarized in Table 6-2, where the minimum load is included for comparison.

> *Table 6-2 Limit states and loads used in anchor design, K12 - model 20.*

Limit state	Gravity anchor			Suction anchor		
	Max load	Average load	Min load	Max load	Average load	Min load
Operation load	<b>2536</b>	2428	2317	<b>3276</b>	2812	2541
Design load (ULS)	<b>4955</b>	4685	4422	<b>6320</b>	5396	4835

One should also note that the anchors are designed for the governing loads according to DNV, and not the MBL of the mooring line. The MBL for the current mooring configuration is in the range 8.5 to 10 MN and is determined out of a stiffness requirement rather than a capacity requirement. This implies that the anchor can be the MBL of the mooring system.

### 6.3 Anchor deformations

Local mooring line analysis shows that large horizontal deformation, i.e. over 40 m, is required to reach MBL. Similarly, large deformation is required before slack occurs in the mooring line. The same analysis shows that the mooring line stiffness is very linear within 10 m of deformation. Results from the local analysis is given in Design of mooring and anchoring, ref. [17], for all the mooring lines. An example of the first anchored southernmost pontoon is shown in Figure 6-3 and Figure 6-4. One can thus conclude that for a permanent anchor displacement of less than 1 m is neglectable for the overall mooring response and 1 m deformation is far above expected creep deformations.

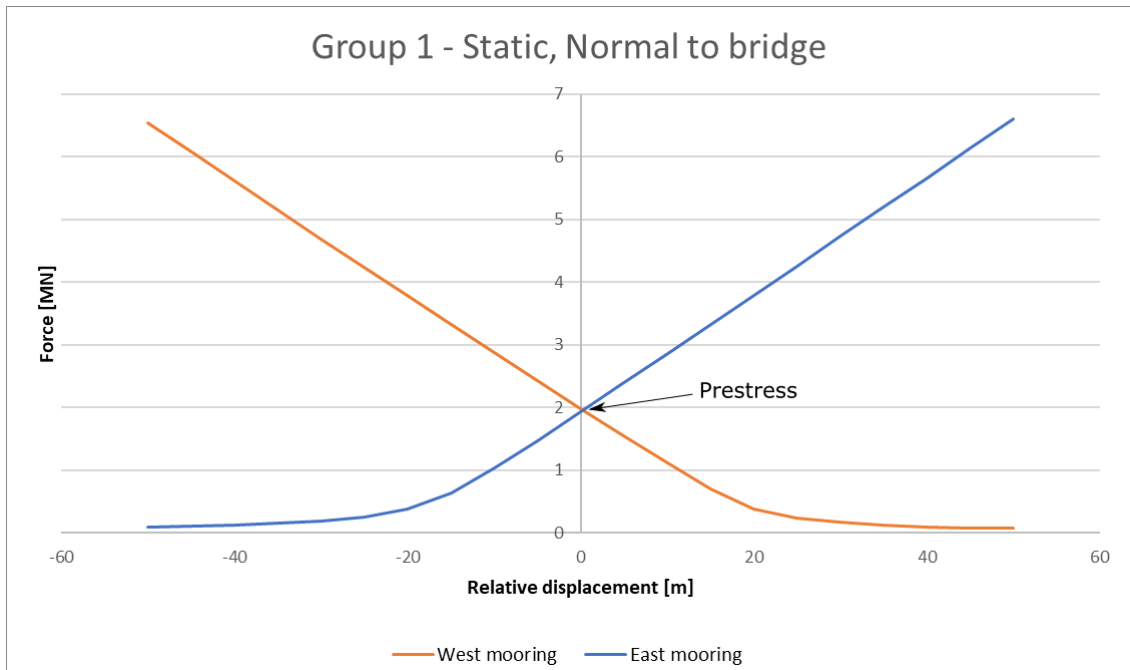


> Figure 6-3 Mooring loads with relative displacement between anchor and pontoon.

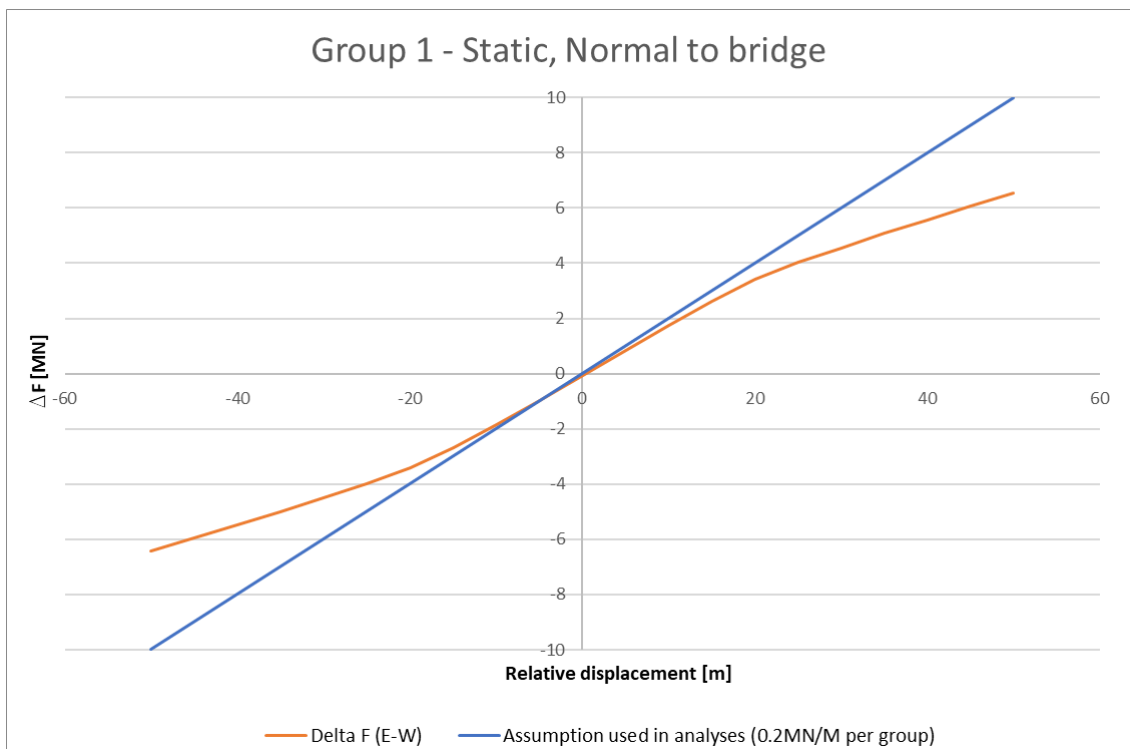


> Figure 6-4 Stiffness of mooring line compared to elastic assumption used in calculation.

## 6.4 Gravity anchor calculations

### 6.4.1 General

A similar gravity anchor as proposed in the last phase by Multiconsult, ref. [14], is used in the current mooring configuration. Diagonal stiffeners are included in the plate walls to ensure a robust load transfer from the padeye and throughout the anchor. Ribs are also used utilized in the design to ensure full friction between the soil and anchor. It is also proposed for the current anchor design to paint and use galvanic anode to avoid corrosion and thereby ensuring 100 years of life service.

The gravity anchors are planned to be placed at areas close to bedrock. The overlain clay is dredged and exchanged with gravel, ensuring a flat surface for the anchor. Thus, cyclic degradation and settlements are expected to be negligible. Assuming a maximum filling height of 3 m and a slope inclination 1:3, the local slope stability is expected to be satisfactorily. Further details regarding marine operations and installation is described in [21].

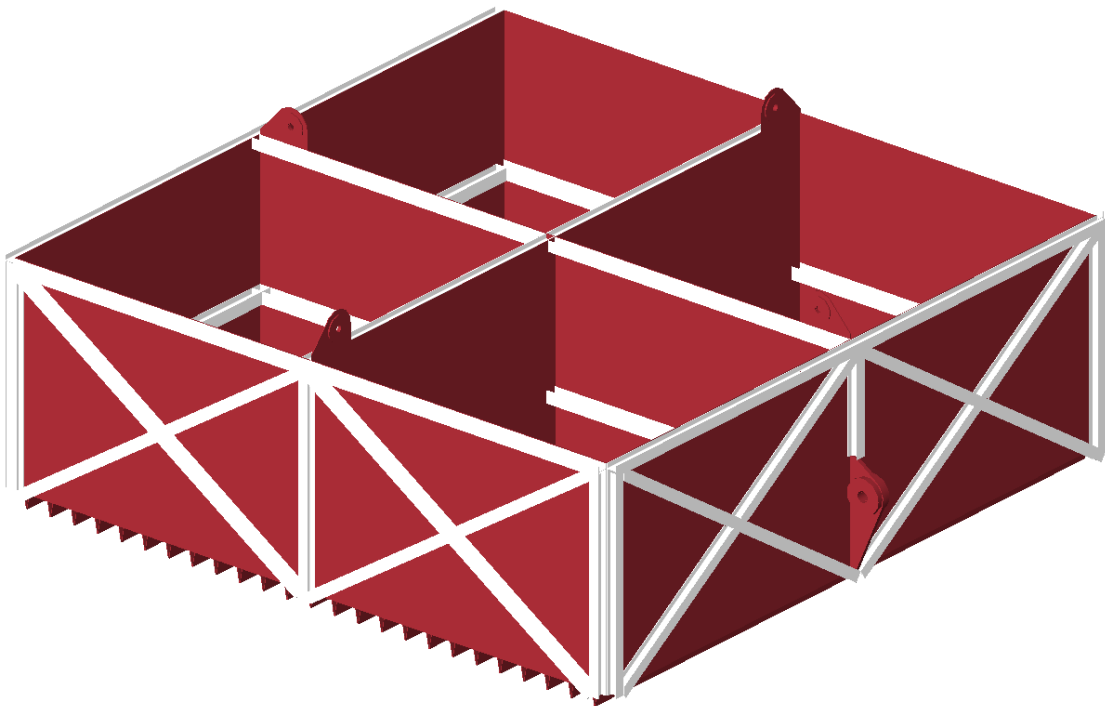


> Figure 6-5 Illustration of gravity anchor type used in calculations.



### 6.4.2 Anchor capacity ULS

Design of gravity anchor was done prior to the mooring loads were calculated, thus the design load from anchor line is assumed to be 6 MN, acting with a load angle between 12 - 22°. The length and width are set to 15 m and the height to 5 m. For the current design ribs of 0.32 m height is proposed, which gives a total steel weight of 160 tons and a storage volume of 1125 m<sup>3</sup>. Olivine as infill material is assumed in the calculations.

The friction angle of the gravel is assumed to be 38° and a safety factor of 1.3, ref. Table 3-1. It's assumed friction can be mobilized at the anchor-soil interface, thus the roughness is set to 1.0. The self-weight reduced with a favourable load factor of 0.9 gives 13.5 MN in vertical load. Janbu's equation is used for determining the anchor capacity:

$$r = \frac{\tau_{mob}}{(\sigma'_v + a) \times \tan \varphi_d} \quad \text{where} \quad \tau_{mob} = \frac{Q_H}{A_{eff}} \quad \text{and} \quad \sigma'_v = \frac{Q_V}{A_{eff}}$$

The anchor capacity is most vulnerable to large load angles, thus by setting  $\theta = 22^\circ$ ,  $F_{d,x} = 6 \text{ MN} \cdot \cos(\theta) = 5.56 \text{ MN}$ , and  $F_{d,y} = 6 \text{ MN} \cdot \sin(\theta) = 2.24 \text{ MN}$

Assuming zero attraction this results in:

$$Q_H = r \cdot \tan \varphi_d \cdot Q_V = 1.0 \cdot 0.6 \cdot (13.5 - 2.24) = 6.76 \text{ MN} > F_{d,x}, \text{ i.e. sufficient capacity}$$

The distance between the ribs is set to 0.6 m and thereby avoiding passive failure between two ribs. Failure due to circular mass transfer (bearing type calculation), is assumed to be non-governing because of the vertical pressure exerted from the anchor. The failure mechanisms which are considered are illustrated below in Figure 6-6. More detailed calculations with respect to loads and structural capacity is presented in other documents.

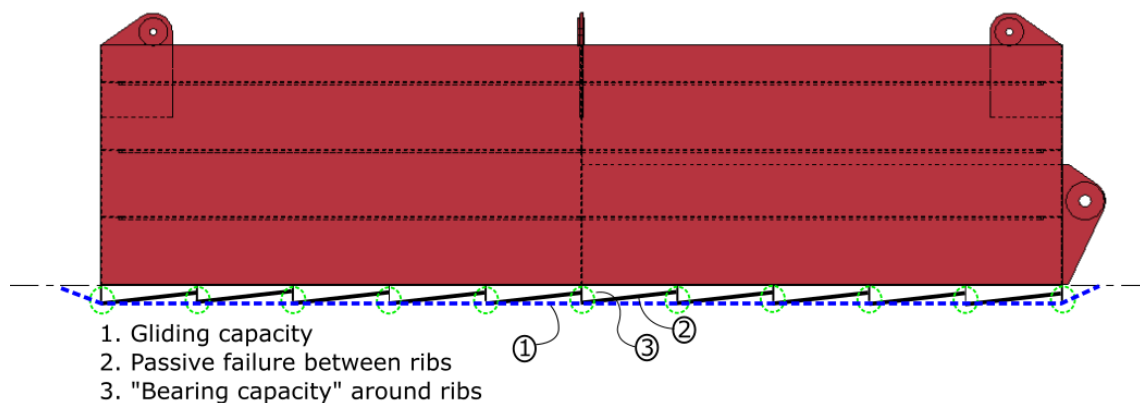


> Figure 6-6 Considered failure mechanisms of gravity anchor.

### 6.4.3 Gravity anchor, seismic capacity ALS

Large deformations are required for the mooring line to reach MBL as illustrated in Figure 6-3. It's deemed highly unlikely that an earthquake will cause permanent deformations larger than 10 m in the bedrock and/or seabed. Furthermore, the earthquake is assumed to act as an impact load on the bridge, thereby requiring time for the bridge to set in motion after the earthquake has occurred. It's therefor assumed that breaking of the mooring line is highly unlikely due to earthquake displacement.

For simplicity the anchor is assumed to have a natural period which matches the maximum pseudo acceleration  $S_e$  at bedrock and adjusted for topography. The non-submerged anchor weight and the added water mass is listed in Table 6-3. It's here assumed that the water volume is equal to 25% of anchor volume. The acceleration  $S_e$  is taken from Table 4-2. The pretension is assumed to act in the horizontal direction together with the seismic load.

The calculations show that external load is higher than the horizontal gliding capacity, without accounting for the vertical seismic load component. It's however highly unlikely that the eigenperiod of the anchor matches the period interval for  $S_e$ . By assuming the acceleration is equal to PGA and adjusting for topography, one can show that the capacity is sufficient. It's thus necessary to perform additional calculations to verify capacity against seismic loading.

> Table 6-3 Summary of seismic conditions.

Anchor	$R_d$ *	$M_{\text{anchor}}$	$M_{\text{fill}}$	$M_{\text{water}}$	$M_{\text{total}}$	$S_{e,\text{max}}$	$F_{\text{seis},x}$	$F_{\text{seis},y}$	Pretension	$E_{d,x}$	$R_d > E_d$
	[kN]	[ton]	[ton]	[ton]	[ton]	[m/s <sup>2</sup> ]	[kN]	[kN]	[kN]	[kN]	[-]
7	11612	159	2475	281	2915	4.65	13549	4516	1600	15149	<b>Not Ok!</b>
8	11612	159	2475	281	2915	4.65	13549	4516	1600	15149	<b>Not Ok!</b>
9	11612	159	2475	281	2915	4.65	13549	4516	1700	15249	<b>Not Ok!</b>
10	11612	159	2475	281	2915	4.65	13549	4516	1600	15149	<b>Not Ok!</b>
11	11612	159	2475	281	2915	4.65	13549	4516	1600	15149	<b>Not Ok!</b>
12	11612	159	2475	281	2915	4.65	13549	4516	1600	15149	<b>Not Ok!</b>
15	11612	159	2475	281	2915	4.65	13549	4516	1700	15249	<b>Not Ok!</b>
16	11612	159	2475	281	2915	4.65	13549	4516	1700	15249	<b>Not Ok!</b>

\*) Design capacity of gliding is calculated without reduction of material factor and pretension.

## 6.5 Suction anchor calculation

### 6.5.1 General

A single cylindrical shell with a flat top cap, as suggested in the last phase by Multiconsult, ref. [14], is considered in the current anchor configuration. The primary objective of these calculations is to determine global anchor dimensions with suitable capacity in terms of ultimate holding capacity and redundancy. It is recommended in a detail design phase to optimize the anchors in terms of cost, self-weight, seismic and ultimate holding capacity.

Marine operations is described in [21]. It's assumed that the suction anchors are installed prior to hook-up such that full set-up effects can develop, which is assumed to be within 6 to 9 months, ref. [6] and [20]. However, it's assumed the installation is performed 1 year prior to hook-up. Simplified calculations are carried out, neglecting installation tolerations, line-soil interaction and possible cyclic degradation. However, this should be studied to ensure to not cause any problems.

A plate thickness of 50 mm is assumed in the calculations, with reinforced plate and inner stiffener with 70 mm thickness and 2.5 m height. It is also proposed for the current anchor design to paint and use galvanic anode to avoid corrosion and thereby ensuring 100 years of life service.

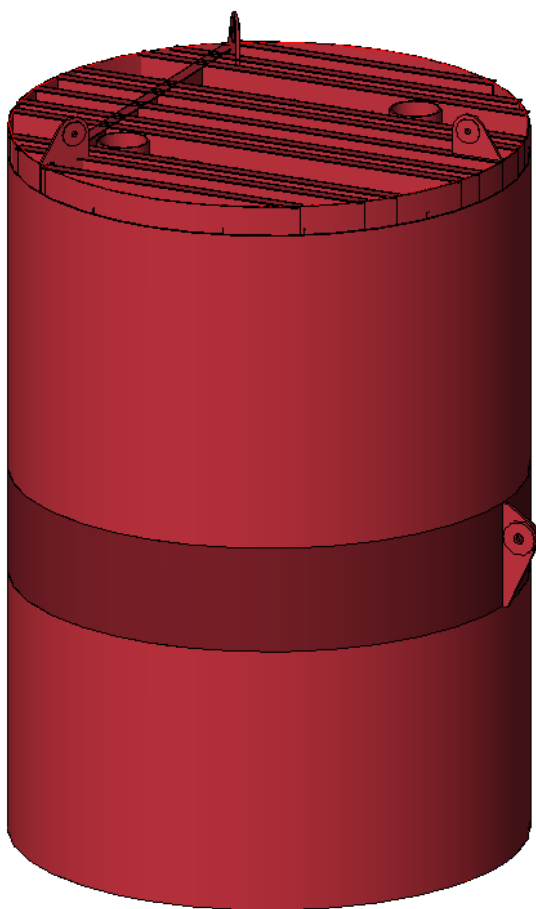


> Figure 6-7 Illustration of anchor type used in calculations.

### 6.5.2 Plaxis model

The suction anchor is modeled in plane strain according to DNVGL-RP-E303, ref. [6]. Profiles of the seabed and bedrock are imported to Plaxis from QGIS as shown in Figure 6-8. However, since the anchors are positioned at fairly flat areas, the model is simplified to be horizontal at seabed.

The anchor is modeled using stiff plates,  $EI = 63E6$ ,  $EA = 4.7E6$ , and is assumed to be much stiffer compared to the soil. It's expected after installation there will be a gap between the soil plug and the top-cap. This is included in the model by off-setting the anchor vertically from the seabed and is described in Table 6-4 as tolerance. The space between is modeled using a weightless, undrained, linear elastic polygon with a low shear stiffness  $G=1000$  kPa. The purpose is to evenly distribute the self-weight of the anchor and avoid any numerical issues.

Based on a Revit model of the suction anchor from last phase, ref. [14], a simple estimation for the anchor weight has been determined. This method is not exact but is believed to give anchor weights in the correct magnitude. The self-weight is distributed across the circular area of the anchor as an external load. One should also note that the plate thickness is assumed to be 50 mm in general, and 70 mm with the padlock. This is to ensure structural integrity and increase the anchor weight, which further described in 6.5.4.

The sides of the anchor are modeled with an interface and a material roughness of 0.65, where the  $I_p$  is assumed to be between 25 and 50%. The side shear of the anchor is calculated with a roughness factor of 0.50. Since the shear capacity is independent of the loading direction, it's introduced to the model by reducing the anchor load with a material factor of 1.2. The horizontal capacity from the active and passive failure zone is not included in the model since the failure zone varies with the load angle.

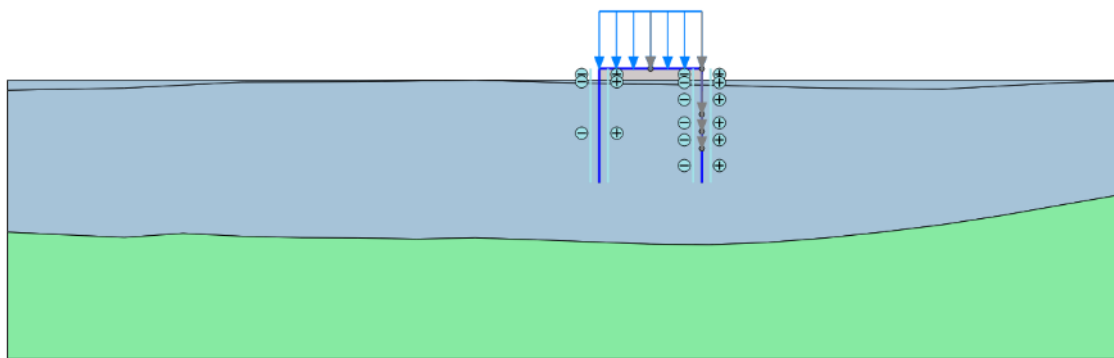


> Figure 6-8 Anchor profile nr. 13 showing true seabed compared to simplified seabed.

The optimal attachment point of the anchor is determined through iteration. The load is applied at the 1/3, 1/2 and 2/3 points of the embedded skirt length. The initial stress is generated using  $K_0$ -procedure and a  $K_0$  of 0.55 in both directions. One should note that for holding capacity calculations that the initial stresses are of little importance since they will be erased with increasing plasticity. A summary of the anchor sizes is presented in the table below.

> Table 6-4 Summary of anchor dimensions and total weight used in calculations.

Anchors	Diameter	Length	Tolerance	Total skirt length	Assumed weight, W
[#]	[m]	[m]	[m]	[m]	[kN]
1, 2, 3, 4, 5, 6	9	11.5	1	12.5	2254
13, 14	9	10	1	11	2054

The peak load duration is expected to be short, thus justifying the assumption of undrained conditions for holding capacity. Cracks and tensile cut-off are thus not introduced in the model. As described in the design brief, ref. Appendix A, the cyclic degradation is assessed to be low and therefore not included.

Since the seabed is flat and the anchors does not influence any slopes in the vicinity, the local slope stability requirement is interpreted as the required bearing capacity pre-hook-up. This is calculated in Plaxis using the c-phi-reduction method both for drained and undrained conditions.

Similarly, the anchor holding capacity is calculated by first applying the load and afterwards calculated the safety factor against failure. The vertical and horizontal ultimate capacity is also calculated for comparison. Note that the horizontal load is assumed to act at 2/3 of the embedded skirt length. The different stages are shown in Figure 6-9.

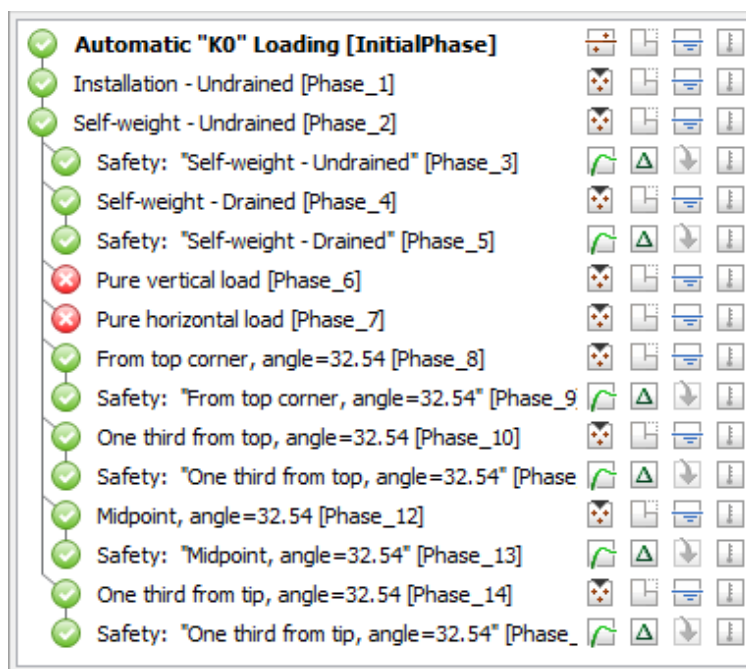


> Figure 6-9 Phases calculated in Plaxis.

### 6.5.3 Local slope stability

The drained and undrained local slope stability is calculated in Plaxis with only the self-weight being present. Typical results are shown in Figure 6-10. Although the bedrock is present in each model, it does not influence the failure zone. Several results are shown in Appendix F.

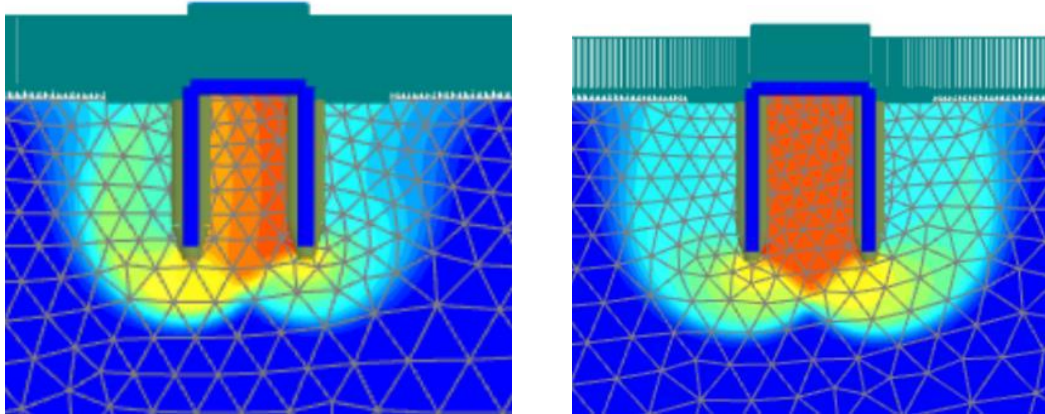


> Figure 6-10 Typical drained and undrained failure zone from self-weight.

The safety factor is well above the required value of 1.6. The set-up factor for 0.65 is debatable for drained conditions. However, as can be seen in Table 6-5, the safety factor is well above the undrained safety factor and thus deemed to not be an issue.

> Table 6-5 Summary of drained and undrained safety factor against failure.

Anchor	Elements	Drained local stability	Undrained local stability
	[-]	[-]	[-]
1	1364	19.99	9.65
2	1316	20.16	9.70
3	1365	20.15	9.71
4	1293	20.17	9.74
5	1521	19.69	9.55
6	1605	19.57	9.54
13	1086	20.12	9.95
14	1108	19.72	9.73

#### 6.5.4 Holding capacity, ULS with loss of two lines

The holding capacity is calculated using the same material models as described in 5.2.2, with the exception of  $G_{ur}/S_{u,c} = 800$ . This will however not have much influence on the model since the soil is assumed to be homogenous with depth.

Loads from 6.2 with the corresponding load angle is applied to each anchor and the safety factor is calculated for each attachment point. For comparison, the vertical and horizontal capacity is also calculated by applying a large load at the assumed optimal points. Typical results are shown in Figure 6-11 and Figure 6-12. As one can observe the vertical load gives similar failure mode as the calculations of self-weight. Furthermore, the horizontal load almost results in a pure rigid body motion without rotation, which is the failure mode that gives the highest capacity.

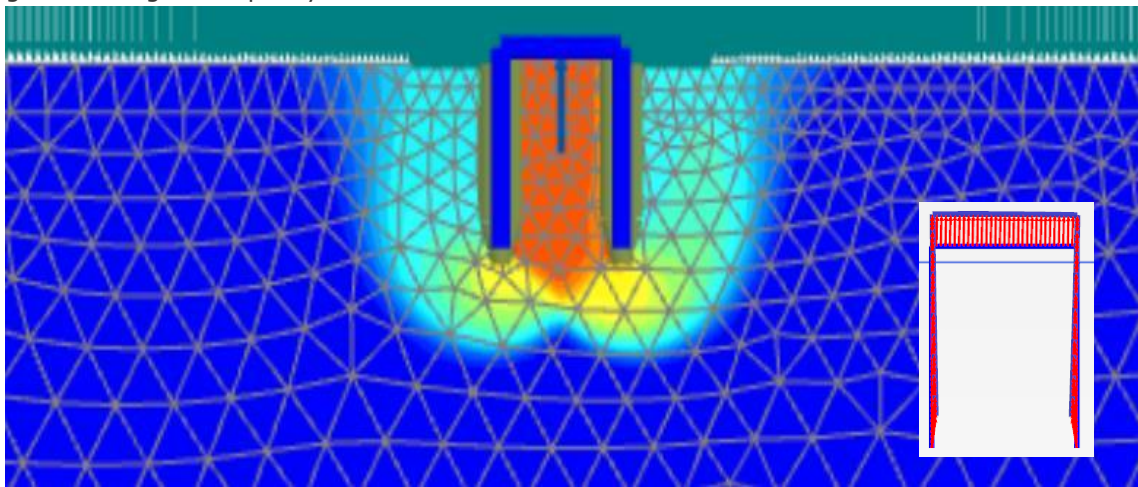


> Figure 6-11 Typical results of vertical undrained failure.

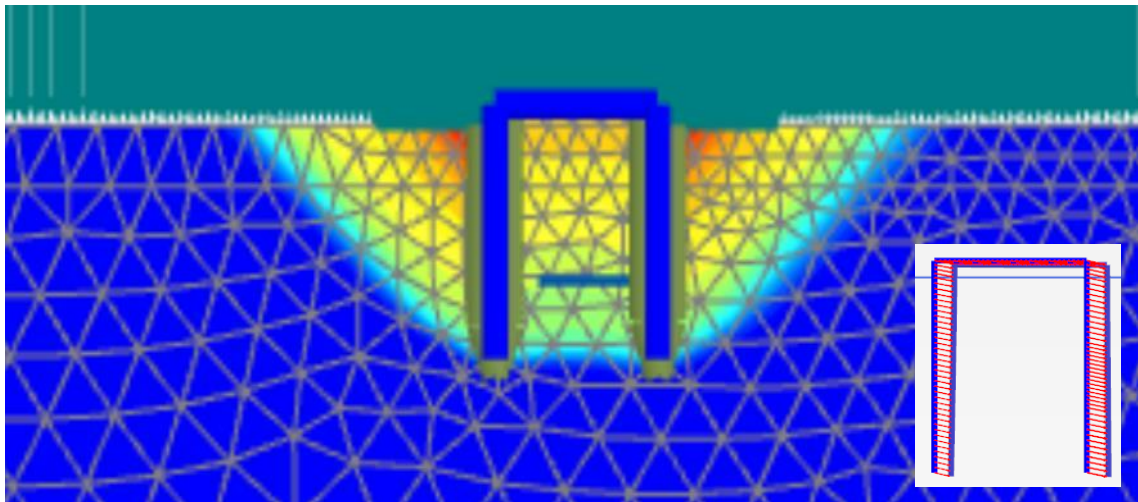


> Figure 6-12 Typical results of horizontal undrained failure.

As shown in Figure 6-13 (a) to (c), the optimal attachment point will vary with the load. One can also observe that for all cases there is a rotation, which implies that the optimal attachment point is not selected. For simplicity, the largest safety factor of the three load points is selected when comparing with the material factor.

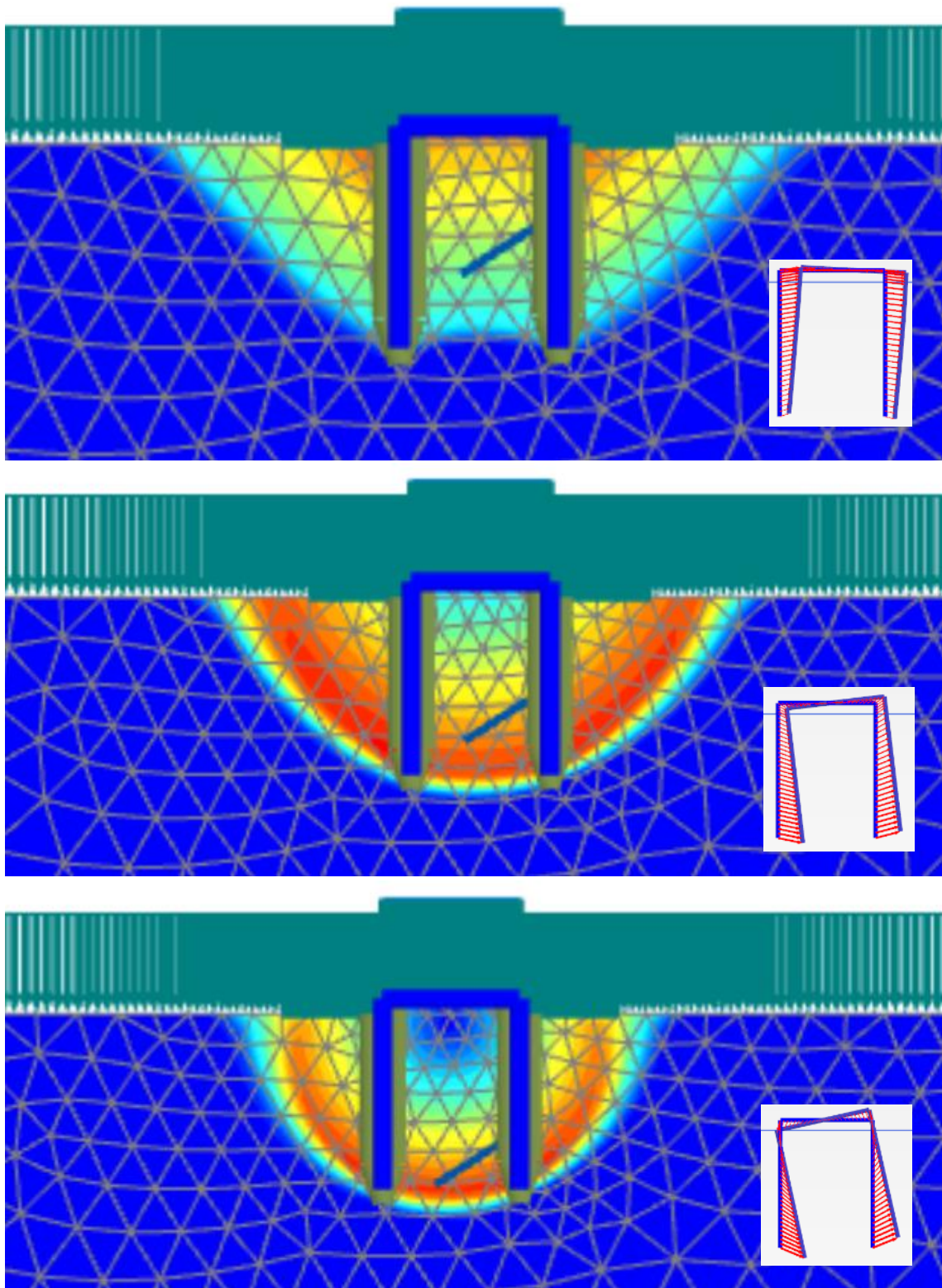


> *Figure 6-13 – Failure modes for anchor profile nr. 2*

- (a) Attachment point  $\frac{2}{3}$  of the embedded length, measured from the skirt tip.
- (b) Attachment point  $\frac{1}{2}$  of the embedded length, measured from the skirt tip.
- (c) Attachment point  $\frac{1}{3}$  of the embedded length, measured from the skirt tip.



The calculation results for the anchor dimensions listed in Table 6-4 are summarized in Table 6-6. The result shows that the holding capacity is sufficiently large since  $\gamma_m > 1.2$  for all anchor sites. Failure modes are shown in Appendix F.

The required submerged weight is calculated from the vertical component from the operational load and reduced with 0.9 for favorable self-weight. For the current concept the anchor plates are rather thick. This is to achieve sufficient self-weight and to ensure structural capacity. Anchor optimization is however recommended in the next phase with respect to alternative design for possible cost reduction.

> *Table 6-6 Key figures from the holding capacity calculation with ULS loads adjusted for loss of two mooring lines.*

Anchor	Load angle	Elements	Required weight, $W'$	Vertical capacity	Horizontal Capacity	Safety factor	Pad eye location
	[°]	[-]	[kN]	[kN]	[kN]	[-]	[kN]
1	32.5	1364	1955	18 028	8368	1.80	2/3 from tip
2	32.5	1316	1779	18 177	8643	2.06	2/3 from tip
3	32.8	1365	1577	18 153	8537	2.40	2/3 from tip
4	32.9	1293	1566	18 043	8375	2.41	2/3 from tip
5	14.8	1521	838	17 837	8204	1.77	1/2 from tip
6	14.8	1605	1968	17 869	8350	1.93	1/2 from tip
13	33.2	1088	1690	16 187	6768	1.73	2/3 from tip
14	32.8	1104	1529	15 760	6798	1.96	2/3 from tip

### 6.5.5 Holding capacity, ULS with loss of two lines – Post run-out

As described in 5.4, one cannot exclude the possibility of run-out for several of the suction anchors. The capacity for different run-out scenarios was carried out in the last phase by NGI, ref. [10]. It's also shown in 5.2.1 that a global failure involving the anchors is highly unlikely.

The impact load from a debris flow will depend on the kinetic energy and will be limited by the anchor size. It's here assumed that the debris will flow over the existing seabed, causing large shear strains at the boundary and thus dissipating some energy. Based on results from Figure 5-4 and static stability calculations, it's believed that the impact force together with the possible remoulding depth of the soil will not exceed the ultimate holding capacity shown in 6.5.4. A scenario where the peak loads, ULS with loss of two lines, occur after a run-out debris is thus assumed to be the most critical situation.

3 m of soil is assumed to be remoulded and the shear strength is reduced with the sensitivity interpreted by NGI, ref. [11],  $S_t = 4$ . The reduction of the active shear strength is illustrated in the figure below, and anisotropic strength is assumed to still be valid in the remoulded soil. Thus, the same NGI-ADP soil model with reduced shear strength has been used in the calculations.

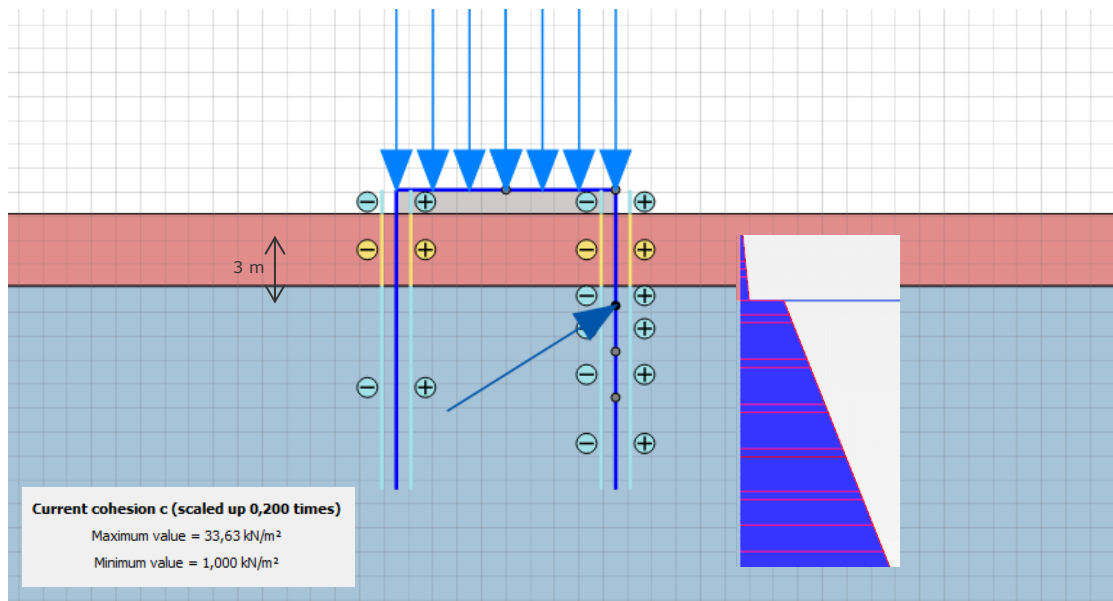


> Figure 6-14 Active shear strength with depth.

The results are summarized in Table 6-7 and shows that the safety factor is still above the required safety factor. The safety factor is reduced 6-12% and the optimal attachment point is lower. Failure modes are shown in Appendix F.

> Table 6-7 Key figures from the holding capacity calculation, post debris-flow.

Anchor	Load angle	Elements	Required weight, $W'$	Side friction	Vertical capacity	Horizontal Capacity	Material factor	Pad eye location
	[°]	[-]	[kN]	[kN]	[kN]	[kN]	[-]	[-]
1	32.5	1489	1955	1097	17 659	7715	1.64	1/2 from tip
2	32.5	1722	1779	1097	17 821	7849	1.88	1/2 from tip
3	32.8	1802	1577	1097	16 623	7760	2.19	1/2 from tip
4	32.9	1674	1566	1097	17906	7664	2.27	1/2 from tip
5	14.8	1540	838	1097	17 538	7674	1.57	1/2 from tip
6	14.8	1647	1968	1097	17 524	7668	1.72	1/3 from tip
13	33.2	1288	1690	839	15 789	6104	1.55	2/3 from tip
14	32.8	1300	1529	839	15 434	6157	1.72	2/3 from tip

### 6.5.6 Anchor capacity seismic condition ALS

As shown in Figure 6-3, large deformations are required for the mooring line to reach MBL. The eigenperiods of the bridge listed in Table 2-1 are much larger than what one would observe in an earthquake. One can thus conclude that the earthquake will act as an impact load on the bridge, thereby requiring time for the bridge to set in motion after the earthquake has occurred. Furthermore, it's highly unlikely that an earthquake will cause permanent deformations larger than 10 m in the seabed. One can thus conclude that failure due of the mooring line MBL is not governing for design, independently of the anchor size.

It's expected that the suction anchor will not be completely out of phase with the surrounding soil and some dissipation will occur due to kinematic constraints. For simplicity the anchor is assumed to be a 1 DOF object which can deform independently of the soil. Assuming that the natural period of the anchor matches the maximum pseudo acceleration  $S_e$ , one can estimate the seismic load.

The non-submerged anchor weight, the mass of the soil plug, and the added water mass is listed in Table 6-8. It's here assumed that the water volume is equal to 25% of anchor volume above seabed. The acceleration  $S_e$  is taken from Table 4-2. The pretension is conservatively assumed to act in the horizontal direction together with the seismic load. The calculations show that external load is lower than horizontal capacity of the intact soil for the current anchor dimensions.

> Table 6-8 Summary of seismic conditions.

Anchor	$R_d$	$M_{\text{anchor}}$	$M_{\text{soil}}$	$M_{\text{water}}$	$M_{\text{total}}$	$S_{e,\text{max}}$	Seismic load	Pretension	$E_d$	$R_d > E_d$
	[kN]	[ton]	[ton]	[ton]	[ton]	[m/s <sup>2</sup> ]	[kN]	[kN]	[kN]	[-]
1	8368	230	1171	16	1416	3.5	4957	2300	7257	Ok
2	8643	230	1171	16	1416	3.5	4957	2100	7057	Ok
3	8537	230	1171	16	1416	3.5	4957	1800	6757	Ok
4	8375	230	1171	16	1416	3.5	4957	1800	6757	Ok
5	8204	230	1171	16	1416	3.5	4957	2000	6957	Ok
6	8350	230	1171	16	1416	3.5	4957	1900	6857	Ok
13	6768	209	1018	16	1243	3.76	4674	2000	6674	Ok
14	6798	209	1018	16	1243	3.76	4674	1800	6474	Ok

### 6.5.7 Settlements creep deformations

The calculations are performed for a typical anchor with key figures as follows:

> *Table 6-9 Key figures for a typical suction anchor used in deformation evaluations*

Item	Value
Anchor diameter, D	9 m
Area, $A = 0.25 \cdot \pi \cdot r^2$	63.6 m <sup>2</sup>
Anchor depth, ds	10-12.5 m
Net weight, W'	~ 2 MN
Characteristic horizontal load, H	3 MN
Overburden, W'/A	31.45 kPa

#### Vertical settlements due to net weight

The safety factor for vertical capacity pre-hook-up is around 10 for undrained conditions and around 20 for drained conditions. Since the suction anchor self-weight will primarily be carried as skirt wall friction at the lower 5 m of the skirts, the long term settlements are assumed to be small, and have insignificant impact on loads and stiffness of the mooring system.

#### Horizontal long term displacements

The horizontal holding capacity for a 12.5 m deep suction anchor is estimated to 8 MN.

A characteristic long term horizontal load of 3 MN is deemed to induce small horizontal displacements to the mooring system. The horizontal load will be transferred through the circumferential areas (active and passive stress, side friction and base area at skirt tip) around 350 m<sup>2</sup>. The average normal and shear stress across these areas will be in the order of 10 kPa, and the net normal stress in the same order. This is not deemed to induce significant displacements. As for the vertical settlements, the conclusion is that this will have insignificant impact on the mooring system. Additionally, the anchor lines may be tightened up if required.

### 6.5.8 Skirt penetration

The skirt penetration is calculated according to appendix A in DNV-RP-E303, ref. [6]. It's assumed that the inner stiffener is placed at the bottom when calculating the tip resistance. The inner stiffener is also included in the wall friction and assumed here to be placed in the center of the suction anchor. The average of the anisotropy factors is roughly the same as  $\frac{S_{u,D}}{S_{u,C}}$  and therefor used in the calculations.

> Table 6-10 Input parameters used in penetration calculation.

Parameter	Input value
$\alpha$	$\frac{1}{S_t} = 0.25$
$A_{wall}$	56.55 m <sup>2</sup> per m
$A_{tip}$	1.86 m <sup>2</sup>
$A_{in}$	63.62 m <sup>2</sup>
$A_{inside}$	28.27 m <sup>2</sup> per m
$\gamma'$	$15.7 \cdot z + 0.025 \cdot z^2 - 10 \cdot z$
$S_{u,D}$	$0.75(4 + 2 \cdot z)$
$S_{u,D}^{av}$	$0.5(S_{u,D}(z) + S_{\{u,d\}}(0))$
$S_{u,tip}^{av}$	$0.75(4 + 2(z + 0.25 \cdot D))$
$S_{u,tip}^{LB}$	$\frac{1}{\gamma_m} \cdot 0.75(4 + 2 \cdot z)$
$N_c$	Shown in Figure 6-15.

The load factor is set to 1.3 according to Table 1, 4.4.1 DNVGL-OS-C101, ref. [19], and a material factor of 1.5 for soil plug failure. Key values are presented in the table below.

> Table 6-11 Summary of penetration calculations results.

Parameter	Anchors 1-6	Anchors 13 & 14
Weight, $W'$	1967 kN	1792 kN
Penetration from self-weight (design resistance)	6.17 m	5.87 m
Skirt length	12.5 m	11 m
$Q_{tip}$	523.9 kN	472 kN
$Q_{tot}$	4452 kN	3598 kN
$\Delta u_n$	-39 kPa	-29 kPa
$Q_d$	5788 kN	4677 kN
$Q_{d,tip}$	681 kN	614 kN
$\Delta u_d$	-60 kPa	-46 kPa

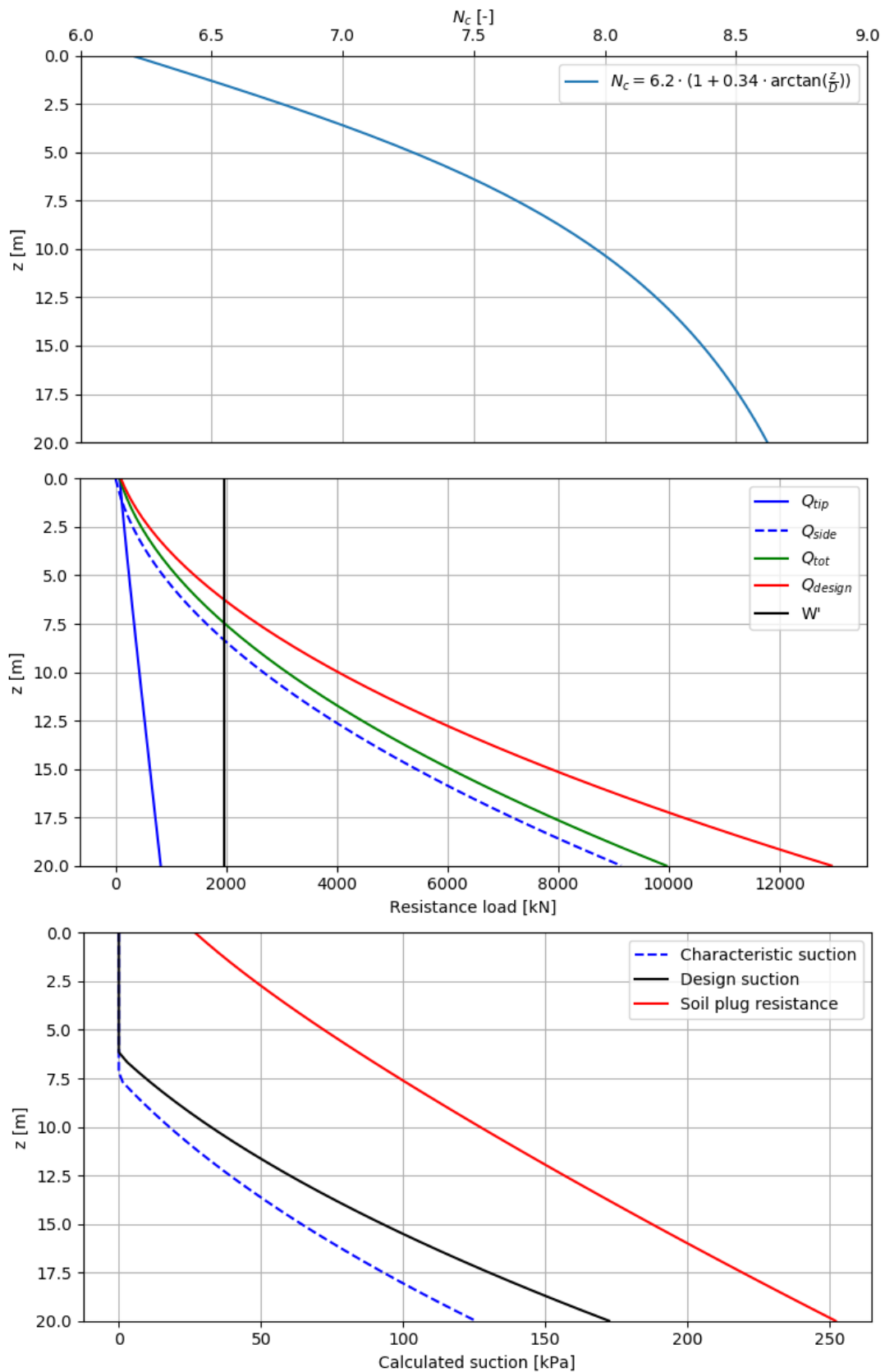


> Figure 6-15 Bearing factor, penetration resistance and required suction calculated with depth for  $D=9$  m and  $L_{skirt} = 12.5$  m.

## 7 LANDFALL GULHOLMANE

### 7.1 Soil conditions

At the North side of Bjørnafjorden, between Gulholmane and the Mainland, the road is proposed to cross the waters on a rock-fill. Figure 7-1 shows the selected road line for alternative K12. Figure 7-2 show the location of the geotechnical boreholes and the water depth in this particular area. The maximum water depth extends down to 2 – 4 m below surface.

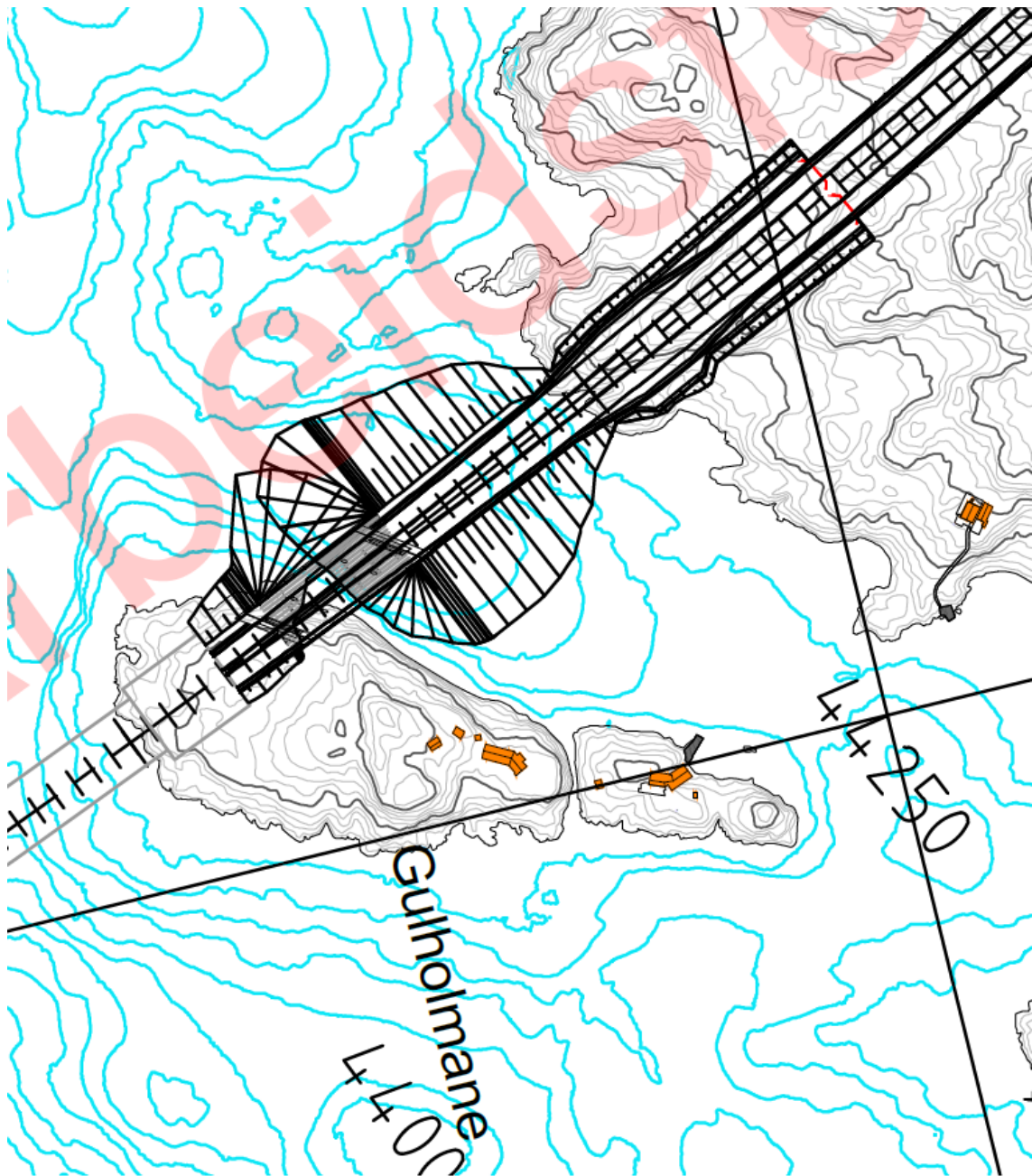
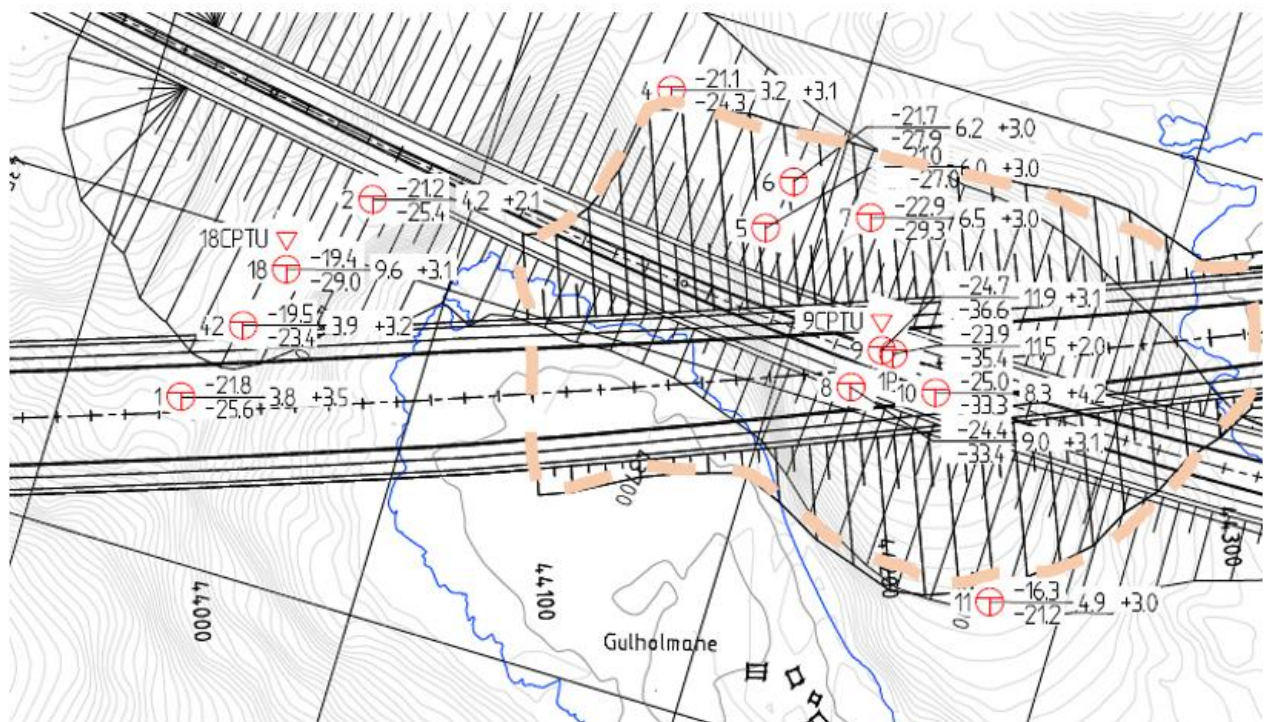
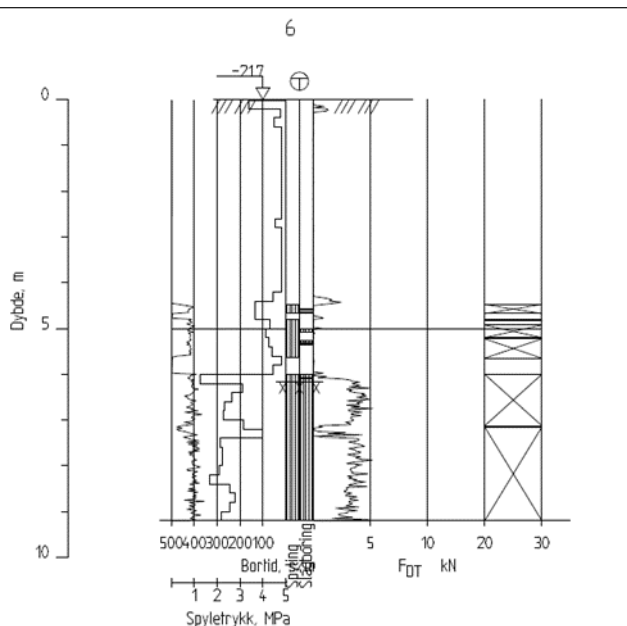


> Figure 7-1 Current road line Alternative K12



- > Figure 7-2 Geotechnical boreholes north of Gulholmane. Road lines indicated on the map are not representative for the current line alternative K12. Approximate extent of rock-fill shown with dashed line

Within the area of the rock-fill nine total soundings have been done down to the rock basement and continued 3 meters into assumed rock. Further, one CPT sounding has been conducted down to firm ground. The total soundings show very low resistance down to a firmer layer above assumed rock level. A typical sounding profile is shown in Figure 7-3.



- > Figure 7-3 Total sounding borehole 6



Interpretation of the CPTU indicates an upper layer of approximately 4 m with loose silty sand, over soft to medium soft clay. Below about 8 m depth the soil appears more layered, with some silt and sand. The interpretation of the undrained active shear strength is shown in Figure 7-4.

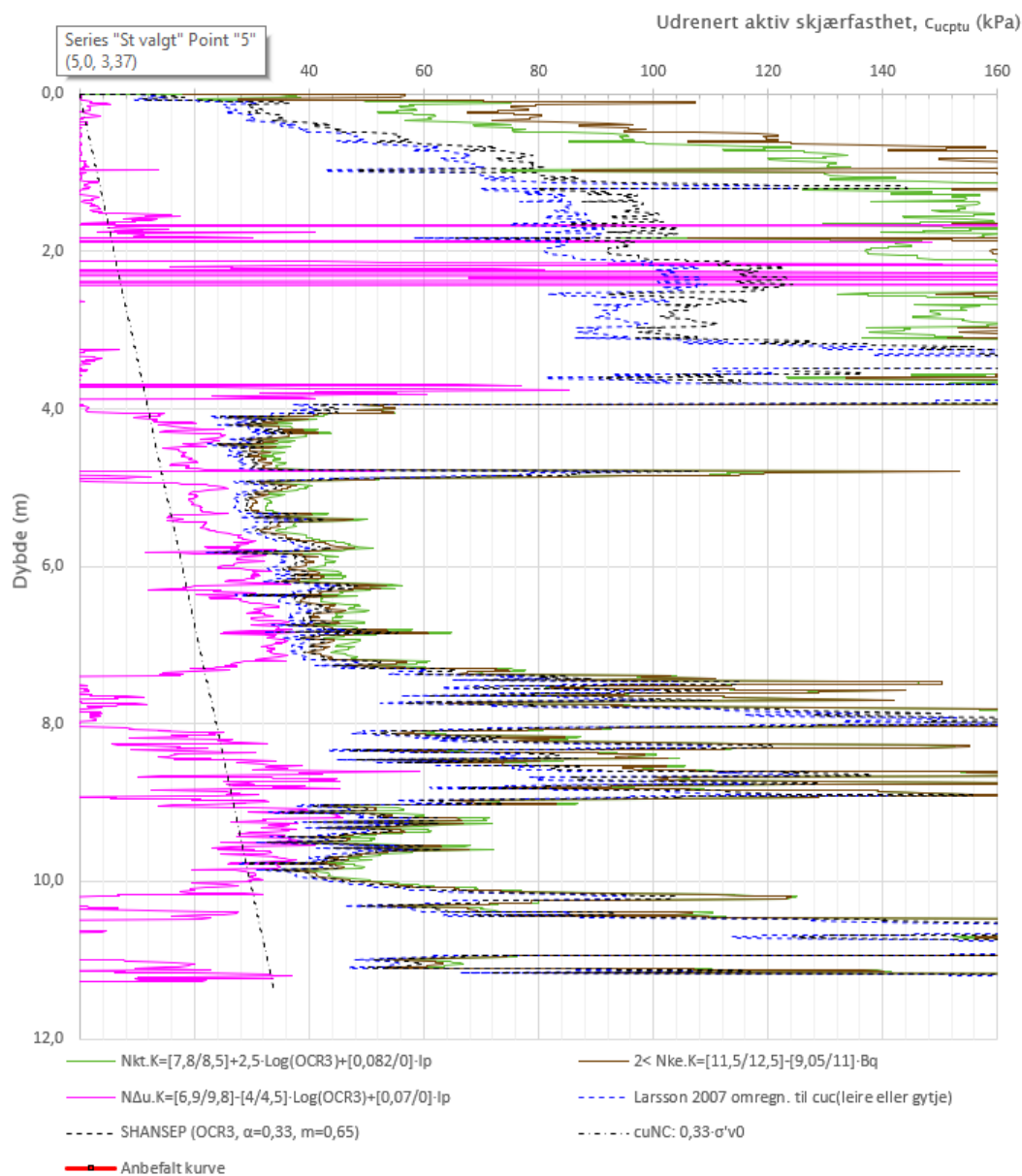


> Figure 7-4 Interpretation of CPTU 9 – Undrained active shear strength

Based on the received data, we assume the soil thickness to be in the range between 3 and 12 m. The soil consists of loose silt or sand in the upper layer, over soft to medium soft clay. Above bedrock there is firmer layer with more sand, probably glacial sediments.

## 7.2 Possible solutions for the rock fill construction

The present plan shows a length of the rock fill in the fjord of about 130 m. The maximum total height is in the order of 30 m from seabed.

### 7.2.1 Alternative 1 – Rock fill directly on top of existing seabed soils

The weight of the rock fill acting on the soft seabed will give a pressure in the order of 350 kPa where the filling is highest. This overburden pressure represents geotechnical issues related to both the risk of seabed slides during fill construction and long-term settlements of the road.

The rock-fill will need to be designed to achieve an acceptable stability situation both during the construction period and when completed. Further, the settlement issue for the completed E39 road will require a high quality of the rock fill to avoid future settlements damage to the road.

Due to the large fill thickness and the soft seabed clay, mitigation measures will most probably be required to establish satisfactory stability conditions for this alternative. The stability issue may be alleviated by extensive counter fill arrangements and dumping fill materials from barges across a predefined area of the seabed. Such precautions will require a comprehensive geotechnical engineering in addition to observations and control during the construction period. However, depending on results from supplementary soil investigation, a solution without complete masse exchange should at this stage not be excluded as a possible solution.

The issue with long term settlements of the road also needs further geotechnical investigations and analyses to be defined. If assuming a thickness range of 5 to 10 m of the normally consolidated clay, a road fill overburden of 350 kPa may induce long term seabed settlements in the order of 1 to 2 m and may take 10 - 20 years to be completed. In addition, there will be settlements in the rock fill, as described for alternative 2.

### 7.2.2 Alternative 2 - Removal of seabed soil prior to rock filling

This alternative will eliminate the geotechnical issues related to fill stability and long-term seabed settlements as described for the Alternative 1 above. This alternative will require dredging of the soft seabed soils across an area of approximately  $125 \times 80\text{m} = 10\,000\text{ m}^2$ . Assuming an average sediment thickness of 5 m across the fill footprint, the soil volume to be dredged may amount to  $50\,000\text{ m}^3$ .

In order to reduce the internal settlement in the rock fill, the fines content in the fill material should be reduced to a minimum. Application of dynamic compaction may also reduce the settlements. Dynamic compaction is not recommended below sea-surface since the effect is very limited. Further, fill construction with a temporary pre-loading may be applied to improve the situation. It is recommended to establish the rock fill as early as possible followed up with settlement measurements in order to implement possible corrective measures.

If assuming a vertical settlement of 1 – 2 % of the fill height, then a settlement of approximately 0,3 - 0.6 m may be anticipated at the deepest part of the fill. A significant portion of these settlements will occur during the construction period.

The rock fill will need to be protected against wave erosion by a filter zone and plaster stones.

## 7.3 Recommendation

In order to establish predictable stability conditions of the fill both during the construction period and beyond, Alternative 2 with seabed dredging of soft soils prior to fill construction is recommended. This alternative will also eliminate the risk of significant long-term settlement damage to the road.

If the availability of rock fill is limited, a bridge solution should be considered.

Before final design of the rock fill a supplementary soil investigation program, including sampling of undisturbed specimen and laboratory testing must be conducted. Depending on the results, a solution without or with partly exchange of existing soil may be possible.

## 8 RECOMMENDED PRIORITIES FOR FUTURE STUDIES

The time series received for the project are for 10.000 years return period, and they are scaled to be valid for the design 2750 years return period. More representative time series should be established for the project.

The suction anchors are exposed for landslide. They are designed to be robust and have spare capacity to handle remoulded soil in the upper 3 m, for anchor loads assuming two random anchors out of service. The robustness should be further investigated by more advanced analysis in order to evaluate debris flow with respect to landslide extent, ploughing depth and flow loads acting on the anchors. A vital part of this exercise will be to estimate the likely ploughing depth based on historic landslides and new geotechnical soundings.

Simplified calculations show that the gravity anchors have insufficient capacity against seismic loading. It's however assumed that sufficient capacity can be achieved by doing more advanced calculations.

The anchors should be further optimized with respect to cost, size and capacity. More detailed calculation of suction anchor capacity should be performed, including soil-line interaction, installation tolerance and possible cyclic degradation.

Detailed structural analysis with fatigue should be assessed in the future together with landing impact analysis and hydrodynamical load.

## 9 ADDITIONAL SOIL INVESTIGATIONS

### 9.1 General

The suggested additional soil investigations should be coordinated with the soil investigations finished in 2019. More detailed seismic investigations are suggested in the areas of the anchor positions and in some slopes that affect the stability conditions. Areas close to anchor positions, not covered by existing investigations, should be included. Distance between profiles should be in the order of 10 m. These investigations should be performed with ROV, including both acoustic profiling and multibeam echo sounder. The investigations will give information on bathymetry, soil layering and depth to bedrock. The investigations can also be used to locate possible boulders at bedrock. The results from the seismic investigation should be available prior to detailed planning of the suggested borings, in order to adjust the position of the borings most optimal.

We recommend soil sampling and CPTU, or alternating CPTU's and soil sampling. This will give information on soil layering, soil parameters and sediment thickness down to firm layer or bedrock. Location and number of borings are not evaluated in detail, and not commented on in the tables below.

### 9.2 Anchor group 1

> *Table 9-1 Soil investigations Anchor Group 1*

WHERE	GEOTECHNICAL CHALLENGE	INTENTION
Anchor locations; 1, 2, 3 and 4	Anchor holding capacity. Effect of landslide; ploughing depth, loads from debris flow	Optimize the anchor design. More precise calculations and predictions with respect to landslide effects. Increased robustness.
Transition between the deep mid area and slopes towards north, north-west and south.	Poor slope stability and run- out effects from landslide	Increase the confidence for the premises to be used in the slope stability calculations. More precise information on the stability conditions. More precise run-out evaluations.

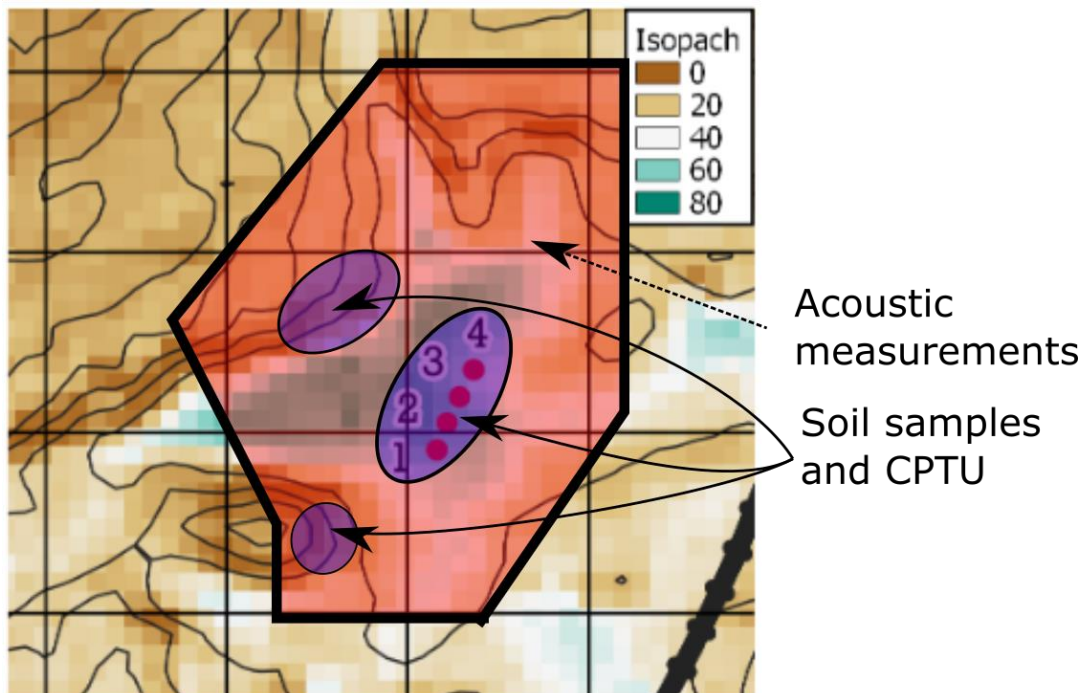


> Figure 9-1 Areas of interest for additional soil investigation - Group 1

### 9.3 Anchor group 2

> Table 9-2 Soil investigations Anchor Group 2

WHERE	GEOTECHNICAL CHALLENGE	INTENTION
Anchor locations; 5 and 6	Anchor holding capacity.	Optimize the anchor design. If critical: More precise calculations and predictions with respect to landslide effects. Increased robustness.
Transition between the deep mid area and slopes towards south-east and east.	Slope stability is slightly below the requirement. Possible run-out effects from landslide and influence by retrogressive failure.	Control of slope stability: Increase the confidence for the premises to be used in the slope stability calculations. More precise information on the stability conditions and check whether slope stability is a challenge. More precise run-out evaluations if required.
Anchor 7 and 8	It is uncertainty related to soil thickness at the anchor positions, assumed to be 6 m. Gravity anchor are suggested. Soil stability issues from the surrounding slopes are not assumed to be critical.	More precise information on soil thickness and soil type/properties, in order to evaluate challenges related to dredging and anchor installation.
Outside surveyed area	Potential debris volume might be found outside the current measured area. However, it might also not be an issue, based on which way the bedrock is sloping.	Ensure that the area of interest is sufficiently surveyed such that one can properly assess the potential debris flow volume.

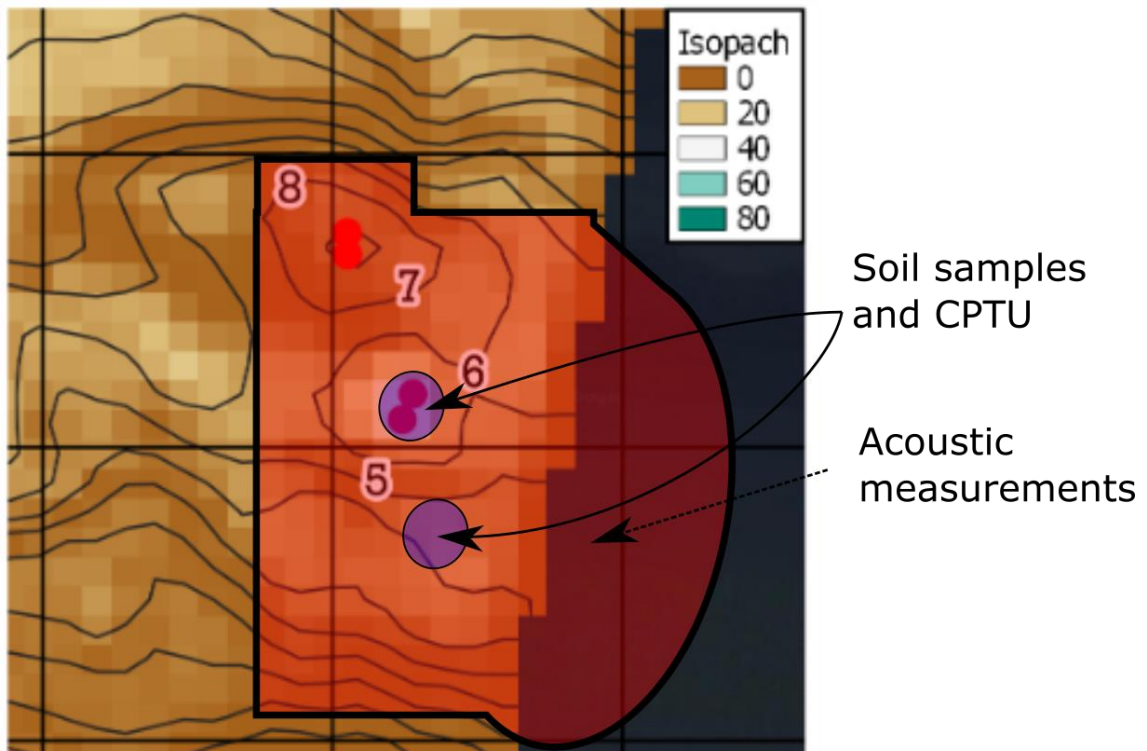


> Figure 9-2 Areas of interest for additional soil investigation - Group 2

#### 9.4 Anchor group 3

For anchor group 3 we recommend acoustic profiling, to confirm the assumptions made and to get more precise information on soil thickness.

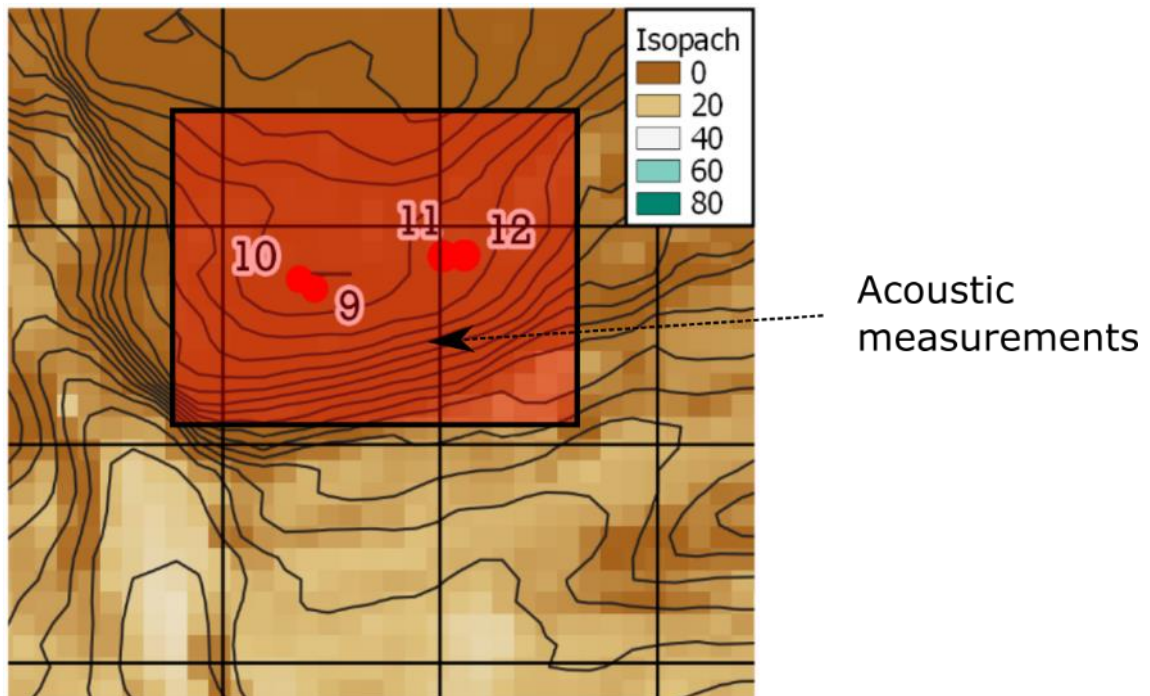


> Figure 9-3 Areas of interest for additional soil investigation - Group 3

## 9.5 Anchor group 4

> Table 9-3 Soil investigations Anchor Group 4

WHERE	GEOTECHNICAL CHALLENGE	INTENTION
Anchor locations; 13 and 14 and towards south and east	Slope stability safety factor is below the requirement towards east and south. The suggested location may be influenced by progressive landslide going backwards and affect the anchors.  Anchor holding capacity.	Control of slope stability: Increase the confidence for the premises to be used in the slope stability calculations. More precise information on the stability conditions and check whether slope stability is a challenge. Check if revised positions of the anchors may be more optimal.  Optimize the anchor design. Increase the robustness.
Anchor 15 and 16	Uncertainty related to soil thickness and effect of earlier landslides.	More precise information on soil thickness

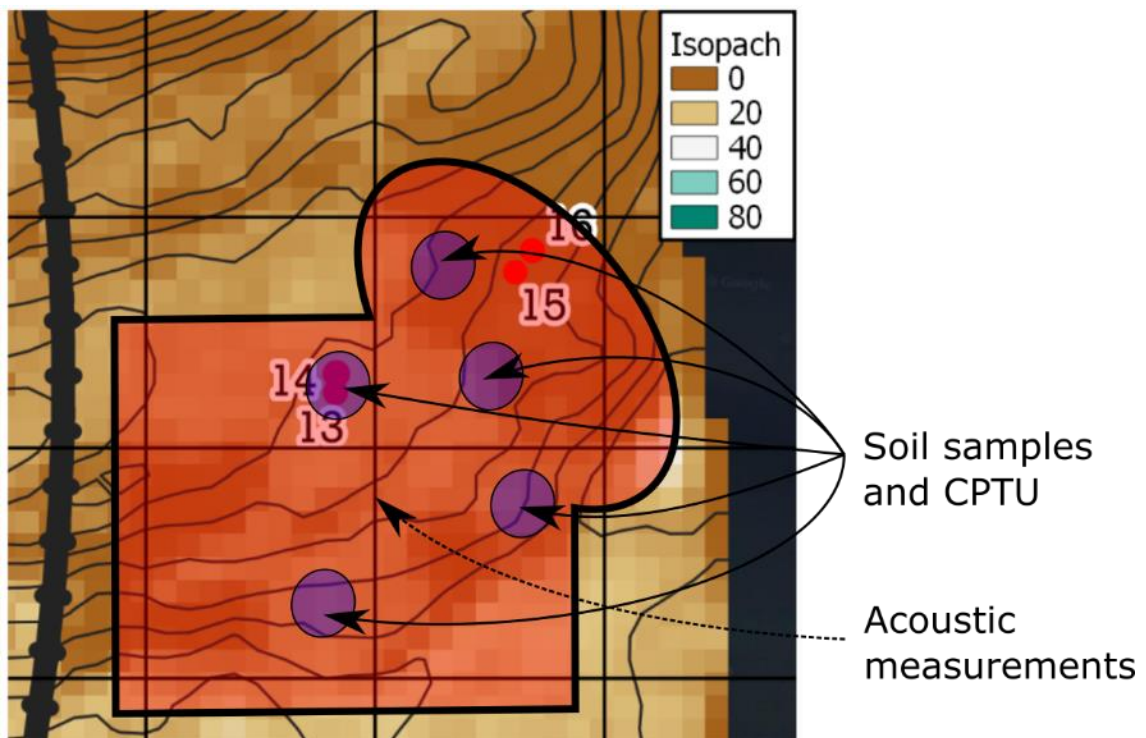


> Figure 9-4 Areas of interest for additional soil investigation - Group 4



## 9.6 Gullholmane

More detailed and confidence information on the soil parameters and properties are required, in order to evaluate possible solutions for the filling. Stability and settlement calculations are required, to check whether a complete mass exchange is required, or solutions without or with partly mass exchange may be possible. Soil samples and CPTU are recommended. Information on depth to bedrock is assumed to be satisfactory. Information on rock surface relatively good covered.

## 10 REFERENCES

- [1] OON, «SBJ-32-C5-OON-22-RE-002, rev.B Concept Selection and Risk Managment,» 29.03.19.
- [2] NPRA, «Design Basis - Bjørnafjorden floating bridges. Doc.no. SBJ-32-C4-SVV-90-BA-001,» 2018.
- [3] Standards Norway, «NS-EN 1990:2002+A1:2005+NA:2016 Eurocode 0: Basis of structural design».
- [4] NPRA, «Design Basis – Geotechnical design Doc.no. SBJ-02 C4-SVV-02-RE-002,» 2018-11-12.
- [5] NPRA, «Design Basis – Mooring and anchor. Doc.no. SBJ-32 C4-SVV-26-BA-001\_3».
- [6] DNV GL, «DNVGL-RP-E303 Geotechnical design and installation of suction anchors,» 2017.
- [7] NGI, «SBJ-31-C3-MUL-02-RE-100 Bjørnafjorden, straight floating bridge phase 3. Geohazard (Base Case),» 2017-06-02.
- [8] «Høydedata,» 2019. [Internett]. Available: <https://hoydedata.no/LaserInnsyn/>.
- [9] NGI, «Bjørnafjorden 2016 Soil Investigations. Measured and Derived Geotechnical Parameters and Final Results. Doc.no. 20150804-04-R rev.0,» 2016.
- [10] Multiconsult/NGI/Aker AS. , «Bjørnafjorden, straight floating bridge phase 3 - Geohazard (Base Case). Doc.no. SBJ-31-C3-MUL-02-RE-100,» rev. O. 2017.
- [11] NGI, «Bjørnafjorden 2016 Soil Investigations. Data Interpretation and Evaluation of Representative Geotechnical Parameters. Operations and preliminary results. Doc.no. 20150804-05-R rev.0,» 2016.
- [12] NORSAR, «Report Probabilistic Seismic Hazard Analysis (PSHA) for Project E39 Akسدal-Bergen (subproject E39 Bjørnafjorden) Tynes/Os kommune i Hordaland,» June 2018.
- [13] Standards Norway, «NS-EN 1998-1:2004+A1:2003+NA:2014: Eurocode 8 Design of structures for earthquake resistance – Part 1: General rules seismic actions and rules for buildings».
- [14] Multiconsult/NGI/Aker AS, «Analysis and design (Base Case) - App. J, Design of anchorages. Doc.no. SBJ-31-C3-MUL-22-RE-110 rev. O.,» 2017 .
- [15] NGF, Geoteknikkdagen - Mapping and modelling of subsea slides in Bjørnafjorden, Western Norway, 2017.
- [16] NPRA, «Report nr. 604. Earthquake design at Norwegian Public Road Administration. Doc no. 20110943-01-R,» 2017-04-06.
- [17] OON, «SBJ-33-C5-OON-22-RE-021-A, K12 - Design of mooring and anchoring,» 2019.
- [18] DNV, «DNVGL-OS-E301 Position mooring,» 2015.
- [19] DNV, «DNVGL-OS-C101 Design of offshore steel structures, general LRFD method,» 2016.
- [20] «NS-EN ISO 19901-7, Dynamisk posisjonering og forankring av flytende innretninger og flyttbare innretninger til havs, 2013,» 2013.
- [21] OON, «SBJ-33-C5-OON-22-RE-023-A, K12 - Execution of construction».